**Universidade de Aveiro** Departamento de Química
**Ano 2013**

**Diana Sofia Ribeiro Duarte Antunes**

# Lipidómica e Proteómica do Catabolismo Muscular Subjacente ao Cancro

# Lipidomic and Proteomic in Cancer-related Skeletal Muscle Wasting

**Universidade de Aveiro** Departamento de Química
**Ano 2013**

**Diana Sofia Ribeiro Duarte Antunes**

# Lipidómica e Proteómica do Catabolismo Muscular Subjacente ao Cancro

# Lipidomic and Proteomic in Cancer-related Skeletal Muscle Wasting

Dissertação apresentada à Universidade de Aveiro para cumprimento dos requisitos necessários à obtenção do grau de Mestre em Bioquímica Clínica, realizada sob a orientação científica da Doutora Maria do Rosário Gonçalves Reis Marques Domingues, Professora Auxiliar do Departamento de Química da Universidade de Aveiro e da Doutora Rita Maria Pinho Ferreira, Professora Auxiliar Convidada do Departamento de Química de Universidade de Aveiro.

Thanks are due to Portuguese Foundation for Science and Technology (FCT), European Union, QREN, and COMPETE for funding the QOPNA research unit (project PEst-C/QUI/UI0062/2011), the research (PTDC/DES/114122/2009; COMPETE, FCOMP-01-0124-FEDER-014707).



Dedico aos meus pais e irmã pelo incansável apoio.

*“Nós nunca nos realizamos. Somos dois abismos: - um poço fitando o céu.”*
Fernando Pessoa

**O júri**

Presidente **Doutor Rui Miguel Pinheiro Vitorino**
Investigador Auxiliar do Departamento de Química da Universidade de Aveiro

**Prof. Doutor Bruno Miguel Rodrigues das Neves**
Professor Auxiliar Convidado do Departamento de Química da Universidade de Aveiro

**Prof. Doutora Rita Maria Pinho Ferreira**
Professora Auxiliar Convidada do Departamento de Química da Universidade de Aveiro

**Prof. Doutora Maria do Rosário Gonçalves Reis Marques Domingues**
Professora Auxiliar do Departamento de Química da Universidade de Aveiro

**agradecimentos**

Às minhas orientadoras Professora Doutora Rosário Domingues e Professora Doutora Rita Ferreira pela orientação científica, disponibilidade, incansável ajuda, motivação e apoio ao longo da realização deste trabalho e acima de tudo pelo exemplo de dedicação e trabalho pela busca de conhecimento científico.

Aos meus colegas de mestrado, em especial à Vanessa, Inês e Vítor pela amizade e apoio, incentivo e todos os momentos de descontração proporcionados que me permitiram aliviar a ansiedade sentida.

A todo o grupo que muito me auxiliou e acompanhou no laboratório, em especial à Deolinda e Ana Isabel pela ajuda constante e incansável no laboratório, assim como paciência e disponibilidade tornando tudo mais fácil e agradável, o que fez muita diferença. Aos restantes companheiros de laboratório Tânia, Edgar, Luísa, Beta, Rita assim como todo o grupo de espectrometria de massa, pela disponibilidade e simpatia com que me receberam sem esquecer os preciosos momentos de descontração.

E por último, mas não menos importante, um especial obrigado à minha família e aos meus grandes amigos pelo apoio incondicional e pela enorme paciência em aturar todos os meus dias de intermináveis crises e neuras que toda esta etapa me proporcionou. Em especial, aos meus pais cujo suporte ao longo da minha vida me permitiu chegar aqui, sem vocês não seria possível.

**palavras-chave** Músculo esquelético, caquexia, cancro, mitocondria, cardiolipina, fosforilação oxidativa.

**resumo** A caquexia associada ao cancro é uma condição fisiopatológica complexa caraterizada por acentuada perda de massa muscular.Recentemente, esta situação foi associada à disfunção mitocondrial. A relação e o papel do proteoma e lipidoma mitocondrial e a funcionalidade deste organelo permanece pouco compreendida, em particular no contexto do catabolismo muscular associado ao cancro. No sentido de melhor compreender os mecanismos moleculares subjacentes às alterações no músculo esquelético na caquexia associada ao cancro, utilizaram-se 23 ratos Wistar divididos aleatoriamente em dois grupos: com cancro da bexiga induzido pela exposição durante 20 semanas a N-butil-N-(4-hidroxibutil)-nitrosamina (grupo BBN, n=13) ou saudáveis (CONT, n=10). No final do protocolo verificou-se que os animais do grupo BBN apresentavam uma perda significativa de peso corporal e de massa muscular. Também foi observado uma diminuição da atividade da fosforilação oxidativa de mitocôndrias isoladas do músculo *gastrocnemius.* a qual foi acompanhada por alterações do perfil de fosfolípidos (PL) da mitocôndria. A alteração do lipidoma mitocondrial caraterizou-se pelo aumento do teor relativo de fosfatidilcolinas (PC) e fosfatidilserina (PS) e uma redução no teor relativo de cardiolipina (CL), ácido fosfatídico (PA), fosfatidilglicerol (PG) e fosfatidilinositol (PI). A análise realizada por GC-FID e HPLC-ESI-MS evidenciou ainda um aumento de ácidos gordos polinsaturados, com um aumento destacado de C22:6 em PC, PE e PS. A diminuição de CL foi acompanhada por diminuição na expressão de citocromo c e aumento da razão Bax/Bcl2, sugestivo de maior suscetibilidade à apoptose e stress oxidativo. Embora em níveis mais elevados, a UCP-3 não parece proteger as proteínas mitocondriais da lesão oxidativa atendendo ao aumento do teor de proteínas carboniladas. Em conclusão, a remodelação de PL da mitocôndria parece estar associada à disfunção da OXPHOS e, consequentemente, do catabolismo muscular associado ao cancro.

**keywords** Skeletal muscle, cachexia, cancer, mitochondria, cardiolipin, oxidative phosphorylation.

**abstract**

Cancer cachexia (CC) is a complex pathophysiological condition characterized by a marked muscle wasting. Recently, this situation has been associated to mitochondrial dysfunction. The interplay and role of mitochondrial proteome and lipidome and also the functionality of this organelle remains poorly understood in the context of cancer-related muscle wasting. To better understand the molecular mechanisms underlying skeletal muscle wasting, 23 *Wistar* rats were randomly divided in two groups: animals with bladder cancer induced by the exposition to N-butyl-N-(4-hydroxybutyl)-nitrosamine for 20 weeks (BBN, n=13) or healthy ones (CONT, n=10). At the end of the experimental protocol, BBN animals demonstrated a significant body weight and muscle mass loss and was also observed an decreased activity of oxidative phosphorylation in mitochondria isolated from *gastrocnemius* muscle, which was accompanied by alterations of this organelle's phospholipids (PL) profile. The mitochondrial lipidome alterations were characterized by an increase of the relative content of phosphatidylcholines (PC) and phosphatidylserine (PS) and a decrease of cardiolipin (CL), phosphatidic acid (PA), phosphatidylglycerol (PG) and phosphatidylinositol (PI). GC-FID and HPLC-ESI-MS analysis also showed an increase of polyunsaturated fatty acids, particularly of C22:6 in PC, PE and PS. The observed decrease in CL class was accompanied by a decrease in the expression of cytochrome c, and an increase of the ratio Bax/Bcl-2, suggestive of a greater susceptibility to apoptosis and oxidative stress. Although in higher levels, UCP-3 does not seem to protect mitochondrial proteins from oxidative damage considering the increased content of carbonylated protein. In conclusion, the PL remodeling seems to be associated to OXPHOS dysfunction and consequently to muscle catabolism associated with cancer.

**Index**

## Figures Index

## Tables Index

**Abbreviations**

ADP – Adenosine diphosphate
Akt – Protein kinase B
AMP – Adenosine monophosphate
AMPk – Adenosine monophosphate kinase
ATP – Adenosine triphosphate
BBN – Bladder cancer- induced by N-butyl-N-(4-hydroxybutyl)-nitrosamine
BSA – Bovine serum albumin
CC – Cancer cachexia
CDP – Cytidine diphosphate
CL – Cardiolipin
CMP – Cytidine monophosphate
Complex I – NADH dehydrogenase
Complex II – Succinate dehydrogenase
Complex III – Ubiquinone cytochrome c oxireductase
Complex IV – Cytochrome c oxidase
Complex V – ATP synthase
Cyt c – Cytochrome c
Da – Dalton
DAG – Diacylglycerol
E1 – Ubiquitin-activating enzyme
E2 – Ubiquitin-conjugating enzyme
E3 – Ubiquitin ligase
eIF4BP-1 – Eukaryotic initiation factor
ETC – Electron Transport Chain
ESI – Electrospray ionization
FA – Fatty acids
FOXO – Forkhead box protein O
HPLC – High performance liquid chromatography
IFN-γ – Interferon gamma
IGF-1 – Insulin growth factor 1
IL – Interleukin
LC – Liquid chromatography
LMF – Lipid-mobilizing factor
MAFbx – Muscle atrophy F-box
MALDI – Matrix-assisted laser desorption/ionization
MS – Mass Spectrometry
MS/MS – Tandem Mass Spectrometry
mtDNA – Mitochondrial DNA
mTOR – Mammalian target of rapamycin
NF-κB – Nuclear factor kappa B
$O_2^{\bullet-}$ - Superoxide radical
OD – Optical density
$OH^{\bullet}$ - Hydroxyl radical
OXPHOS – Oxidative phosphorylation
PA – Phosphatidic Acid
PC – Phosphatidylcholine
PE – Phosphatidylethanolamine
PG – Phosphatidylglycerol
PI – Phosphatidylinositol
PI3K – Phosphatidylinositol 3-kinase
PIF – Proteolysis-inducing factor
PL – Phospholipid
PS – Phosphatidylserine
$R^{\bullet}$ - Alkyl radical
$ROO^{\bullet}$ - Peroxyl radical

ROOH – Hydroperoxide

ROS – Reactive oxygen species

SDS-PAGE – Sodium dodecyl sulfate polyacrylamide gel electrophoresis

TBS – Tris-buffered saline

TLC – Thin layer chromatography

TNF-α – Tumor necrosis factor-alpha

UPP – Ubiquitin proteasome pathway

# CHAPTER I

# Introduction

# I. Introduction

Cancer is a major health concern and the worldwide leading cause of morbidity and mortality [1]. Deaths from cancer are expected to increase, with an estimated 13.1 million deaths in 2030 [1]. The majority of patients with advanced cancer undergo involuntary loss of weight usually denominated as cachexia [2, 3]. Due the high incidence of cancer cachexia, more research should be developed aiming to better understand the underlying molecular mechanisms and, ideally, develop measures to prevent muscle wasting, and so improve patients' quality of life.

Cachexia, derived from the Greek *kakos* and *hexis*–"bad condition" is a wasting syndrome characterized by progressive loss of muscle with or without loss of fat mass [4]. This condition is observed in many diseases such as cancer, chronic heart failure, and chronic obstructive pulmonary disease (COPD), and is estimated to be responsible for the deaths of 22% of cancer patients [2, 4-13]. Cancer cachexia (**CC**) also seems to be responsible for a decreased response to chemotherapy leading to death when the weight loss is higher than 30% [7, 10, 14, 15]. The most prominent phenotypic feature of cancer cachexia is muscle wasting and once skeletal muscle comprise more than 40% of the body weight [4, 16, 17], its wasting contributes to increased disability, fatigue, poor quality of life, and increased mortality in cancer patients [2, 6, 7, 10, 15-17]. Among the cellular mechanisms underlying muscle wasting, the imbalance between protein synthesis and degradation towards increased proteolysis has been suggested as one of the most relevant processes involved in the pathogenesis of cancer-related cachexia [2, 10]. The involvement of mitochondrial dysfunction in skeletal muscle wasting was recently reported [18-21]. However, the underlying molecular mechanisms centered on mitochondria are not well elucidated.

## 1.1. Cancer cachexia pathophysiology

Cancer cachexia is a complex metabolic syndrome underlying illness and characterized by a marked weight loss in adults or growth failure in children [3, 4]. Anorexia, inflammation, insulin resistance and increased muscle protein breakdown are frequently related with wasting disease [4].

Asthenia or lack of muscular strength is one of the most prominent symptoms and reflects the muscle wasting [10, 12, 17]. Indeed, muscle wasting has been reported as an

important feature in the pathophysiology of cachexia and a major cause of fatigue in patients [22-24]. Several studies on cachexia suggest the importance of the inflammatory response characterized by increased levels of pro-inflammatory cytokines, acute phase proteins and metabolic disturbances such as glucose intolerance, anemia, low levels of plasmatic albumin, among others [4]. Body weight loss is by far the most important parameter required to define the cachexia score in patients with cancer [4]. Besides whole body and lean body mass loss, catabolic drivers (including the ones involved in immune and inflammatory response) are important to predict how CC will affect patient's quality of life, and physical performance [4]. Imunosupression response accounts for up to 20% and might be an early marker of cachexia [4]. Besides immune disturbance, metabolic alterations have been considered to result from a variety of interactions between the host and the tumor in cancer cachexia (**Figure 1**) [7, 25-27], mediated by tumor-derived pro-inflammatory cytokines. Systemic inflammation initiates with the induction of the acute phase response and the mobilization of fat reserves, which together with pro-cachectic factors secreted by the tumor, promotes waste of muscular tissue and fat stores [25]. However, it is not certain whether the tumor cell production of pro-inflammatory cytokines or the host inflammatory cell response is the primary cause of cachexia [7].

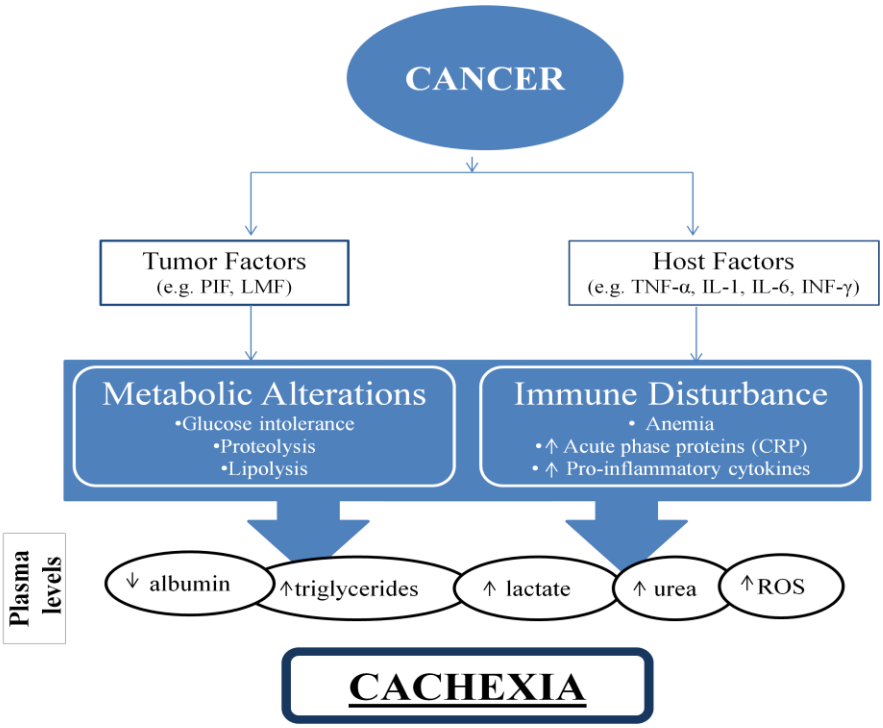


**Figure 1:** Pathophysiological changes underlying cancer cachexia [adapted from 26, 27].

## 1.2. Mediators of cancer cachexia

The mediators of cachexia are associated with both waste of fat tissue and muscular tissue and can be divided into two categories:

(i) host factors, such as tumor necrosis factor-α (**TNF- α**), interleukin-1 (**IL-1**), interleukin-6 (**IL-6**) and interferon-γ (**IFN-γ**); (ii) tumor factors that have a direct catabolic effect on host tissues, such as lipid-mobilizing factor (**LMF**), which acts on adipose tissue, and proteolysis-inducing factor (**PIF**), which acts on skeletal muscle [17, 26]. Pro-inflammatory cytokines were associated with a significant loss of skeletal muscle mass in mice bearing MAC16 adenocarcinoma and mice bearing cell lines (JHU022, JHU012) [28, 29]. TNF-α is a cytokine primarily produced by macrophages responsible for the stimulation of the NF-κB pathway, which is involved in cytokine mediated proteolysis [2, 10, 30], and has been correlated with the increase of ubiquitin gene expression in rat *soleus* muscle [31]. The involvement of this cytokine in the

induction of cachexia appears to vary with tumor type and each may rely on the concomitant production of other cytokines or factors responsible for the cachexia [12].

Furthermore, TNF-α and the tumor factor PIF have been suggested as the major inducers of skeletal muscle atrophy in cachectic patients through the activation of the ubiquitin-proteasome pathway (**UPP**) [2, 7]. PIF mediates catabolism in animals bearing tumors presenting muscle loss as in mice bearing MAC16, being absent in animals bearing tumors but with no evidences of cachexia [23, 32]. Since PIF is expressed in tumors and correlates with weight loss, it is likely to be associated with cancer-related cachexia [33, 34]. Interleukin-6 (IL-6) has a major role in the inflammatory process and has been suggested to induce cachexia in mice by increasing tumor burden and protein degradation in muscle through the activation of proteolytic pathways [2]. The association between IL-6 and cancer cachexia was confirmed with the administration of an anti-mouse IL-6 antibody to murine colon adrenocarcinoma tumor-bearing mice that reversed key parameters of cachexia [2]. Another cytokine that has been proposed to play a role in cancer cachexia is IFN-γ, which is produced by activated T and NK cells and its biological activities overlap with those of TNF-α [2, 27, 30]. Nevertheless, no significant correlation between IFN-γ serum levels and weight loss was observed in CC patients though the administration of a monoclonal antibody against this cytokine reversed the wasting syndrome induced by Lewis lung carcinoma in mice [2, 30, 35]. Another mediator implicated in CC-related fat loss is the lipid-mobilizing factor (**LMF**) through increased lipolysis [2, 7, 9, 15]. Loss of adipose tissue occurs more rapidly than lean tissue with the progression of cancer cachexia [2]. Despite the association with cancer cachexia, fat tissue wasting is not well defined [24], being skeletal muscle protein degradation the main cause of weight loss [36, 37]. Moreover, in a study performed with animal models submitted to fasting-refeeding periods it was observed an increased protein degradation in normal rats but not in tumor bearing rats, suggesting that muscle wasting occurs despite of the fed state [38].

## 2. Mechanisms underlying cancer-related skeletal muscle wasting

CC-related muscle wasting has been associated with increased proteolysis, decreased protein synthesis, or a combination of these two cellular processes. Protein

degradation has been suggested to be the major cause of skeletal muscle loss, and involves cellular mechanisms activated by mediators such as TNF-α and PIF [7, 10, 17, 39].

The skeletal muscle contains several proteolytic systems, two of which have been suggested to play a major role in cancer-related skeletal muscle wasting [40]. These include the non-lysosomal calcium ($Ca^{2+}$)–dependent protease system and the ATP-dependent ubiquitin-proteasome pathway [37, 41]. The non-lysosomal $Ca^{2+}$-dependent protease system consists of a family of $Ca^{2+}$-activated cysteine proteases known as calpains. These proteases are activated by an increase in cytosolic calcium, suggestive of injury [30, 42]. Calpains degrade the structures that keep myofibrillar proteins assembled in the myofibrils, acting as initiators of myofibrillar protein degradation [12]. In fact, increased calpains levels were observed in the skeletal muscle of cachectic tumor-bearing rats [43].

The ubiquitin-proteasome pathway is the main catabolic system involved in cancer-related increase of muscle degradation [7, 28]. UPP is activated in catabolic states resulting in muscle atrophy [30]. The major function of the UPP is tagging damaged proteins with a small protein called ubiquitin. The ubiquitinated proteins then enter the S26 proteasome, which breaks them into small peptides [10, 42, 44]. In normal states, the UPP degrades damaged and defective proteins produced by errors in gene transcription, mRNA translation, or oxidative stressors [12]. However, in disease states such as cancer, the activity of the UPP increases, leading to accelerated ubiquitination and subsequent degradation of proteins. Ubiquitination is performed by the action of several enzymes: ubiquitin-activating enzyme (**E1**), ubiquitin-conjugating enzyme (**E2**) and an ubiquitin ligase (**E3**). Two muscle-specific ubiquitin ligases, muscle ringer finger 1 (**MuRF1**) and muscle atrophy F-box (**MAFbx**) also called atrogin-1, have been suggested as key regulators of skeletal muscle proteolysis under catabolic conditions [45, 46].

In tumor-bearing animals, increased expression of the UPP in skeletal muscle was associated with a subsequent increased rate of muscle protein degradation [23, 44]. Moreover, ATP depletion decreases protein degradation in cachectic tumor-bearing rats, supporting the theory that the ATP-dependent Ub-proteasome pathway is primarily responsible for skeletal muscle degradation [30, 37]. CC-related muscle wasting also relies on impaired protein synthesis in skeletal muscle through the Akt pathway, a key signaling mechanism that regulates muscle mass. The two main branches of this pathway are the

Akt/mTOR pathway which controls protein synthesis, and the Akt/FOXO pathway which controls protein degradation [47, 48]. Decrease of Akt-dependent signaling in human skeletal muscle has been associated with CC [49]. The mammalian target of rapamycin (**mTOR**) is a protein that is activated under specific conditions, and its downstream mediators enable the efficiency of translation [50]. Akt is a member of the phosphatidylinositol 3-kinase (**PI3K**) pathway [51], corresponding to an upstream regulator of mTOR, and plays a central role in integrating anabolic and catabolic responses. mTOR phosphorylation, and subsequently phosphorylation of its downstream targets leads to increased protein synthesis [46, 49]. This kinase is also involved in cellular stress and apoptotic signaling, through the control of the forkhead box protein O (**FOXO**) 1 and FOXO3 transcription factors (**Figure 2**) [51, 52].

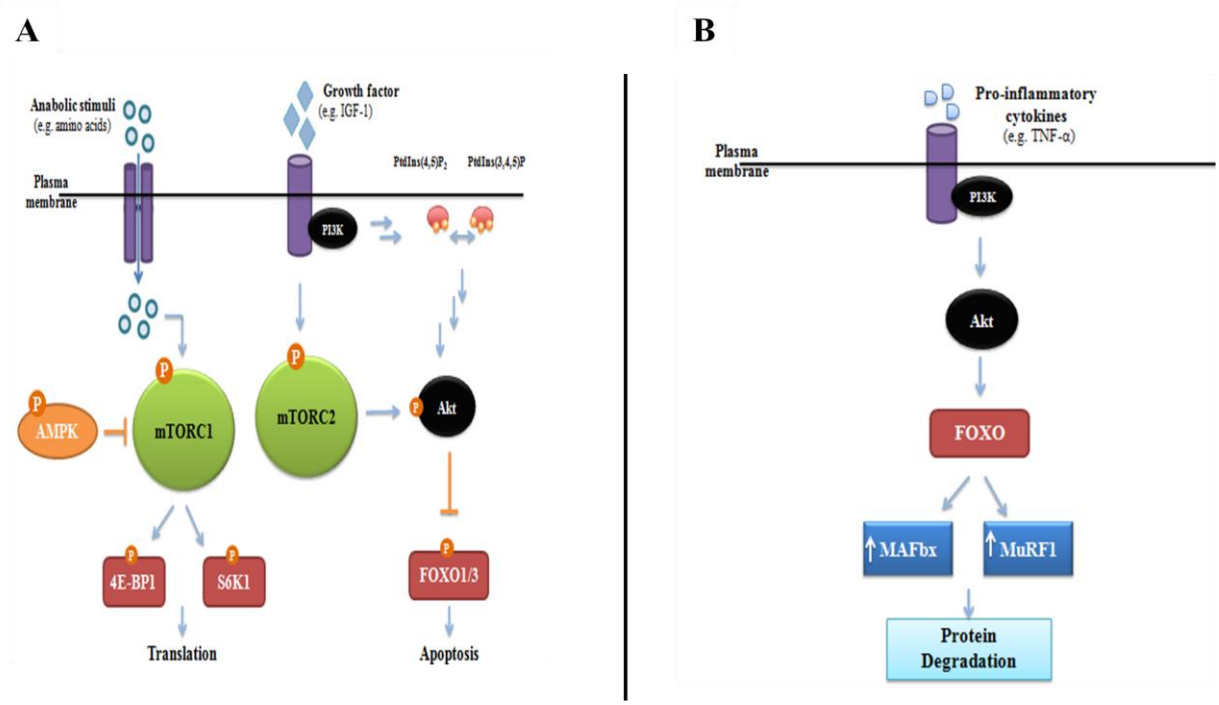


**Figure 2:** Schematic representation of the Akt/mTOR and Akt/FOXO pathways in anabolic (A) and catabolic conditions (B). P phosphorylation, activation or inactivation; PI3K phosphatidylinositol 3-kinase; Akt protein kinase B; FOXO forkhead protein box O; AMPK AMP-activated kinase; 4E-BP1 eIF4E-binding protein 1; S6K1 S6 kinase; MAFbx muscle atrophy F-box; MuRF1 muscle ringer finger 1 [adapted from 51, 52, 53].

Evidences suggest that impaired signaling Akt pathway may be involved in the suppression of protein synthesis and induction of protein degradation in catabolic conditions [54]. In fact, a study demonstrated that Akt in skeletal muscle of cancer cachectic patients is reduced by almost 55% relatively to levels in skeletal muscle from normal patients [49].

## 3. The role of mitochondria in muscle wasting

### 3.1. Mitochondrial dysfunction in wasting conditions

Mitochondrion is an intracellular organelle found in most eukaryote cells and plays an important role in cellular ATP production, in the regulation of cell death by apoptosis, in the synthesis of key metabolites for protein synthesis, pyruvate oxidation and oxidation of fatty acids, calcium buffering and homeostasis [55-57]. This cross talk between cell and mitochondria might leads to cell adaptation to physiological changes or the cell death. The ATP production occurs mainly from glucose and fatty acid oxidation and to a lesser extension from amino acid oxidation. The acetyl-CoA resultant from β-oxidation pathway enters in the Krebs cycle and is used in ATP generation. Both oxidative pathways are related to the mitochondrial electron transport chain (**ETC**), whose protein content and activity, such as cytochrome c oxidase, define the mitochondrial oxidative capacity. Electrons generated in the Krebs cycle from the oxidation of acetyl-CoA are carried from reduced nicotinamide adenine dinucleotide (NADH) and succinate to complex I (NADH dehydrogenase) and complex II (succinate dehydrogenase), providing the electron transport chain. The ETC is located into the mitochondrial inner membrane and consists of complexes I-IV, containing electron carriers such as coenzyme Q or ubiquinone, and cytochrome c, which transport the electrons from one complex to the next with oxygen acting as the final electron acceptor. In this process of electron transport is generated an electrochemical gradient that provides the energy required to drive the synthesis of ATP by complex V, ATP synthase (**Figure 3**). This electrochemical gradient states the coupling between oxidative and phosphorylative reactions, corresponding to oxidative phosphorylation (**OXPHOS**) [58, 59]. The utilization of fatty acids as an energy source requires the optimal functionality of the mitochondrial electron chain and OXPHOS. NADH is involved into the electron transport chain at complex I and electrons

are transferred from acyl CoA dehydrogenases via the electron-transfer flavoprotein (ETF), ETF dehydrogenase and ubiquinone to complex III as depicted in Figure 3. Deficiencies in the ETF pathway lead to impaired fatty acid oxidation [60].

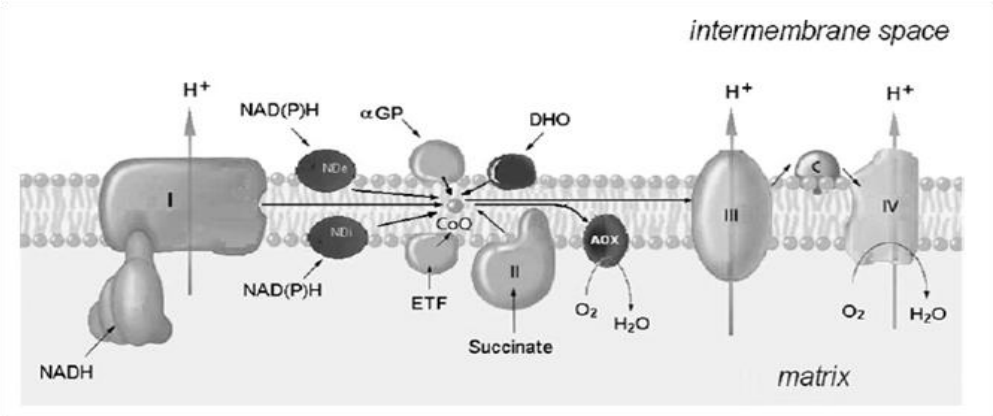


**Figure 3:** Representation of the electron transport chain with the protein complexes and their substrates in relation with the inner mitochondrial membrane. Complex I (NADH dehydrogenase); complex II (succinate dehydrogenase); complex III (ubiquinone cytochrome c oxireductase); complex IV (cytochrome oxidase), complex V (ATP synthase); NDi and NDe, internal and external alternative NAD(P)H dehydrogenases; AOX, alternative oxidase; GP, glycerol-3-phosphate; ETF, electron transfer flavoprotein; DHO, dihydroorotate; CoQ, Coenzyme Q; C, cytochrome c [adapted from 59].

Mitochondria generate more than 90% of cell energy by OXPHOS, which occurs in the inner mitochondrial membrane and converts reducing equivalents and oxygen into energy and water [61]. This organelle is also a primary source of endogenous reactive oxygen species (**ROS**), which are byproducts of OXPHOS activity [55, 56]. Indeed, from the oxygen utilized by the mitochondria during respiration, 0.4-4.0 % is converted in superoxide radical ($O_2^{\bullet -}$), and when its production overwhelm the antioxidant capacity oxidative damage of biomolecules occurs [61, 62]. Complexes I and III are the principle sites of ROS and are at the same time its main targets, together with ATP synthase [61, 63, 64]. Regarding mitochondrial lipids, these are predominantly phospholipids, being phosphatidylcholine, phosphatidylethanolamine and cardiolipin the most representative classes [67]. Increased ROS production and mitochondrial dysfunction have been associated with oxidative damage of mitochondrial phospholipids [63, 65, 66].

The deregulation of mitochondrial function has been implicated in pathophysiological conditions as CC, since is directly related to decreased muscle oxidative capacity [68]. Furthermore, the mitochondrial dysfunction in the skeletal muscle with a consequent diminished oxidative phosphorylation efficiency and impaired mitochondrial dynamics has also been associated with systemic inflammation and skeletal muscle wasting [68]. Indeed, the activation of TNF-α-induced NFκB was shown to decrease the activity of regulators involved in mitochondrial biogenesis and affect downstream oxidative proteins, leading to impaired muscle oxidative capacity [69].

The dysfunction of this organelle can lead to a cascade of events whereby mitochondrial damage causes additional damage [70]. The reduced ATP synthesis, suggestive of mitochondrial bioenergetics dysfunction, ultimately leads to skeletal muscle wasting [21]. Several studies have described changes in mitochondria shape, number, and function in wasted skeletal muscle [19, 20, 71]. *Gastrocnemius* muscle from tumor-bearing mice was found to have an abnormally low mitochondrial respiratory chain activity, and indirect evidence also suggests that the mitochondrial oxidative energy metabolism may be compromised relatively early in the wasting process [20, 71]. In the control of energy metabolism, mitochondrial uncoupling proteins (UCPs) assume an important role, once the uncoupling of oxidative phosphorylation leads to decreased ATP synthesis rate [2, 17, 72]. In skeletal muscle UCP-3 overexpression was related to cancer cachexia in animal models [21, 72-74]. Moreover, upregulation of UCP3 has been associated with the activation of proteolytic pathways in wasted muscle [75].

Ushmorov *et al.* [71] studied the mitochondrial oxidative phosphorylation from *gastrocnemius* muscle of C57/BL6 mice bearing the fibrosarcoma MCA-105 and observed a reduction of 25% in mitochondria oxygen consumption. This study highlighted a reduction in complex IV activity in skeletal muscle of cachectic mice, which was reverted by supplementation with cysteine and ornithine [71]. By modulating ROS production at mitochondria, pro-inflammatory cytokines such as IL-1, IL-6, TNF-α, and IFN-γ, promotes muscle wasting [76]. Indeed, it was reported that TNF- α inhibits the mitochondrial ETC in different cell lines [77]. Nevertheless, the role of these cytokines in CC-related skeletal muscle mitochondrial dysfunction was not yet demonstrated.

In overall, despite being the most powerful intracellular source of ROS, mitochondria are also a primary target for the oxidative damage. The biomolecules that are

particularly susceptibility to ROS include lipids, proteins from the oxidative phosphorylation and mtDNA. The oxidative modification of these molecules leads to impaired function of mitochondria and impacts cell viability [65, 66]. Thus, it seems particularly important to explore the structural changes promoted by ROS in mitochondrial biomolecules and their relevance in wasted muscle.

### 3.1.1. Biomolecular alterations underlying muscle wasting-related mitochondrial dysfunction

Among the main targets of ROS in mitochondria are the membrane lipids, the OXPHOS complexes proteins from metabolic pathways, and mtDNA (**Figure 4**) [61, 78].

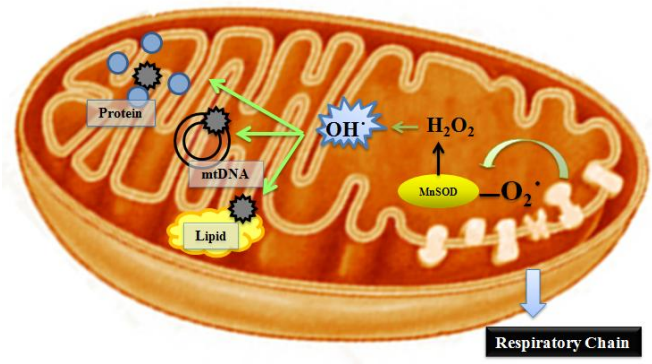


**Figure 4:** Sources of reactive oxygen species and their main targets of reactive oxygen species [adapted from 78].

Membrane phospholipids are essential for mitochondria integrity and functionality since they can impact electron transport chain activity, mitochondrial protein import, membrane fluidity and permeability, and ultimately ATP synthesis [79]. Given the nearly absent variation in the mitochondrial phospholipid composition among different cells is supposed that great changes cannot be tolerated. Indeed, alterations in phospholipid content and also phospholipid damage have been linked to several pathological disorders [80]. The main phospholipid targets of peroxidation are not fully defined [81]. However, mitochondrial lipid peroxidation products led to impaired barrier function of membranes by interacting with proteins and/or with the lipid moieties of the membrane [82]. It is well

known that the anionic phospholipid cardiolipin (**CL**) has been suggested as a particularly susceptible PL in mitochondria [83, 84]. Lipids with a high degree of unsaturation are more susceptible to oxidation and cardiolipin contains a higher ratio of unsaturated to saturated fatty acid residues compared with the other phospholipids of the inner mitochondrial membrane [65]. In fact, loss of CL content is the most commonly reported pathological alteration of the CL profile. A selective loss of CL content could occur due to CL degradation, decreased CL synthesis resulting from impaired function of enzymes involved or decreased availability of CL precursors such as phosphatidylglycerol [80]. This CL loss, together with alterations in its acyl chain composition and/or CL peroxidation have been associated with mitochondria dysfunction, being responsible for alterations in the stability of mitochondrial membranes, increased permeability and decreased mitochondrial respiratory rate [80, 85]. Indeed, disorders underlying mitochondrial dysfunction associated with the inhibition of catalytic activity due to the loss of CL have been described for both complexes III and IV [80]. The identification and characterization of oxidized cardiolipin was also achieved using a combination of thin layer chromatography and electrospray ionization/mass spectrometry (ESI-MS) [84, 86]. Though in low levels in the inner membrane of mitochondria, phosphatidylglycerol (PG) accumulates in mitochondria when CL synthesis is decreased, partially compensating some functions of CL [87]. Moreover, similarly to CL, PG also seems to affect electron transfer efficiency and mitochondrial respiratory rate since its proximity to $O_2$ transfer pathway and PG's contribution in the stabilization of the complex IV [88].

Besides, injury to mitochondria induced by lipid peroxidation can lead to additional ROS production and be associated with mitochondrial dysfunction [81]. Regarding this lipid-oxidative damage, the uncoupling protein UCP-3 has been proposed to be involved in the protection of lipids from oxidative damage [89]. In fact, uncoupling of mitochondrial respiratory chain is related to decreased ROS production [90].

The oxidative damage of proteins generally leads to its loss of function [66]. Free radicals can directly induce the detachment of the pro-apoptotic factor cytochrome c from the inner mitochondrial membrane into the cytosol [91]. Indeed, mitochondrially-generated ROS has been shown to decrease the content of cardiolipin in the membrane, which interaction is required for cytochrome c attachment and an efficient respiratory activity [80, 85]. This release interrupts the transfer of electrons between ETC complexes III and IV, leading to

radical species production that could accelerate apoptotic processes [92]. In fact, the release of cytochrome c from mitochondria activates the cytoplasmatic proteases known as caspases. This process is regulated by Bax/Bcl-2 family proteins [93, 94]. In healthy cells, the major part of the pro-apoptotic Bax is located in the cytosol, although under apoptotic signaling this protein is transferred to outer mitochondrial membrane. An imbalance in this shift results in the consequent release of cytochrome c and other pro-apoptotic factors from mitochondria, the so-called mitochondrial outer permeabilization [95]. Oxidative damage to proteins may be caused by reactions of amino acid residues with ROS with the introduction of carbonyl groups in some residues, namely in lysine, arginine, proline, and threonine [66, 96, 97], and loss of thiol groups [66]. Carbonyl groups could be inserted into proteins by secondary reaction of the nucleophilic side chains of cysteine, histidine and lysine residues, with aldehydes produced during lipid peroxidation or with reactive carbonyl derivatives generated as a consequence of the reaction of reducing sugars, or their oxidation products with lysine residues of proteins. Hence, the presence of carbonyls is not necessarily indicative of oxidation of amino acid residues in proteins [97]. The insert of these groups may lead to inter- and intramolecular cross-links with protein amino groups and trigger loss of function. Therefore, accumulation of protein oxidation products in mitochondria may lead to loss of energy production and concomitant increased production of oxidants such as $O_2^{\bullet-}$ and $H_2O_2$, potentiating mitochondrial dysfunction [65]. These modifications can also increase the susceptibility to proteolytic degradation since oxidized proteins are more easily targeted by the UPP, which is up-regulated by ROS [66, 98]. The detection of oxidatively modified proteins has been performed by immunoblotting using antibodies specific for these modifications, and subsequently identified by mass spectrometry [63, 97, 99]. Mitochondrial proteins from OXPHOS complexes I-V are particularly susceptibility to oxidation by carbonylation processes [100]. These carbonylated proteins were targeted by affinity chromatography-stable isotope labeling and were then identified by tandem mass spectrometry (MS/MS). Carbonylation of fatty acid binding proteins was also found, suggesting a possible decrease in fatty acid metabolism. Proteins involved in the citrate cycle also seem prone to carbonylation [101].

In addition to lipids and proteins, mtDNA is particularly susceptible to oxidation. Mitochondrial DNA is a double-stranded ring encoding 24 genes involved in local mitochondrial protein synthesis and 13 essential protein subunits of the OXPHOS

complexes I, III, IV and V [56, 102]. The close proximity to the electron transport chain, the lack of protective histones and the impaired DNA repair activity make mtDNA extremely susceptible to ROS [65, 66], which damage leads to mitochondrial dysfunction with the consequent loss of cell energy [65, 103]. This damage can occur by an indirect mechanism or by direct interaction with hydroxyl radical (**$OH^{\bullet}$**). Indirect mechanism involves the peroxides through oxidation of SH groups of $Ca^{2+}$ channels in the endoplasmic reticulum, which increases intracellular calcium and stimulates $Ca^{2+}$ - dependent endonucleases and ultimately leading to incorrect DNA fragmentations. $OH^{\bullet}$ causes modification of bases leading to DNA strand breakdown during replication and pairing errors [66]. The accumulation of mutations in the mtDNA can lead to alterations in cell-signaling pathways, which in turn can induce cell dysfunction and apoptosis [66]. Several studies have suggested an association between mtDNA mutations and a decreased activity of complexes I and IV, particularly in long-lived postmitotic cells such as cardiomyocytes, skeletal muscle fibers, and neurons [65, 66, 104, 105]. Evidences shown decreased complexes I, III and IV activities associated with damage to mtDNA in mitochondria isolated from the *gastrocnemius* muscle of aging mice [106, 107]. Furthermore, alterations were not verified in complex II, which has no mtDNA coded component [106, 108]. However, *in situ* hybridization experiments indicate a strong association between mtDNA deletions and complexes II and IV abnormalities in old *rhesus* monkeys with senescent loss of skeletal muscle [109, 110]. These mtDNA deletions have been demonstrated to be tissue-specific, being more pronounced in the skeletal muscle and heart [111].

### 3.2. Mitochondrial phospholipid profile in wasted muscle

The mitochondrial membrane phospholipids regulate mitochondrial activity of the ETC, mitochondrial protein import and ATP synthesis [81, 112], which are known to be impaired in wasted conditions [21, 71, 100]. Changes in mitochondrial lipid-lipid and lipid-protein interactions impacts integrity, fluidity and permeability of this organelle, leading to its dysfunction [81, 113, 114].

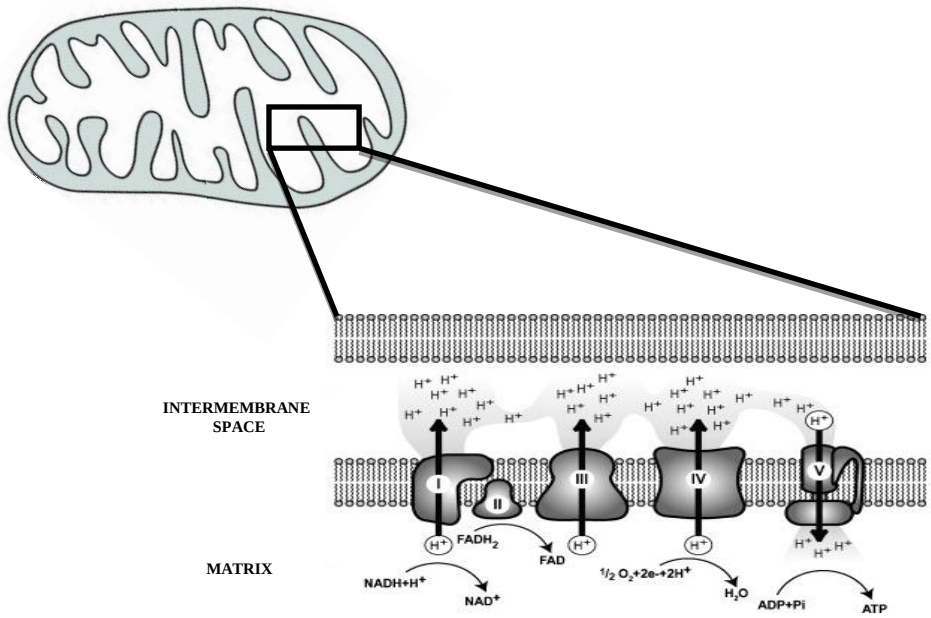


**Figure 5:** Mitochondrial electron transport chain. Complex I (NADH dehydrogenase); complex II (succinate dehydrogenase); complex III (ubiquinone cytochrome c oxireductase); complex IV (cytochrome oxidase), complex V (ATP synthase) [adapted from 112, 115].

Among phospholipids, phosphatidylcholine (**PC**), phosphatidylethanolamine (**PE**) and cardiolipin are the most abundant phospholipids in mitochondria [67]. Cardiolipin is a complex phospholipid that is specific of the inner mitochondrial membrane, and is not found in other subcellular membranes [80, 116]. PC, PE and CL are glycerophospholipids, also called phospholipids synthesized from the universal precursor phosphatidic acid (**PA**) [117, 118]. The glycerophospholipids have a role in cell structure and are involved in cell signaling and cell proliferation, thus they have been considered as potential biomarkers for several diseases[80]. Phospholipids usually consist of a glycerol backbone to which are attached two fatty acids (*sn*-1 and *sn*-2 acyl chains) and a phosphate group [117]. The phosphate group can bind to a polar molecule by phosphodiester bonds, forming the head group of phospholipid (**Figure 6**) [117]. The different combinations of length, degree of unsaturation of acyl chains and the constitution of the polar head group, makes phospholipids a groupwhich is divided in several distinct classes depending on the group of the polar head. Each phospholipid class has different combinations of fatty acids attached to glycerol (**Figure 6**) [119, 120].

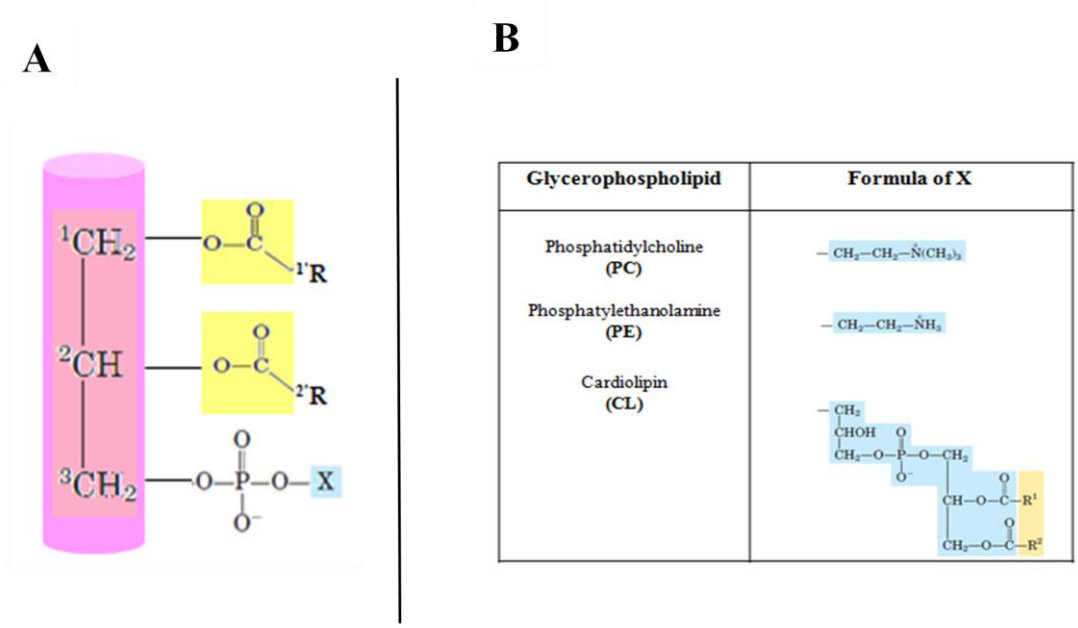


**Figure 6:** General structure of glycerophospholipids (A) and of PC, PE and CL (B). R1, R2, R1' and R2' represent the fatty acyl chains esterified to glycerol backbone. PC – Phosphatidylcholine, PE – Phosphatylethanolamine, CL – Cardiolipin [adapted from 120].

Mitochondria can synthesize several acidic phospholipids autonomously, including phosphatidic acid (PA), cytidine diphosphate-diacylglycerol (**CDP-DAG**), phosphatidylglycerol (**PG**), and cardiolipin. In contrast, phosphatidylcholine (PC), phosphatidylserine (**PS**), phosphatidylinositol (**PI**), and sterols are synthesized in other organelles and transported to mitochondria. CDP-DAG is an important PA derived since is utilized for the synthesis of PE and PC. Imported phosphatidylserine is rapidly decarboxylated within the mitochondrion to form PE [116].

CL is a dimeric and negatively charged phospholipid that may be involved in protein import into mitochondria though interaction with positively charged signal sequences of precursor proteins [28]. This phospholipid has four acyl side chains attached to two glycerol molecules, in contrast to the typical lipids with two acyl chains and one glycerol backbone [80, 117]. Several studies have analyzed the fatty acids composition of CL in different tissues and 18:2 and 18:1 are the most abundant ones in rat heart, liver, kidney and skeletal muscle [121]. Moreover, it has been shown that the membranes containing CL with unsaturated fatty acyl chains, are linked to cytochrome c with higher binding affinity than those containing saturated CL [85]. CL is synthesized from PA via

several enzymatic steps common with other phospholipids [80, 117]. The biosynthesis of the phosphatidic acid occurs in the endoplasmatic reticulum and in the outer mitochondrial membrane [117]. The mitochondrial inner membrane contains all the enzymes of the CL pathway, namely those responsible for the formation of phosphatidic acid from acyl-CoA fatty acid and glycerol 3-phosphate, production of phosphatidyl-CMP, its transfer to another glycerol 3-phosphate and consequent hydrolysis of the latter yielding phosphatidylglycerol. The final reaction of this pathway whereby PG is combined with CDP-diacylglycerol to yield CL is catalysed by CL synthase (**Figure 7**) [117, 122].

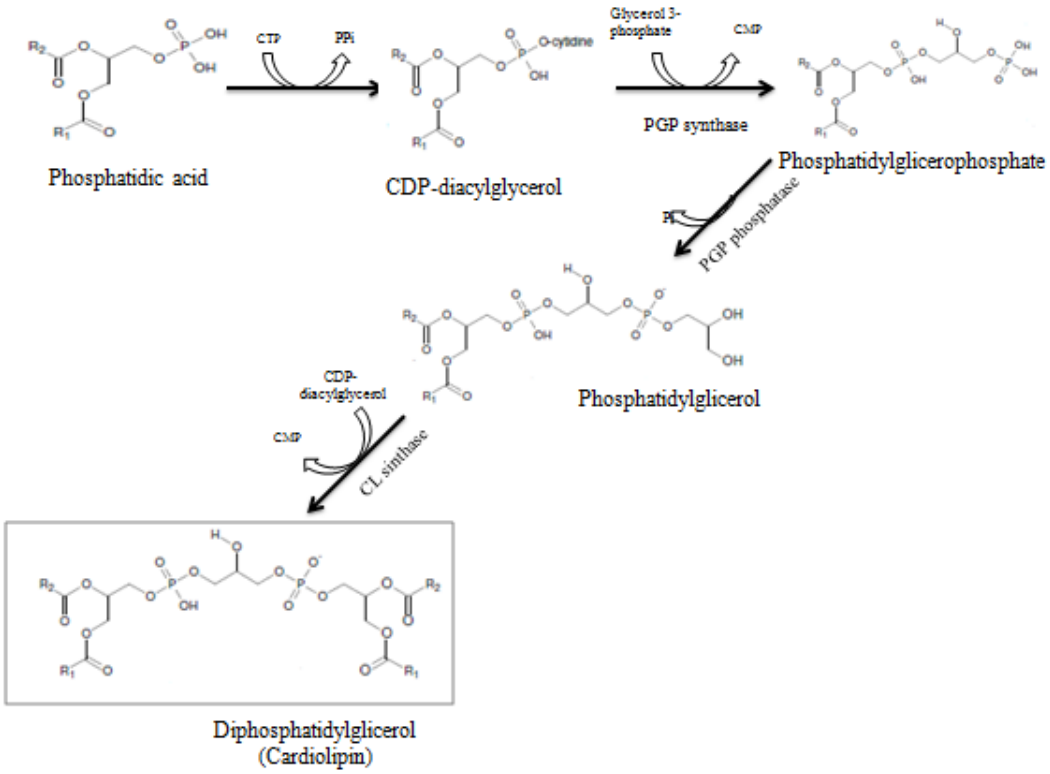


**Figure 7:** Pathway of cardiolipin (CL) biosynthesis [adapted from 117].

PC, PE and CL have different saturated and unsaturated fatty acid, and therefore with different susceptibilities to oxidation, which increases exponentially as a function of the number of double bonds *per* fatty acid [123]. In fact, the major phospholipid components of the mitochondrial membranes are rich in unsaturated fatty acids and consequently are susceptible to oxygen radical attack because of the presence of double bounds, which can undergo peroxidation through a chain of oxidative reactions [124].

Cardiolipin is particularly susceptible to oxidation by reactive oxygen species (**ROS**) due to the presence of the unsaturated fatty acyl chains linoleic acid or docosahexanoic acid, and also due to its close association with electron transport chain [80, 124]. In fact, the loss of CL has been attenuated by quenching or preventing the production of mitochondrial ROS in skeletal muscle [80], suggesting an association between the mitochondrial dysfunction and lipid peroxidation in skeletal muscle.

One of the most reactive ROS responsible for lipid peroxidation is $OH^{\bullet}$. Lipid peroxidation by the $OH^{\bullet}$is initiated by the suptake of one hydrogen atom from an allylic position, leading to the production of alkyl radicals ($R^{\bullet}$). This modification promotes the reorganization of the adjacent double bonds culminating in the production of other alkyl radicals, with formation of distinct intermediates with the radical species located in different positions of the fatty acyl chain. The alkyl radicals will react with oxygen leading to the formation of peroxyl radicals ($ROO^{\bullet}$), which in turn produce one lipid hydroperoxide (ROOH) by acquiring one hydrogen atom. This lipid hydroperoxide can undergo other reactions leading to several oxidation products with different structures such as hydroxyl, hydroperoxi, epoxy and poly-hydroxy derivatives usually named long-chain oxidations products. Besides the decomposition of the lipid hydroperoxides may lead to the formation of the alkoxyl radicals which may undergo posterior beta cleavage of the fatty acyl chain with formation of oxidation products with shortened fatty acyl chain that included dicarboxylic acids, aldehydes and hydroxyaldehydes, usually named short-chain products (**Figure 8**) [125-128].

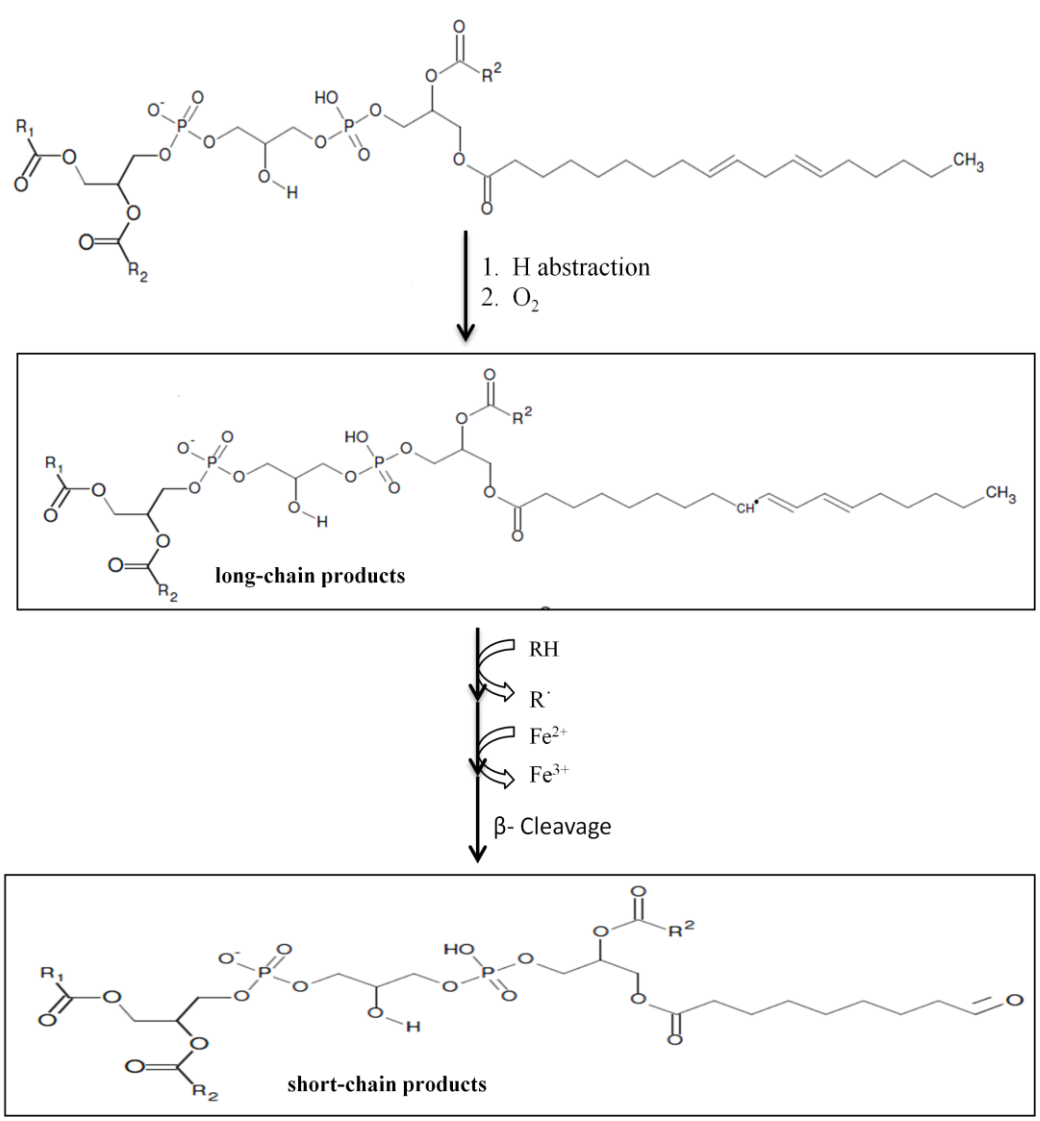


**Figure 8:** Generation of the long chain and short chain oxidation products by radical oxidation [adapted from 128].

The peroxidation products are responsible for the loss of structural and functional characteristics of the membrane due to the increase the polarity of phospholipids and consequently decreasing the fluidity and increasing membrane permeability, or even cause disruption of the membrane integrity [81, 113, 129].

Mass Spectrometry (MS) has been used to identify and analyze phospholipids [79, 83, 119]. Several studies have been performed in order to identify non-oxidized glycerophospholipids and the products derived from its oxidation [130, 131]. The products observed in MS/MS of oxidized phospholipids allows the identification of changes in fatty

acyl chain and specific characteristics such as presence of new functional groups in the molecule and its localization in the hydrocarbon chain [130]. The different oxidation products may be responsible for distinct biological effects thus increasing the relevance of identifying each specific oxidation product in order to understand their specific biological significance and effects [117].

Several studies concerning lipid alterations underlying pathological conditions were carried out by MS. Many researchers used lipidomic approaches for the study of phospholipids and their oxidation products in diverse injuries such as traumatic brain injury [83, 130]; in models of γ-radiation-induced [132, 133] or induced pro-apoptotic and pro-inflammatory stimuli [134]; in the study of cardiolipin loss and/or oxidation [80], among others.

Glycerophosphocholines (PC) are the most studied class of oxidized phospholipids by electrospray ionization mass spectrometry (ESI-MS) and oxidized products have been identified by MS in biological fluids and tissues [125, 128]. Saturated and unsaturated short-chain products containing terminal aldehyde and carboxylic groups were identified, some of which substituted with hydroxyl, keto and hydroperoxide groups, derived from the oxidation of diacylphosphatidylcholine *in vitro,* generated under Fenton reaction conditions ($H_2O_2$ and $Fe^{2+}$) [125]. Reversed-phase liquid chromatography–mass spectrometry (LC-MS) also allowed the identification of these oxidation products [127].

Cardiolipin is a phospholipid that has been reported, in several studies, to be oxidized either *in vitro* and *in vivo* conditions [83, 86, 134]. Since CL is a mitochondria-specific phospholipid and is critical for maintaining the integrity and function of membrane and osmotic stability, any disturbance of the CL profile leads to functional impairment. Indeed, loss of CL content, alterations of CL fatty acyl profile or increased CL peroxidation, have been correlated with mitochondrial dysfunction in several tissues in a variety of pathological conditions [80]. CL is associated with many mitochondrial proteins, namely the respiratory chain complexes I, III, IV, and V, the carrier family (ADP–ATP-carrier, phosphate carrier, uncoupling protein), and peripheral membrane proteins such as cytochrome *c* and creatine kinase [80, 85, 135]. In fact, cytochrome c requires an electrostatic interaction to CL for successful electron transfer from reduced cytochrome c to molecular oxygen [80, 85, 123]. Therefore, the oxidized molecular species of CL derived from lipid peroxidation contributes to the permeabilization of the mitochondrial membrane, the release of cytochrome c and other pro-apoptotic factors into the cytosol [80,

136, 137] and compromises the activity of mitochondrial respiratory enzymes [80]. Moreover, CL levels have been found increased in the outer mitochondrial membrane during apoptosis [88]. Few data exist concerning evaluation of CL profiling in cancer cachexia (CC). Alterations in CL were found in brown adipose tissue from rats with CC [138]. A significant CL content increase (+55%) was also observed in liver mitochondria during CC [139].

Regarding CL oxidation, Bayir *et al.* [83] identified hydroxy and hydroxyl-hydroperoxy derivatives using ESI-MS in mitochondria of rat brain after traumatic brain injury. Tyurina *et al.* [133] also verified hydroxy and hydroxyl-hydroperoxy derivatives by ESI-MS for CL in γ-radiation-induced lung injury. An *in vitro* study performed with MALDI-TOF-MS and thin-layer chromatography identified phosphatidic acid and dyacilphosphatidyl-hydroxyacetone as oxidation products of CL induced by lipossomes γ-radiation and were generated from cleavage on central glycerol molecule [132].

Maciel *et al.* [140] identified new short chain products resulted from β-cleavage of alkoxyl radicals at C9 and C13 of cardiolipin oxidation, in nephrotoxic disturbances induced by an aminoglycoside antibiotic associated with mitochondrial dysfunction and lipid peroxidation in rat kidney tissue. Tyurin *et al.* [134] identified CL hydroperoxides accumulated in apoptotic cells and mouse lung of C57BL/6 mice after pro-apoptotic and pro-inflammatory stimuli, similarly to that observed for PS.

Oxidation of CL have been correlated with Cyt c release to the cytosol and the externalization of PS in apoptotic cells. In fact, the interaction of cytochrome c with oxidized phosphatidylserine (PS) has also been related with its migration across the cell membrane. Similarly to CL/cyt c interactions in mitochondria, the formation of PS/cyt c complexes in the cytosol leads to oxidized PS, which seems to be essential for the transduction of apoptotic signals [85]. Bayir *et al.* [83] also proposed the presence signaling role of PS hydroperoxides derivatives in traumatic brain injury. PS hydroperoxides were also identified by ESI-MS in cells and tissues under inflammatory/oxidative stress conditions [134]. An oxidative lipidomic analysis of γ-radiation-induced lung injury allowed to verify an non-random oxidation of phospholipids, with identification of hydroxy and hydroxyl-hydroperoxy derivatives by of PS while more abundant PLs, such as PC and PE, remained non-oxidized [133].

Concerning the phosphatidylethanolamine oxidative products, few studies are known. A study relying on three different oxidation systems and using multiple reaction

monitoring identified short-chain products with terminal aldehyde and carboxylic derived from phosphatidylethanolamines derivatives. The systems used were autoxidation in presence of Cu (II), UV radiation and myeloperoxidase (MPO) [136].

## 4. Aims of this thesis

In order to better elucidate the molecular mechanisms underlying cancer-related skeletal muscle wasting, the aims of the present study were to:

i) Evaluate how bladder cancer-induced cachexia affects mitochondrial OXPHOS activity and susceptibility to oxidative damage and/or apoptosis;

ii) Characterize the impact of bladder-cancer related cachexia on mitochondrial lipid profile of *gastrocnemius* muscle;

iii) Evaluate how mitochondrial lipidome profile relates to alterations in mitochondrial OXPHOS functionality and proteins suggestive to susceptibility to apoptosis;

Data integration will allow a better understanding of bladder cancer-induced muscle wasting pathogenesis and will ideally give clues for the development of strategies to counteract muscle wasting in oncologic patients.

# CHAPTER II

# Material and Methods

# II. Material and Methods

## 1. Experimental Design

In order to achieve the proposed aims for this study, the experimental approach shown in Figure 9 was performed. Briefly, 23 Wistar rats, randomly divided in two groups: animals with bladder cancer induced by the exposition to N-butyl-N-(4-hydroxybutyl)-nitrosamine in the drinking water for 20 weeks (BBN, n=13) and healthy animals (CONT, n=10). After 28 weeks of the beginning of the protocol, all animals were sacrificed and *gastrocnemius* dissected out for mitochondria isolation with recourse to sequential steps of enzymatic digestion, mechanical disruption and differential centrifugation. The mitochondrial fractions were used for OXPHOS activity assessment, lipidomic characterization and the analysis of protein targets using western blotting. The experimental groups and methodological approaches used are described in the following sections.

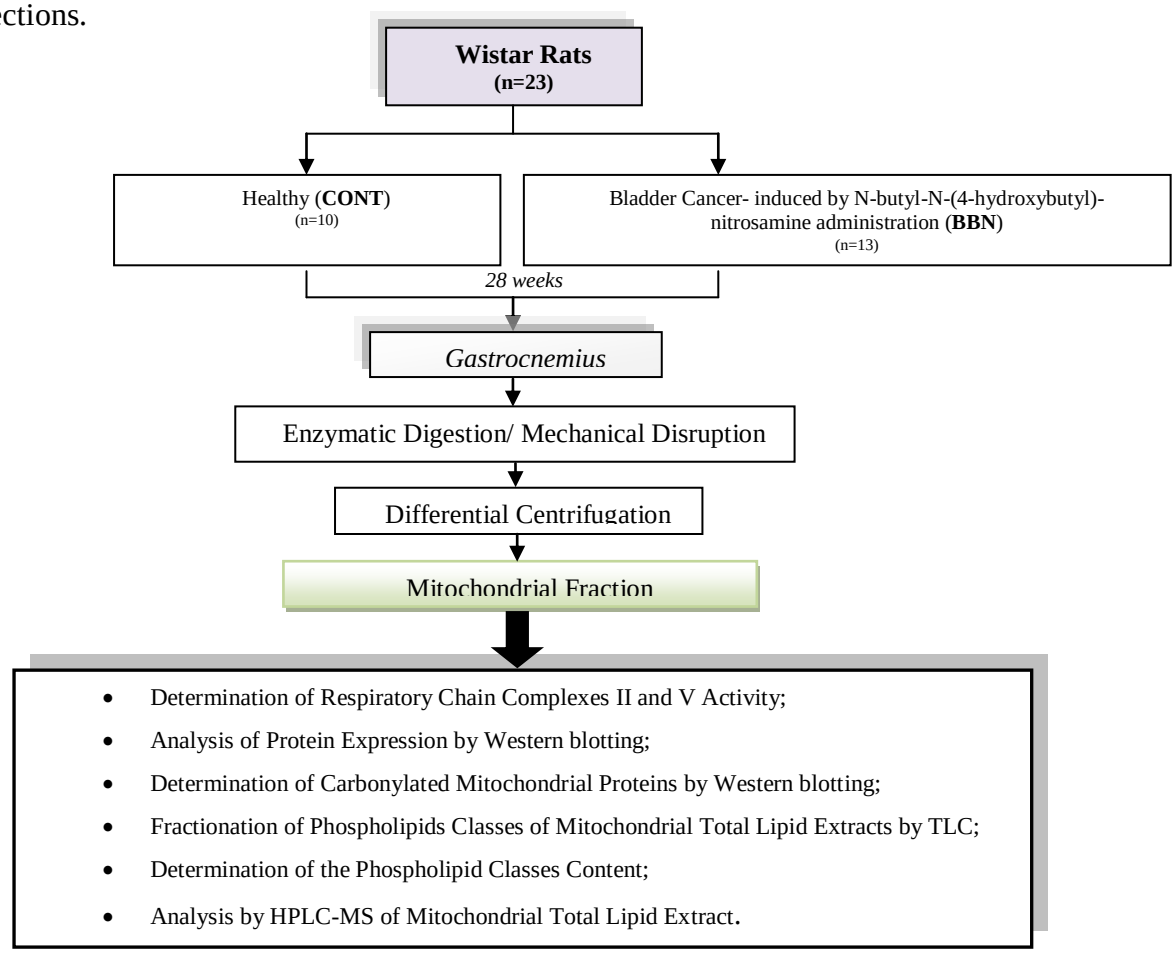


**Figure 9:** Scheme of the methodological procedures used in the analysis of different biochemical parameters in *gastrocnemius* muscle of rats with bladder cancer-related cachexia and controls.

## 2. Chemicals

*N*-butyl-*N*-(4-hydroxybutyl)-nitrosamine (BBN) was purchased from Tokyo Kasey Kogyo (Japan). All other reagents and chemicals used were of highest grade of purity commercially available. Rabbit polyclonal anti-ETFDH antibody (cat. no. Abcam ab91508), rabbit polyclonal anti-ETFβ antibody (cat. no. ab73986), mouse monoclonal anti-ATPβ antibody (cat. no. ab14730), rabbit polyclonal anti-UCP-3 antibody (cat. no. ab3477) were acquired from Abcam (Cambridge, UK). Mouse monoclonal anti-cytochrome c antibody (cat. no. BD556433) was obtained from BD Biosciences (Pahrmingen). Mouse monoclonal anti-Bcl-2 antibody (cat. no. sc-7382) and rabbit polyclonal anti-Bax antibody (cat. no. sc-493) were acquired from Santa Cruz Biotechnology, INC. (CA, USA). Rabbit polyclonal anti-DNP antibody was obtained from DakoCytomation (Hamburg; Germany). Secondary peroxidase-conjugated antibodies (anti-mouse IgG and anti-rabbit IgG) were obtained from GE Healthcare (Buckinghamshire, UK). The lysophosphatdylcholine (LPC), phosphatidic acid (PA), phosphatidylcholine (PC), phosphatidylethanolamine (PE), phosphatidylglycrol (PG), phosphatidylinositol (PI), phosphatidylserine (PS), sphingomyelin (SM), and cardiolipin (CL) standards were purchased from Sigma-Aldrich (Madrid, Spain), triethylamine (AcrosOrganics), chloroform (HPLC grades), methanol (HPLC grades), ethanol (Panreac), primuline (Sigma), purified milli-Q water (Millipore, USA). All the reagents were used without further purification. TLC silica gel 60 plates with concentration zone (2.5x20cm) were purchased from Merck (Darmstadt, Germany).

## 3. Animal Protocol

The animal protocol was accomplished using twenty three female *Wistar* rats. The animals were obtained at the age of 5 weeks from Harlan (Barcelona, Spain). The rats were used in this study after a week of acclimatization. During the experimental protocol, animals were housed in groups of 4 rats/cage, in a controlled environment at a room temperature of 22±3ºC and 60±10% of relative humidity with 12:12h light-dark cycle, with free access to food and water. The animals were randomly divided into two groups: control group (CONT; n=10 rats) and urothelial carcinogenesis group (BBN; n=13

rats). The following protocol was approved by *the Portuguese Ethics Committee for Animal Experimentation*.

In order to induce urothelial carcinogenesis, one group of animals was treated with N-butyl-N-(4-hydroxybutyl)-nitrosamine (BBN group), which was administered in the drinking water, in light impermeable bottles, at a concentration of 0.05%. No chemical supplementation was added to the drinking water of control animals. The urothelial carcinogenesis group was exposed to BBN for 20 weeks and was maintained with normal tap water until the end of the experiment. After 28 weeks of the beginning of the protocol, all animals were sacrificed with 0.4 % sodium pentobarbital (1 mL/Kg, intraperitoneal), blood was collected from heart. The urinary bladders were inflated *in situ* by injection of 10% phosphate-buffered formalin (300 mL), ligated around the neck to maintain proper distension and then were immersed in the same solution for 12 h. After fixation, the formalin was removed; the urinary bladder was weighed and cut into four strips and was routinely processed for haematoxylin and eosin staining.

### 4. Mitochondria Isolation from *Gastrocnemius* Muscle

The *gastrocnemius* muscles were extracted during animals' sacrifice for the preparation of isolated mitochondria, as previously described [141] with some alterations. All the procedures were performed on ice or below 4ºC. Briefly, muscles were washed three times with 20mM MOPS, 110 mM KCl, 1 mM EGTA, pH 7.5. The blood-free tissue was minced with scissors and then incubated in the before mentioned buffer with 0.25 mg/mL trypsin (Promega, Wisconsin, USA). After 25 min on ice, albumin fat-free (Sigma, St. Louis, MO, USA) was added to a final concentration of 10 mg/mL. The tissue was subsequently rinsed three times with buffer and then homogenized with a Potter homogenizer (Teflon pestle). The homogenate was centrifuged at 14.500 g for 10 min. The resulting pellet was re-suspendend with 20 mM MOPS, 110 mM KCl, 1 mM EGTA, pH 7.5. The resulting suspension was centrifuged at 750 g for 10 min, and the resulting supernatant was centrifuged at 12.500 g for 10 min. The mitochondrial pellet was re-suspending in a small volume of buffer (250mM sucrose, 10 mM Tris–HCl, 0.1 mM EGTA, pH 7.4), and it was stored at -80 ºC for further use.

## 5. Determination of Total Protein Concentration by DC assay

The amount of total protein was determined in mitochondrial fractions by the DC protein assay (Bio-Rad, Hercules, CA, USA), based in Lowry *et al.* [142]. Briefly, 20 µl of S reagent from the Bio-Rad kit was added to 1 ml of A reagent (to make A´ reagent). Then, 50 µl of A´reagent and 400 µl of B reagent was added to 5 µl of sample and incubated at room temperature for 15 min. Standard solutions of bovine serum albumin (BSA) between 0.16 to 10 mg/ml were prepared and treated in parallel with the samples. At last, the absorbance of all the samples was measured at 750 nm in a microplate reader (Multiscan 90, ThermoScientific).

## 6. Determination of Respiratory Chain Complexes II and V Activities

The respiratory chain complexes II and V activities were determined spectrophotometrically after disruption of mitochondrial fractions by a combination of freeze-thawing cycles in hypotonic media (25 mM potassium phosphate, pH 7.2). Complex II activity was determined according to Birch-Machin *et al.* [143]. Briefly, mitochondria were pre-incubated with 25mM potassium phosphate buffer, pH 7.2, 5mM $MgCl_2$ and succinate at 30ºC for 10 min. Antimycin A (2 µg/mL), rotenone (2 µg/mL), 2mM KCN and 50 µM of DCIP were added and the absorbance variation was measured at 600 nm for 3 min. Then, 65µM of ubiquinone was added and a new determination at 600 nm for 3 min was performed. ATP synthase activity was measured according to Simon *et al.* [144]. The phosphate produced by hydrolysis of ATP reacts with ammonium molybdate in the presence of reducing agents to form a blue-color complex, the intensity of which is proportional to the concentration of phosphate in solution. This reaction was carried out by incubation with a test solution (3.3g of ammonium molibdate, ferrous sulfate (4 g/500 mL), 0.37M of sulfuric acid) for 15 min, followed by measure of absorbance at 610 nm. Oligomycin was used as an inhibitor of mitochondrial ATPase activity. Standards of inorganic phosphate were performed to measure the released phosphate in the ATP hydrolysis. The absorbance was determined using a microplate reader (Multiscan 90, ThermoScientific).

## 7. Analysis of Protein Expression by Western blotting

In order to evaluate the expression of mitochondrial proteins, these was separated according to their molecular weight on polyacrylamide gels in denaturing and reducing conditions, by applying an electric current of 200 V. A given sample sample corresponding to 20 μg of protein was loaded on a 12.5% or 15% SDS-PAGE, prepared according to Laemmli [145]. After separation, proteins were transferred to a nitrocellulose membrane (Millipore® 0.45 μm of porosity) by electroblotting at 200 mA for 2 h in transfer buffer (25 mM Tris, 192 mM glycine, 20% methanol). To avoid non-specific binding the nitrocellulose membrane was blocked in a solution of 5% (w/v) nonfat dry milk in TBS-T (100 mM Tris pH 8.0, 150 mM NaCl and 0.05% Tween 20) for 1 h at room temperature. The membrane was then incubated with primary antibody diluted 1:1000 in blocking solution (anti-ETFDH, anti-ETFβ, anti-ATPβ, anti-UCP3, anti-Bcl-2, anti-Bax or anti-cytochrome c) for 2 h at room temperature or overnight at 4ºC. After three washes with TBS-T the membrane was incubated with secondary antibody horseradish peroxidase-conjugated anti-rabbit or anti-mouse for 1 h at room temperature. The membrane was washed three new times with TBS-T and the blots were developed using chemiluminescence ECL reagents (Amersham Pharmacia Biotech®) according to the manufacturer's instructions, followed by exposure to X-ray films (Kodak Biomax Light Film, Sigma®). Films were scanned using a Gel Doc XR + System (Bio-Rad®) and bands intensity quantified with the QuantityOne imaging software (version 4.6.3, Bio-Rad®).

## 8. Determination of Carbonylated Mitochondrial Proteins by Western Blotting

Carbonylated proteins were assayed according to Robinson *et al.* [99]. Briefly, a given volume (V) of sample containing 20 μg of protein was derivatized with 2,4-dinitrophenylhydrazine (DNPH). The sample was mixed with 1 V of 12 % SDS plus 2 V of 20 mM DNPH/10% TFA, followed by 30 minutes incubation in dark. After the incubation period 1.5 V of 2 M Tris-base/18.3% of β-mercaptoethanol was added for neutralization. The derivatized proteins were applied in a 12.5 % SDS-PAGE, prepared according to Laemmli [145]. After separation by molecular weight, proteins were transferred for a nitrocellulose membrane blots, blocked with 5% (w/v) nonfat dry milk in TBS-T for 1 h and then incubated for 2 h at room temperature with rabbit anti-DNP

antibody diluted 1:5000 in blocking solution. After three washes with TBS-T the membrane was incubated for 2 h at room temperature with secondary antibody horseradish peroxidase-conjugated anti-rabbit diluted 1:1000 in blocking solution. The membrane was washed three new times with TBS-T and detection was carried out with chemiluminescence ECL reagents (Amersham Pharmacia Biotech®) according to the manufacturer's instructions. Then, the membrane was exposed to X-ray films (Kodak Biomax Light Film, Sigma®). Films were scanned using a Gel Doc XR + System (Bio-Rad®) and bands intensity quantified by QuantityOne imaging software (version 4.6.3, Bio-Rad®).

## 9. Determination of Mitochondria Lipid Peroxidation levels

Lipid peroxidation was assayed spectrophotometrically in mitochondrial fractions according to Bertholf *et al.* [146] by measuring the formation of thiobarbituric acid reactive substances (TBARS). So, to sample aliquots of 75 µL was added 150 µL of TCA 10% followed by vortex and centrifugation for 5 min at 15000 rpm. To 125 µL of the resulting supernatant, 125 µL of TBA 1% was added. The color reaction was developed by incubating the mixtures at 100 ºC for 10 min. Finally, TBARS levels were measured at 540 nm using a microplate reader (Multiscan 90, ThermoScientific).

## 10. Phospholipids Extraction

Total lipid content, including phospholipids were extracted from the mitochondrial fractions using the Bligh and Dyer method [147]. Briefly, 3.75 mL of chloroform:methanol 1:2 (v/v) was added to 1mL of *gastrocnemius* mitochondrial fraction (corresponding approximately to 8 mg of protein), well -vortexed and incubated on ice for 30 min. Then, 1.25 mL of chloroform and 1.25 mL of mili-Q $H_2O$ were added. After vortexed well, the mixture was centrifuged at 1000 rpm for 5 min at room temperature to obtain a two-phase system: the aqueous phase on top and the organic phase below from which lipids were obtained. At last, the extracts were dried in a nitrogen flow, re-suspended in 300 µL of chloroform and stored at -20 ºC for subsequent analysis.

## 11. Quantification of Phospholipids by Phosphorous Assay

The total content in phospholipids of the total lipid extract, as well as the amounts of each phospholipid class present in each spot separated by TLC, were determined by a phosphorous quantification method according to Bartlett and Lewis [148]. To quantify the total PL extract, 10 µL of the total lipid extract were transferred to a glass tube and dried under a nitrogen flow. To quantify the different classes separated by TLC, the spots were scraped off from the plates directly to glass tubes for quantification. Then, 650 µL of perchloric acid (70%, w/v) was added to the samples, which were then incubated at 180 ºC for 1h in a heating block (Stuart, U.K.). To all tubes were added 3.3 mL of mili-Q $H_2O$, 0.5 mL of ammonium molibdate (2.5g ammonium molibdate/100 mL of $H_2O$) and 0.5 mL of ascorbic acid (10g ascorbic acid/100 mL of $H_2O$) and vortexed well after the addition of each solution, followed by incubation in a water bath at 100 ºC for 5 min. Standards from 0.1 to 2 µg of phosphate underwent the same sample treatment. Samples from TLC were centrifuged at 4000 rpm for 5 min to separate PLs from silica. Finally, the absorbance of standards and samples was measured at 800 nm, in a microplate reader (Multiscan 90, ThermoScientific). The relative content of each PL class was calculated by relating the amount of PL in each spot to the total amount of PLs in the sample.

## 12. Separation of Phospholipids Classes by Thin-Layer Chromatography (TLC)

Phospholipids classes from the total lipid extract were separated by thin-layer chromatography (TLC) using plates of silica gel 60 with concentration zone 2.5 x 20 cm. Prior to separation the silica plates were washed with a solution of chloroform: methanol (1:1 v/v) and dried in the hotte for 15 min. Then, plates were sprayed with a solution of boric acid in ethanol (2.3% w/v) and dried in an oven at 100 ºC for 15 min. Then, twenty µL of sample of total lipid extract was applied in the TLC. The spots on TLC were dried in nitrogen flow and developed in solvent mixture with chloroform/ethanol/water/triethylamine (30:35:7:35, v/v/v/v). After complete elution, and after eluent evaporation, the TLC plates were sprinkle with a primuline solution (50 µg/100 mL acetone:water, 80:20, v/v), and visualized with a UV lamp (λ=254 nm). Identification of the different classes of PLs was carried out by comparison with phospholipids standards.

For further analysis, the spots were scraped off from the plates, and the phospholipids present in each spot were quantified using the phosphorous assay. The percentage of each PL class was calculated, relating the amount of phosphorus in each spot to the total amount of phosphorus in the sample, thus giving the relative abundance of each PL class.

## 13. Fatty Acid Quantification by Gas Chromatography with Flame Ionization Detector (GC-FID)

In order to identify and quantify the fatty acids present in total lipid extracts, GC-FID was performed, according to Pimentel *et al.* [149]. For that, fatty acid methyl esters were formed by addition of KOH in methanol solution. Then, twenty µL of total lipid extract was transferred to centrifuge tubes and dried in nitrogen current. Then, 1 mL of methyl heptadecanoate (C17:0) internal standard solution (0.75g/L in n-hexane with 1:100 dilution) was added. Plus, 200 µL of KOH (2M) in methanol was added, the mixture was vortexed well (1-2 min) and was then centrifuged at 2000 rpm for 5 minutes. The upper phase was collected to eppendorf and the solvent was dried in a nitrogen flow. Finally, the sample was ressuspended in 20 µL of *n*-hexane, and 4 µL of this solution was injected to GC. Fatty acids were identified by the retention times previously determined by the same procedure with a mixture of standard fatty acids. Peak areas corresponding to each fatty acid were calculated for a relative quantification of fatty acids.

### 13.1. GC-FID Conditions

The GC injection port was programmed at 250 ºC and the detector at 270ºC. Oven temperature was programmed in three ramps, 50ºC for 3 min, 25ºC/min until 180ºC for 6 min and 40ºC/min until 260ºC for 3 min, respectively. The carrier gas was hydrogen flowing at 1.7 mL/min. The column used was DB1 with 30 m, internal diameter of 0.250 mm and 0.10 µm film thickness. Data acquisition and analysis was carried out with TotalChrom Navigator Software.

## 14. 4 Identification of Phospholipid Molecular Species by High-Performance Liquid Chromatography – Mass Spectrometry (HPLC-MS)

The identification of PL molecular species and evaluation of changes in cancer-related cachexia phospholipid classes were carried out by LC-MS using a HPLC system (Waters Alliance 2690) coupled to an electrospray (ESI) linear ion trap mass spectrometer (ThermoFinnigan, San Jose, CA, USA). The mobile phase A is composed of 10% water and 55% acetonitrile with 35% (v/v) of methanol. The mobile phase B is composed of acetonitrile 60%, methanol 40% with 10mM ammonium acetate. For injection, 15 µL of total lipid extract were diluted in the mobile phase A and reaction mixture was introduced into Ascentis Si HPLC Pore column (15 cm x 1.0 mm, 3 µm) (Sigma-Aldrich). The solvent gradient started with 0% of A and linear increased to 100% of A during 20 min, and maintain in these conditions for 35 min, returning, to the initial conditions in min. The flow rate in the column was 16 µL/min obtained using a pre-column split (Acurate, LC Packings, USA). LC-MS was performed with an internal standard [150].

### 14.1. Electrospray Mass Spectrometry Conditions

LC-MS and ESI-MS were acquired in an electrospray linear ion trap mass spectrometer (ThermoFinnigan, San Jose, CA, USA). MS data was obtained using the following electrospray conditions: electrospray voltage was 4.7 kV in negative mode and 5 kV in positive mode; capillary temperature was 275 ºC and the sheath gas flow of 25 U. An isolation width of 0.5 Da was used with a 30-ms activation time for MS/MS experiments. Full scan MS spectrum and MS/MS spectrum were acquired with a 50-ms and 200-ms maximum ionization time, respectively. Normalized collision energy$^{TM}$ (CE) varied between 17 and 20 (arbitrary units) for MS/MS. Data acquisition and analysis was carried out with a Mass Lynx data system V4.0 (Waters, Manchester, UK) and a Xcalibur data system (V2.0), respectively.

## 15. Statistical Analysis

Data is presented as mean ± standard deviation (of raw data or expressed as percentage of control). The Kolmogorov -Smirnov test was used to test normality of

distribution for all data. Significant differences among groups were evaluated with the unpaired student's *t* test, using GraphPad Prism® software (version 5.00). The level of significance was set at $p < 0.05$.

# CHAPTER III

# Results

# III. Results

## 1. Characterization of animal's response to BBN administration

After 20 weeks of oral exposition BBN (N-butyl-N-(4-hydroxybutyl)-nitrosamine) followed by 8 weeks of tap water, rats evidenced a significant 17% loss of body weight ($p$<0.001), which seems related to signs of nodular hyperplasia in the bladder, and simple hyperplasia and dysplasia (in more than 75% of the animals). No histopathological changes in the urothelium were observed in control rats. No changes in food consumption were noticed. The 17% loss of body weight observed in BBN rats might be viewed as moderate cachexia according to the cachexia score for humans (CASCO) [4]. BBN-related body weight decrease was accompanied by a 12% reduction in *gastrocnemius* muscle mass ($p$<0.05 vs. CONT) (**Table 1**). No significant differences of muscle-to-body weight ratio were observed between groups (data not shown).

**Table 1:** Characterization of the animals used in the study.

| Experimental group | Body weight (g) | Muscle mass (g) |
|---|---|---|
| **CONT** | 309.0 ± 21.1 | 3.3 ± 0.3 |
| **BBN** | 256.6 ± 4.1*** | 2.9 ± 0.1* |

Data are expressed as mean ± standard deviation. (*p<0.05 vs CONT; *** p< 0.001vs CONT)

## 2. Effect of Bladder Cancer-related Cachexia on Mitochondrial Metabolic Activity

In order to evaluate the effect of cancer-related cachexia on bladder mitochondrial functionality, the activity of the respiratory chain complexes II and V was spectrophotometrically measured in the mitochondrial fractions of *gastrocnemius* muscle (**Table 2**) and a decreased activity of both complexes was observed ($p$<0.001 vs CONT).

**Table 2:** Effect of cancer-related cachexia on OXPHOS complexes II and V activities in CONT and BBN rats.

| Experimental group | Succinate:ubiquinone reductase (µmol/min/g) | ATP synthase (µmol/Pi/min/mg) |
|---|---|---|
| **CONT** | 4.805 ± 0.3599 | 11.18 ± 0.9436 |
| **BBN** | 2.908 ± 0.2426*** | 6.980 ± 0.6050*** |

Data are expressed as mean ± standard deviation**.** (*** $p$< 0.001vs CONT)

The 40% decrease of succinate:ubiquinone reductase activity and 38% diminishing of ATP synthase activity, was accompanied by a significant decrease of ATP synthase subunit beta expression (**Figure 10B**). The same tendency was noticed for the electron transporter cytochrome c (**Figure 10A**).

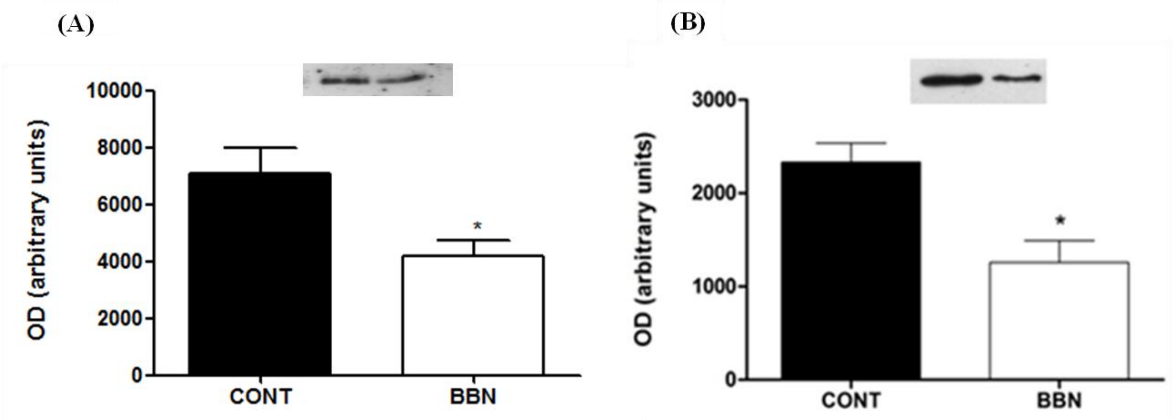


**Figure 10:** Cytochrome c (A) and ATP synthase β (B) expression evaluated by western blotting in gastrocnemius muscle from BBN and control animals. Representative western blots are present above the corresponding graph. Values are expressed as mean ± standard deviation. (*$p$<0.05 vs CONT).

The expression of ETFβ and ETFDH was also analyzed and decreased levels of both proteins were verified in mitochondria of BBN rats (**Figure 11**). The decreased content of these proteins corroborate the lower OXPHOS activity observed since energy production depends on ETF/ETFDH activity and ETFDH is also responsible for

ubiquinone reduction in the mitochondrial membrane [151]. Concomitantly, mitochondrial levels of the uncoupling protein UCP-3 were increased due to BBN exposition ($p$<0.001; **Figure 11C**), and its uncoupling action results in OXPHOS inefficiency [72, 74].

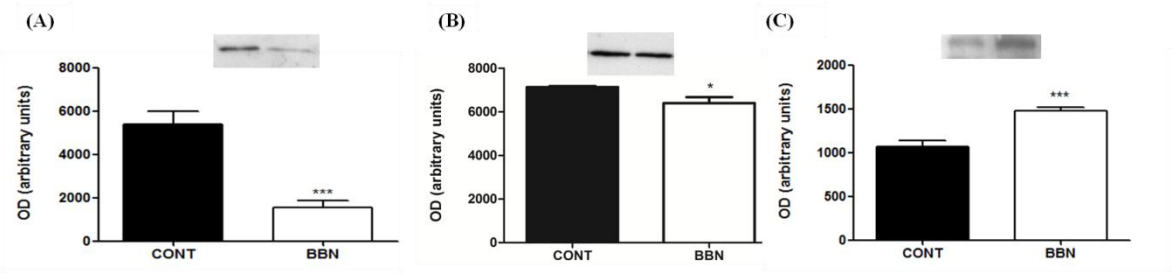


**Figure 11:** Effect of BBN on ETFβ (A), ETFDH (B) and UCP3 (C) expression evaluated by western blotting. Representative immunoblots are presented above the corresponding graph. Values are expressed as mean ± standard deviation. (*$p$<0.05 vs CONT; ***$p$<0.001 vs CONT)

### 3. Effect of Bladder Cancer-related Cachexia on Mitochondria Susceptibility to Oxidative Damage and/or Apoptosis

To evaluate the effect of bladder cancer-related cachexia on mitochondrial proteins susceptibility to oxidative damage, the total content of carbonylated proteins was measured by western blotting after derivatization with dinitrophenylhydrazine (**Figure 12**). The results obtained show an increase of carbonylation levels in BBN mitochondria (***$p$< 0.001 vs CONT). No distinct band patterns of carbonylated proteins were observed between groups, being proteins with MW in the range of approximately 10-60 kDa particularly susceptible to oxidative damage (**Figure 12**).

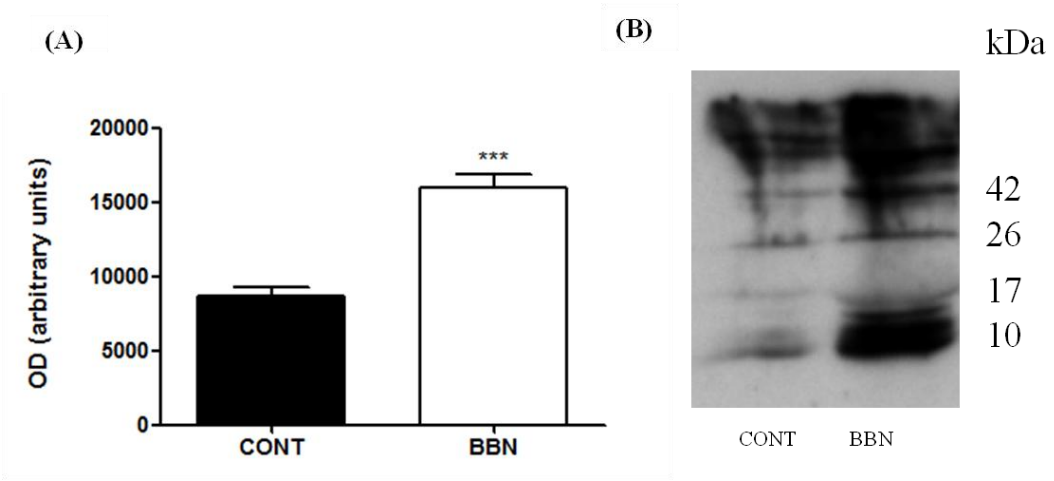


**Figure 12:** Effect of BBN on carbonyl content and profile in mitochondria (A). Representative image of western blotting data is presented (B). Values are expressed as mean ± standard deviation. (****p*< 0.001vs CONT)

The expression of apoptosis-regulating proteins Bax and Bcl-2 was also analyzed to evaluate the susceptibility of mitochondria to apoptosis on cancer-related cachexia (**Figure 13**). Bax/Bcl-2 ratio was higher in BBN mitochondria suggesting a higher susceptibility of wasted muscle to apoptosis (**Figure 13C**).

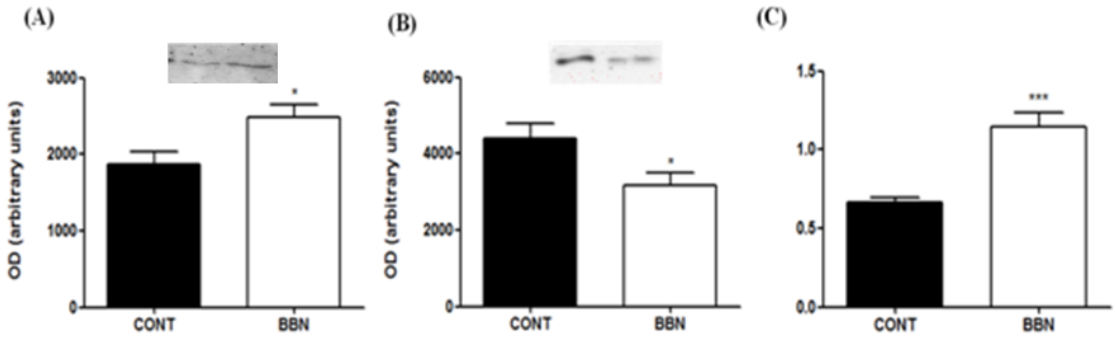


**Figure 13:** Effect of BBN in Bax (A), Bcl-2 (B) and Bax/Bcl-2 ratio (C) expression evaluated by western blotting in mitochondria of *gastrocnemius* muscle from CONT and BBN groups. Representative western blots are present above the corresponding graph. Values are expressed as mean ± standard deviation. (*$p$<0.05 vs CONT ;*** $p$< 0.001vs CONT)

## 4. Effect of Bladder Cancer-related Cachexia on Mitochondria Susceptibility to Lipid Peroxidation

To evaluate the susceptibility of BBN administration on mitochondrial lipids to peroxidation, TBARS were evaluated in isolated mitochondria and no significant differences were observed in the mitochondria from BBN-treated animals (**Figure 14**), in opposite to the verified for mitochondrial proteins.

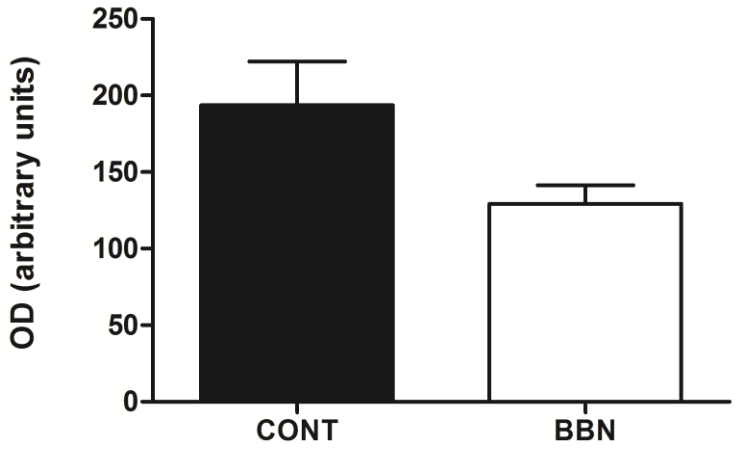


**Figure 14:**Effect of BBN on *gastrocnemius* mitochondria thiobarbituric acid reactive substances (TBARS).Values are presents as mean ± standard deviation of 5 replicates (*p<0.05 vs. CONT).

## 5. Effect of Bladder Cancer-related Cachexia on Phospholipid Profile of Mitochondria

In order to evaluate possible changes in mitochondria phospholipid profile between controls and cachexia, PL profileof total lipid extracts of mitochondria isolated from *gastrocnemius* muscle was evaluted using a lipidomic approach. The results obtained will be presented in the following sections.

### 5.1. Evaluation of Phospholipids Profile in Mitochondria

To evaluate the effect of bladder cancer-related cachexia in mitochondria PL profile, the total lipid extract was fractionated by thin-layer chromatography (TLC) (**Figure 15**). The identification of PL classes was accomplished by comparison with PL

standards applied in the same TLC plate. This approach allowed the separation and identification of mitochondrial phospholipids (PL) classes from *gastrocnemius* muscle tissue: phosphatidylcholines (PC), phosphatidylethanolamines (PE), cardiolipin (CL), phosphatidylserine (PS), phosphatidic acid (PA), phosphatidylglycerol (PG), phosphatidylinositol (PI) and sphingomyelin (SM).

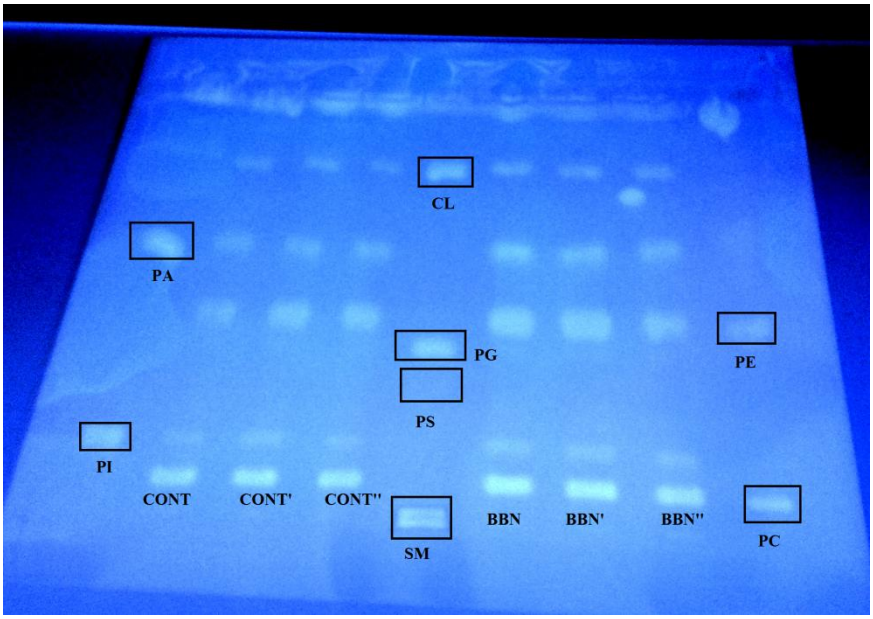


**Figure 15:** Separation of phospholipid classes by thin-layer chromatography from the total lipid extracts obtained from mitochondria of rats control (CONT) and with bladder cancer-related cachexia (BBN). PI – phosphatidylinositol; PA - phosphatidic acid; SM – sphingomyelin; PS - phosphatidylserine; PG – phosphatidylglycerol; CL – cardiolipin; PC - phosphatidylcholine; PE – phosphatidylethanolamine.

After the separation by TLC, the relative PL content (%) present in each spot was evaluated by phosphorous assay (**Figure 16**) as described by Bartlett and Lewis [148]. This analysis was carried out in triplicate for each experimental group.

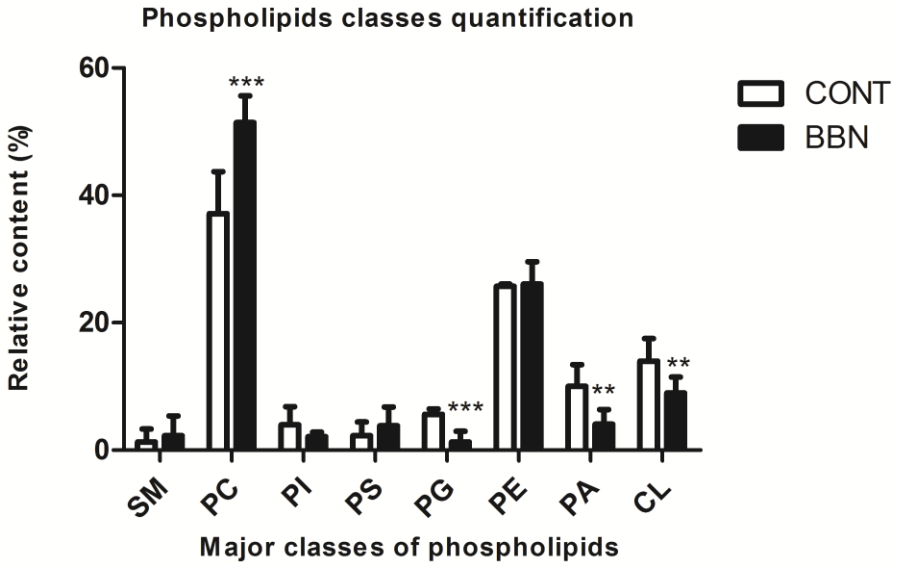


**Figure 16:** Relative content of phospholipid (PL) classes in the total lipid extracts obtained from mitochondria of skeletal muscle of rats, controls (CONT) and bladder cancer-related cachexia (BBN) conditions. The PL classes were separated by thin-layer chromatography and the phosphorous content of each spot was determinate by relating to the amount of phosphorous total lipid extract. SM – sphingomyelin; PC - phosphatidylcholine; PI – phosphatidylinositol; PS - phosphatidylserine; PG – phosphatidylglycerol; PE – phosphatidylethanolamine; PA - phosphatidic acid; CL – Cardiolipin. Values are expressed as mean ± standard deviation from triplicate experiments is shown. (**$p$<0.01 vs CONT; ***$p$<0.001 vs CONT).

The most abundant PL class in all mitochondrial samples was phosphatidylcholine (CONT=37%; BBN=51%) and phosphatidyethanolamine (CONT=26%; BBN=26%), followed by cardiolipin (CONT=14%; BBN=9%). These results are in accordance with the literature that reported these three PL classes as the most abundant in mitochondria [67]. The oral administration of N-butyl-N-(4-hydroxybutyl)-nitrosamine for 20 weeks led to alterations in mitochondrial phospholipid profile detected by changes in phospholipids relative content (**Figure 16**). In the control group, the relative abundance of classes followed the order PC>PE>CL>PA>PG>PI>PS>SM and in cancer-related cachexia group this order was changed for PC>PE>CL>PA>PS>SM>PI>PG . From the analysis of Figure 16 we can depict the significantly decreased in the relative content of PG, PA and CL in BBN mitochondria ($p$<0.001 for PG; $p$<0.01 for CL and PA) while PC were significantly increased in the case of mitochondria of rats treated with BBN ,($p$<0.001). No significant variation was observed for PE content. SM and PS showed a tendency to increase in rat

mitochondria from bladder cancer-related cachexia although not in a statistically significant way. PI class showed a tendency to decrease.

To integrate the alterations verified in PL classes in mitochondria from animals with cancer-related cachexia, data was clustered in metabolic pathways using the Metscape plugin from Cytoskape platform [152]. The general overview of phospholipids biosynthesis allows comprehending the effect of urothelial carcinoma on the remodeling of PL classes (**Figure 17**). The glycerophospholipid (PG) and phosphatidylinositol phosphate metabolic pathways are down-regulated in cachectic mitochondria (**Figure 18**). This is in accordance with data obtained from TLC that showed that PG content was decreased in cachexia group ($p$<0.01; Figure 16). Since PG is a precursor of CL (**Figure 17**) this is a statistically significant decrease in the levels of CL, with cachexia (KEGG reaction RE1197, Figure 18)

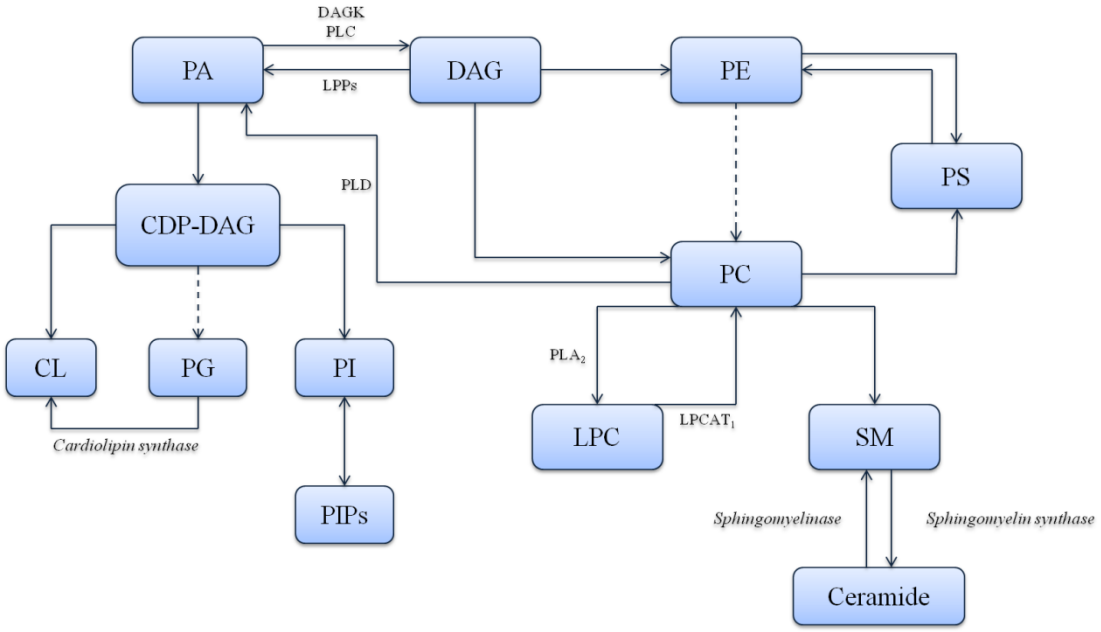


**Figure 17:** Main phospholipids biosynthetic pathways. Broken arrows indicate more than one step. DAGK – diacylglycerol kinase, CDP-DAG – cytidine diphosphate diacylglycerol, PLC – phospholipase C , LPPs – phosphate phosphohydrolases, PLD – phospholipase D, $PLA_2$- phospholipase $A_2$, $LPCAT_1$- lysophosphatidylcholine acyltransferase 1.

Concerning phosphatidylinositol phosphate metabolism, the decrease in PI content although not statistically significant may be due to the increase of phospholipases action

(KEGG reaction REF3273, Figure 18). Decrease of PI class can be also due to phosphorylation, with formation of phosphoinositides phosphorylated (PIPs) (**Figure 17**), which play a main role in apoptotic cellular events [153]. Phosphatidic acid constitutes the molecular basis for the formation of all other phospholipids and showed decreased levels in BBN group. In overall, phospholipids synthesized autonomously by mitochondria, namely PA, PG and CL showed a decreased relative content which seems related with mitochondrial dysfunction observed.

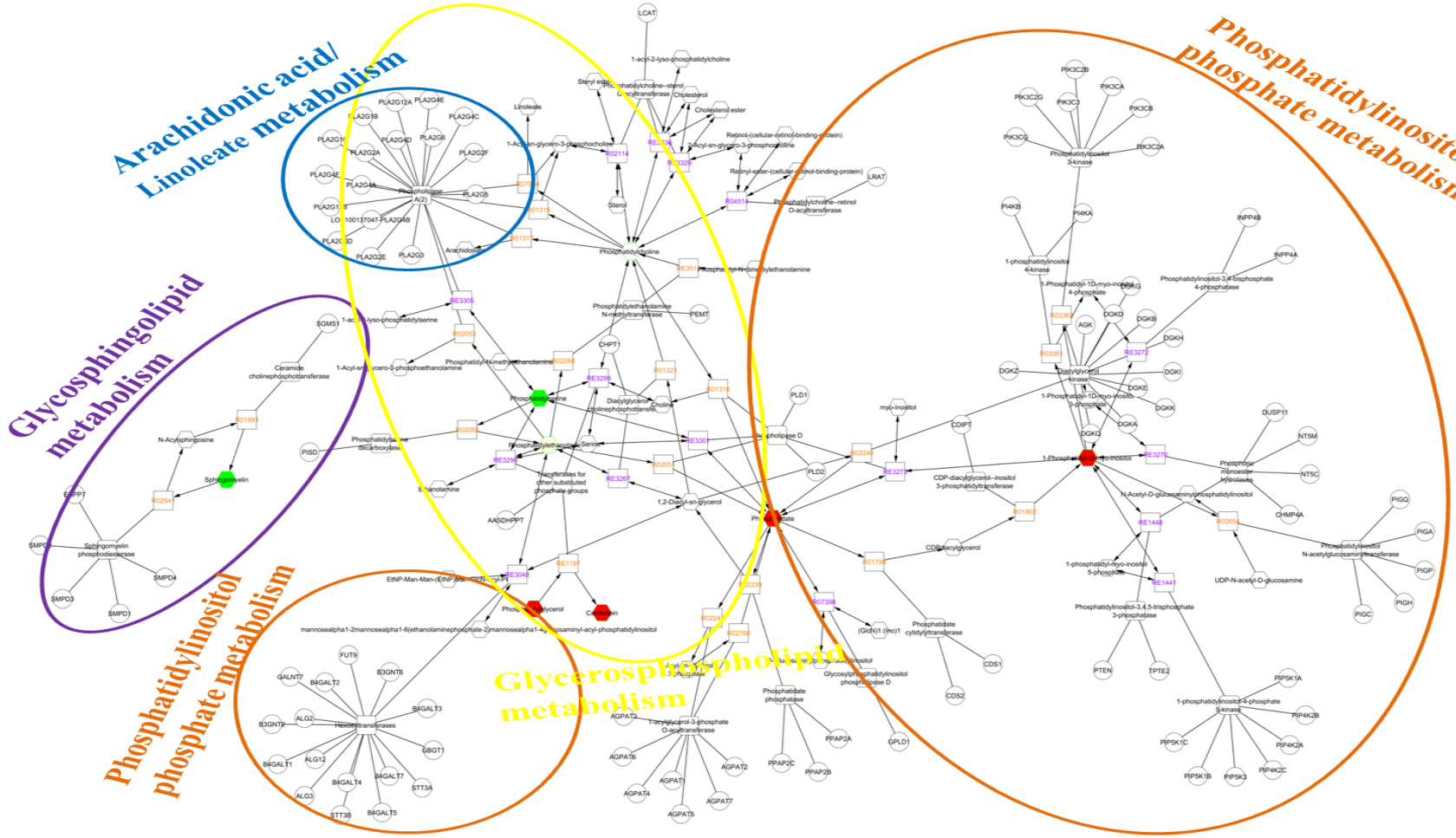


**Figure 18:** Phospholipid metabolic pathways. PL classes found up- and down-regulated (highlighted in green and red, respectively) in mitochondria from animals with cancer-related cachexia and the reactions and enzymes involved. Metscape plugin from Cytoskape platform was used in data clustering.

### 5.2.Evaluation of Fatty Acids Profile in Mitochondria by GC-FID

In order to evaluate if the fatty acid profiling in total lipid extracts change in BBN treated rats , analysis of the fatty acids was performed by GC-FID (**Figure 19**). The results obtained showed a statically increases in the C18:2 and a decrease C18:0 content. Also a tendency of a decrease in the saturated fatty acids relative content (C18:0 and C16:0) accompanied by an increase in the polyunsaturated fatty acids levels (C18:2 and C22:6) is observed Alterations in phospholipid fatty acyl composition impacts mitochondria membrane fluidity and permeability, and consequently its integrity [79]. Though no statistically significant, is interesting to highlight the increase of docosahexanoic acid content (C22:6), since it has been related to an increase of mitochondrial membrane permeability [155].

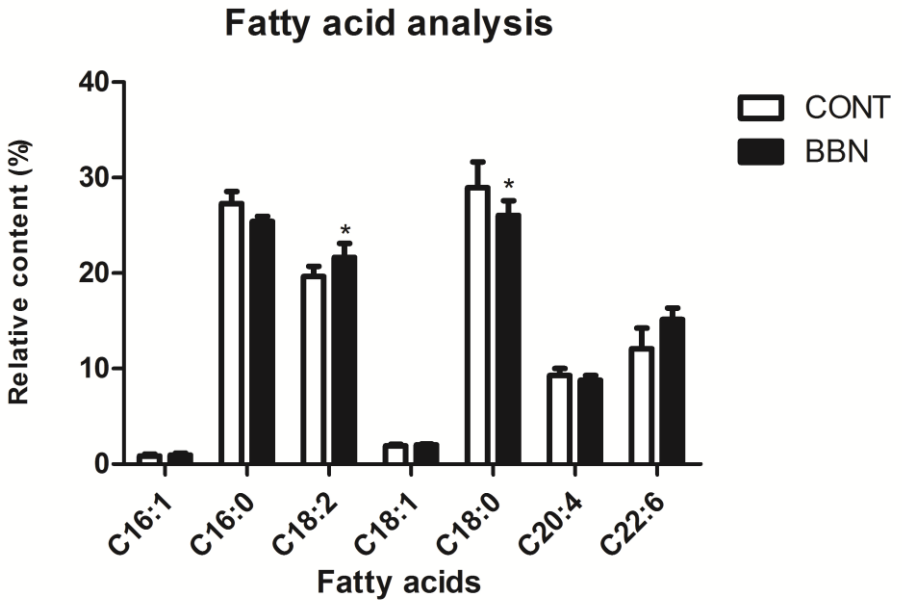


**Figure 19:** Quantification of fatty acid content of mitochondrial total lipid extracts by GC-FID. Values are expressed as mean ± standard deviation from triplicate experiments is shown. (*$p$<0.05 vs CONT).

### 5.3. Evaluation of Phospholipid Classes Profile in Mitochondria by HPLC-MS

To assess the effects of bladder cancer-related muscle wasting on molecular profile within each PL class, lipid extracts from isolated mitochondria of the *gastrocnemius* muscle were analyzed by HPLC-MS. With this approach a separation of phospholipid classes and sequential analysis of molecular species by MS and MS/MS of each class was achieved. This analysis was further complemented with the assessment by tandem mass spectrometry (MS/MS) to identify the fatty acyl composition in each PL molecular species. The identification of PC, SM and LPC classes was performed with ESI-MS in positive mode, with formation of $[MH]^+$ ions. Molecular species of PE, PA, PS, PI, PG and CL were analyzed by ESI-MS in negative mode, that allow the identification of the $[M-H]^-$ ions and also of the $[M-2H]^{2-}$ for CL. An example of LC-chromatogram showing the elution of each phospholipid class is shown in Figure 20.

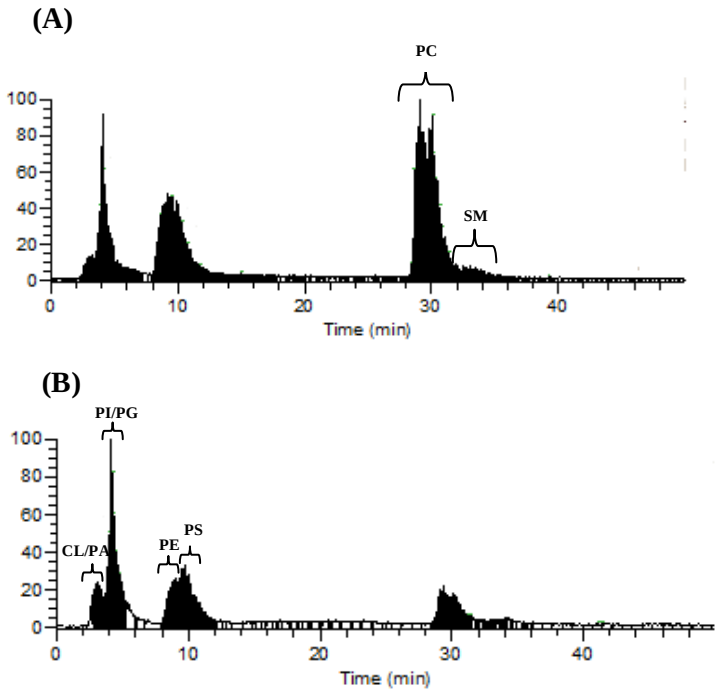


**Figure 20:** Example of total ion chromatograms from the HPLC-MS analysis obtained in the positive mode (A) and in the negative mode (B) from CONT group. Representation of the zone of each PL class elutes and the mode carried out for the analysis.

### 5.3.1. Evaluation of Phosphatidylcholine Profile in Mitochondria

PCs are the most abundant phospholipids found in cell membranes and play an important role in mantaining the membrane structure. PCs ionize preferentially in the positive mode, forming $[MH]^+$. In Figure 22, it is shown HPLC-MS spectra obtained for PC class of total lipid extract in control and cachexia conditions. The identification of PCs as well as their fatty acyl chains composition along the glycerol backbone was achieved by ESI-MS and interpretation of ESI-MS/MS spectra of each ion identified in the MS spectra, as resumed in Table 3. We were able to identify not only diacyl species, but also alkylacyl species. Diacyl and alkyl-acyl species of phospholipids with the same fatty acid compositions but are characterized by a mass difference of 14 Da, due to their attachment to the glycerol backbone of phospholipid by ether or ester bonds (**Figure 21**).

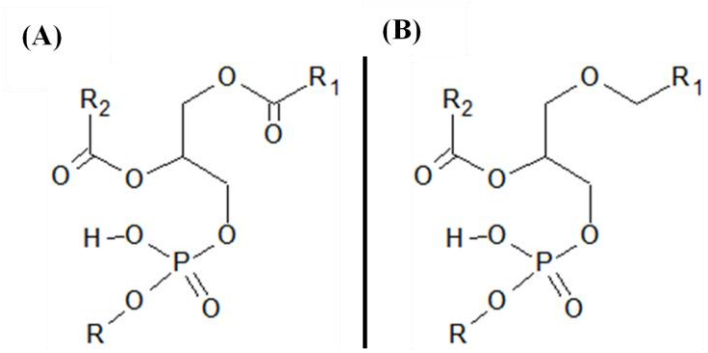


**Figure 21:** Alkylacyl (A) and diacyl (B) phospholipid structures. R represents the headgroup and R1 an R2 represent the fatty acid chain attached to the *sn*-1 and *sn*-2 positions respectively.

By the analysis of MS spectra of PC (**Figure 22**) we can verified that the profile of PC molecular species are the same in the control and cachexia although the PC class relative content increase with cancer-related cachexia according to TLC analysis. The HPLC-MS spectra of PC show major ions at *m/z* 758.7 (PC 16:0/18:2; 16:1/18:1), 782.7 (16:0/20:4), and 806.7 (18:2/22:6) (**Figure 22**). By comparison of profiles in CONT and BBN, there is a slightly increase of the ion at *m/z* 806.7 (18:2/22:6) and at *m/z* 734.6 (16:0/16:0). Increased PC(C18:2/22:6) is in accordance with the increase of longer fatty acid chains observed in GC-FID analysis.

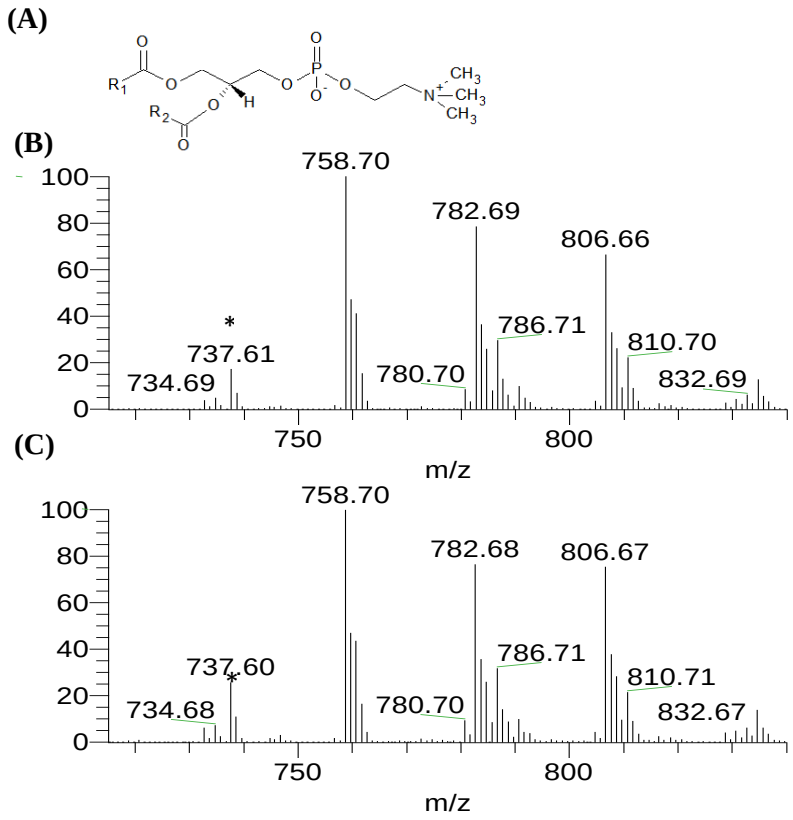


**Figure 22:** General structure of Phosphatidylcholine (PC) (A); HPLC-MS spectra of PC class in the positive mode with formation of $[MH]^+$ ions (B) in control (CONT) and (C) in cachexia situations (BBN). Y-axis: Relative abundance considering the highest abundant ion as 100 %; X-axis: *m/z* for each ion. *737.6 peak correspondent to the eluent.

**Table 3:** Identification of the $[MH]^+$ ions observed in the HPLC-ESI-MS spectra PC. The identification of the fatty acyl composition was done according to the interpretation of the correspondent MS/MS. C:N – number of carbons in the chain : number of double bonds.

| | Diacyl Species | | |
|---|---|---|---|
| **Phosphatidylcholine (PC)** | **$[MH]^+$ *m/z*** | **Molecular Species (C:N)** | **Fatty Acyl Chains** |
| | 732.6 | 32:1 | 16:0/16:1 |
| | 734.6 | 32:0 | 16:0/16:0 |
| | 758.7 | 34:2 | 16:0/18:2 |
| | | | 16:1/18:1 |
| | 760.7 | 34:1 | 16:0/18:1 |
| | 780.7 | 36:4 | 16:1/20:4 |
| | | | 18:1/18:3 |
| | 782.7 | 36:4 | 16:0/20:4 |

**Table 3:** Continued.

| | | | |
|---|---|---|---|
| **Phosphatidylcholine (PC)** | **Diacyl Species** | | |
| | **$[MH]^+$ *m/z*** | **Molecular Species (C:N)** | **Fatty Acyl Chains** |
| | 784.7 | 36:3 | 18:1/18:2 |
| | 786.7 | 36:2 | 18:0/18:2 |
| | 806.7 | 40:8 | 18:2/22:6 |
| | 808.7 | 38:5 | 18:1/20:4 |
| | 810.7 | 38:4 | 18:1/20:3 |
| | 814.7 | 38:2 | 16:1/22:1 |
| | | | 18:1/20:1 |
| | 834.7 | 40:6 | 18:0/22:6 |
| | **Alkylacyl Species** | | |
| | 718.6 | 32:1 | O-16:0/16:1 |
| | 746.7 | 34:1 | O-16:0/18:1 |

PC fragmentation in the MS/MS allowed to identify the fatty acyl composition of PC species. MS/MS spectra of $[MH]^+$ ions of PC, is characterized by the loss of the headgroup phosphocholine (*m/z* 184), not observed in the MS/MS spectra acquired in the ion trap mass spectrometers, loss of the head group (loss of 183) and the loss of the fatty acids as carboxylic acids ($[M+H-R_1COOH]^+$) [128, 156] (**Figure 23**).

**(A)**

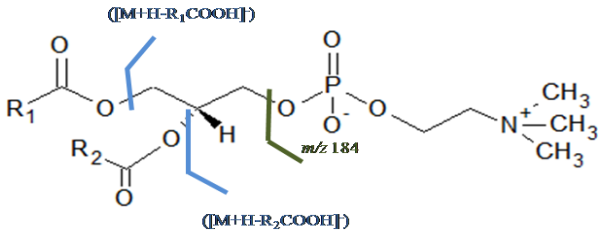


**(B)**

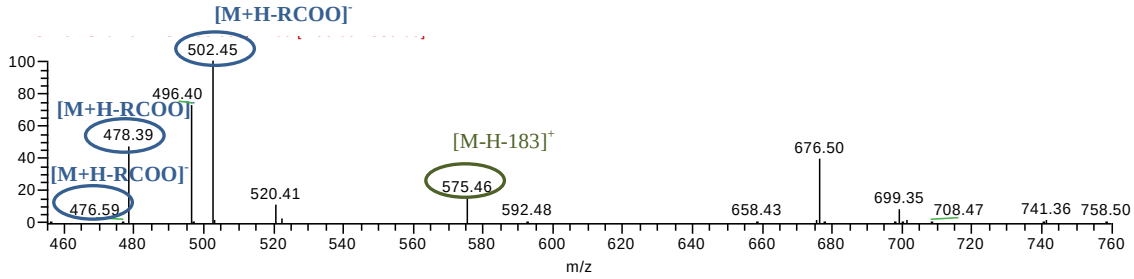


**Figure 23:** Characteristic fragmentation of PC in the positive mode (A); HPLC-ESI-MS/MS spectrum of ion at *m/z* 758 corresponding to PC 16:0/18:2 and PC 16:1/18:1 mixture in the positive mode (B). Ions at *m/z* 502,5; 478,4; 476,6 correspond to the loss of the fatty acid 16:0, 18:2 and 18:1 as a carboxylic acid ([M-H-RCOOH]-), ion at *m/z* 575.5 corresponds to the loss of the phosphocholine headgroup.

### 5.3.2. Evaluation of Sphingomyelin Profile in Mitochondria

As PC, SM species are choline-containing species, which ionize in positive mode as $[MH]^+$. The HPLC-MS spectra obtained for SM is presented in Figure 24 and the identification of the $[MH]^+$ ions resumed in Table 4. Since sphingomyelin class has an additional nitrogen atom they exhibit odd *m/z* values, in contrast with PC that showed even *m/z* values.

Analyzing SM spectra (**Figure 24**), it is possible to see that both are similar, thus indicating that no changes in SM molecular profile occurred after BBN administration. The HPLC-MS spectra of SM shows that the most abundant ion identified was at *m/z* 731.7 (d18:1/18:0), followed by the ion at *m/z* 701.7 (d18:1/16:1) for control and 703.6 (d18:1/16:0) for cancer-related cachexia situations, which corresponds to the unique alteration in both profiles. Since SM elutes close to PC class and given that in total lipid extract PCs are present in high amount, it was possible to identify in SM spectra some

PCs molecular species at *m/z* 758.6 and 782.6. However, the SM species formed as odd value of *m/z* allows us to differentiate between PCs and SMs.

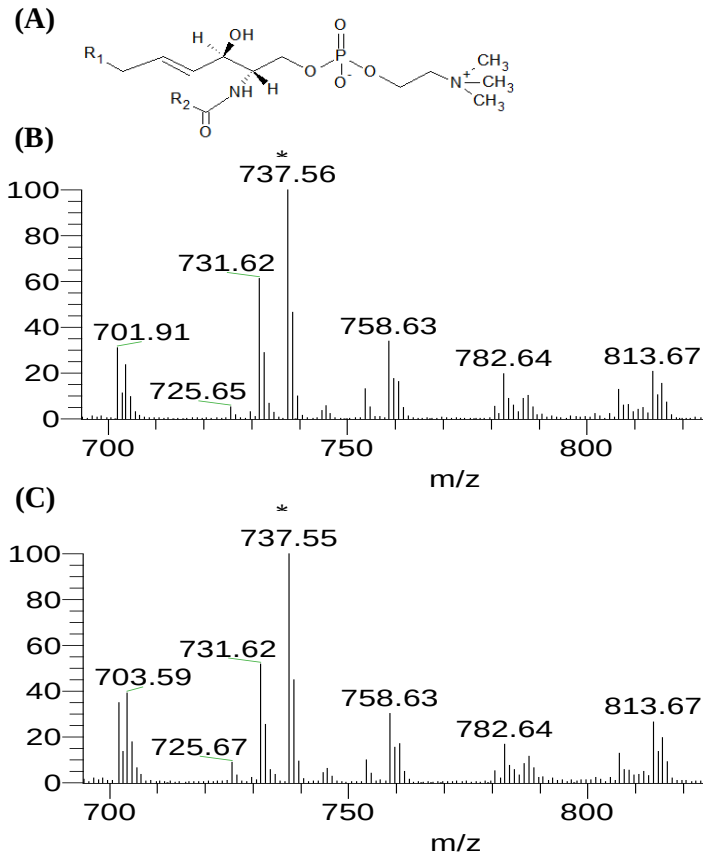


**Figure 24:** General structure of Sphingomyelin (SM) (A); HPLC-MS spectra of SM class in the positive mode with formation of $[MH]^+$ ions (B) in control (CONT) and (C) in cachexia situations (BBN). Y-axis: Relative abundance considering the highest abundant ion as 100 %; X-axis: *m/z* for each ion. *737.6 peak correspondent to the eluent.

**Table 4:** Identification of the $[MH]^+$ ions observed in the HPLC-ESI-MS spectra of SM. The identification of the fatty acyl composition was done according to the interpretation of the correspondent MS/MS. C:N – number of carbons in the chain : number of double bounds.

| | $[MH]^+$ *m/z* | Molecular Species (C:N) | Fatty Acyl Chains (Sphingoid base/Acyl) |
|---|---|---|---|
| **Sphingomyelin** | 701.7 | 34:2 | d18:1/16:1 |
| | 703.6 | 34:1 | d18:1/16:0 |
| | 725.7 | 36:4 | d18:1/18:3 |
| | 731.7 | 36:1 | d18:1/18:0 |

**Table 4:** Continued.

| | $[MH]^+$ *m/z* | Molecular Species (C:N) | Fatty Acyl Chains (Sphingoid base/Acyl) |
|---|---|---|---|
| | 733.6 | 36:0 | d18:0/18:0 |
| | 753.7 | 38:4 | d18:0/20:4 |
| | 759.7 | 38:1 | d18:1/20:0 |
| | 761.7 | 38:0 | d18:0/20:0 |
| | 787.6 | 40:1 | d18:1/22:0 |
| | 813.6 | 42:2 | d18:1/24:1 |
| | 815.6 | 42:1 | d18:1/24:0 |

### 5.3.3. Evaluation of Lysophosphatidylcholine Profile in Mitochondria

LPCs were not detected in the TLC plate due to its very low abundance; however we were able to identify in the HPLC-MS spectra molecular species of this PL class. The molecular species of LPC class were analyzed in the positive ion mode, with formation of $[MH]^+$ ions. The HPLC-MS spectra are shown in Figure 25 and the identification of the molecular species are resumed in Table 5.

Examining the LPC profiles obtained (**Figure 25**) we observe differences among them. The most prominent ion is the one at *m/z* 538.5 (O-20:4) corresponding to the main ion in the BBN situation. Also the ions at *m/z* 496.5, 522.5, 524.5, 546.5 and 560.5, corresponding to LPC(16:0), LPC(18:1), LPC(18:0), LPC(20:3), LPC(O-22:2), are increase in BBN situation.

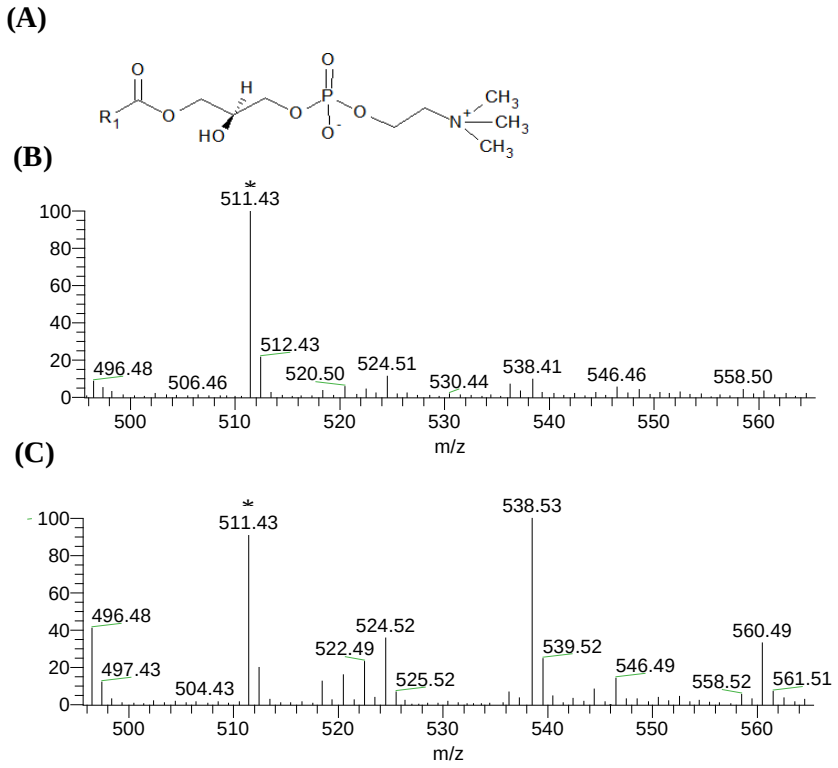


**Figure 25:** General structure of Lysophosphatidylcholine (LPC) (A); HPLC-MS spectra of LPC class in the positive mode with formation of $[MH]^+$ ions (B) in control (CONT) and (C) in cachexia situations (BBN). Y-axis: Relative abundance considering the highest abundant ion as 100 %; X-axis: *m/z* for each ion. *511.4 peak corresponds to an not identifiable specie.

**Table 5:** Identification of the $[MH]^+$ ions observed in the HPLC-ESI-MS spectra of LPC. Fatty acyl composition was attributed by the analysis of MS/MS spectra. C:N – number of carbons in the chain : number of double bonds.

| | **Diacyl Species** | |
|---|---|---|
| **Lysophosphatidylcholine (LPC)** | **$[MH]^+$ *m/z*** | **Molecular Species (C:N)** |
| | 496.5 | 16:0 |
| | 522.5 | 18:1 |
| | 524.5 | 18:0 |
| | 546.5 | 20:3 |

**Table 5:** Continued.

| | Alkylacyl Species | |
|---|---|---|
| | **$[MH]^+$ *m/z*** | **Molecular Species (C:N)** |
| | 538.5 | O-20:4 |
| | 560.5 | O-22:2 |

### 5.3.4. Evaluation of Phosphatidylethanolamine Profile in Mitochondria

The molecular species of PE class were analyzed in the negative mode, with the formation of $[M-H]^-$ ions. The PE profile spectra of control and BBN are shown in Figure 26 and the identification of $[M-H]^-$ ions are resumed in Table 6. The identification of PE class spectra was confirmed by neutral loss map of 141 Da in the MS/MS acquired in the positive mode and allow to identify diacyl and alkylacyl species as summarized in table 6.

By analysis of MS spectra of PE (**Figure 26**) we can observe differences between both conditions studied. The most abundant ion identified was at *m/z* 790.5 PE(18:0/22:6; 18:1/22:5), followed by the ion at *m/z* 746.6 PE(18:0/18:0) and 774.6 PE(O-18:0/22:6), respectively. Interestingly the ion at *m/z* 762.6 PE(16:0/22:6) was higher in comparison with the one at *m/z* 746.6 PE(18:0/18:0) in BBN situation. Higher PE with longer fatty acyl chains, namely PE(16:0/22:6) are in accordance with augment in longer fatty acid analysis. On the other hand, the ion at *m/z* 746.6 PE(18:0/18:0) is also in accordance with the fatty acid profile that showed decrease in C18:0.

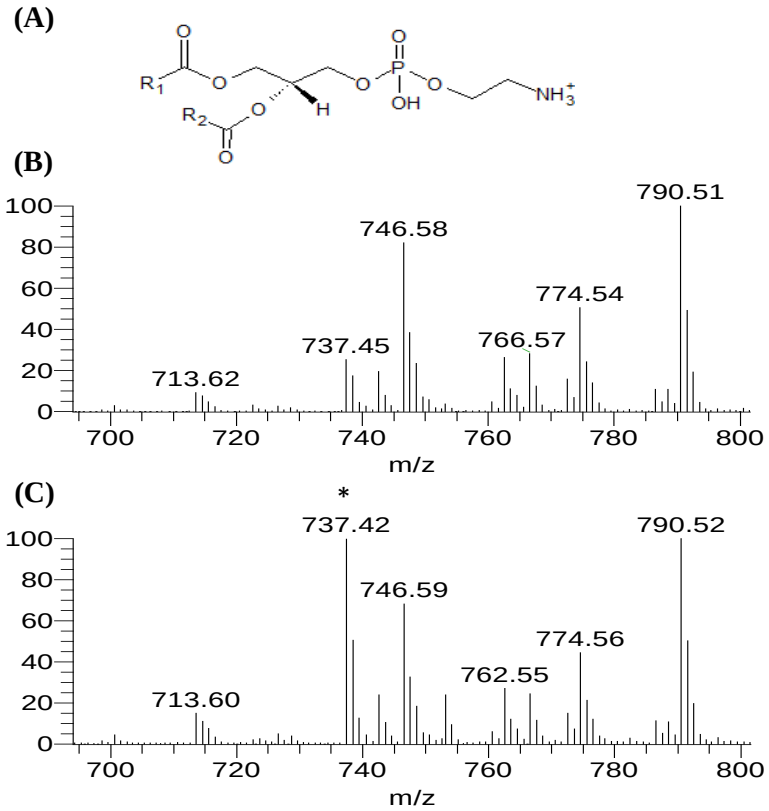


**Figure 26:** General structure of Phosphatidylethanolamine (PE) (A); HPLC-MS spectra of PE class in the negative mode with formation of [M-H]- ions (B) in control (CONT) and (C) in cachexia situations (BBN). Y-axis: Relative abundance considering the highest abundant ion as 100 %; X-axis: m/z for each ion. *737.6 peak correspondent to the eluent.

**Table 6:** Identification of the $[M-H]^-$ ions observed in the HPLC-ESI-MS spectra of PE. The identification of the fatty acyl composition was done according to the interpretation of the correspondent MS/MS. C:N – number of carbons in the chain : number of double bonds.

| | Diacyl Species | | |
|---|---|---|---|
| **Phosphatidylethanolamine (PE)** | **$[M-H]^-$ *m/z*** | **Molecular Species (C:N)** | **Fatty Acyl Chains** |
| | 700.6 | 34:2 | 16:0/18:2 |
| | | | 16:1/18:1 |
| | 714.6 | 34:2 | 16:0/18:2 |
| | | | 16:1/18:1 |
| | 716.6 | 34:1 | 16:0/18:1 |

**Table 6:** Continued.

| | | | |
|---|---|---|---|
| | 740.4 | 36:3 | 18:1/18:2 |
| | 742.5 | 36:2 | 18:0/18:2 |
| | | | 18:1/18:1 |
| | 744.6 | 36:1 | 18:0/18:1 |
| | 746.6 | 36:0 | 18:0/18:0 |
| | 762.6 | 38:6 | 16:0/22:6 |
| | 764.5 | 38:5 | 18:1/20:4 |
| | 766.5 | 38:5 | 18:0/20:4 |
| | 768.5 | 38:3 | 18:1/20:2 |
| | 770.4 | 38:2 | 18:0/20:2 |
| | 772.5 | 38:1 | 18:0/20:1 |
| | 790.5 | 40:6 | 18:0/22:6 |
| | | | 18:1/22:5 |
| | 792.5 | 40:5 | 18:0/22:5 |
| | 794.4 | 40:4 | 18:0/22:4 |
| | 798.4 | 40:2:00 | 18:0/22:2 |
| | **Alkylacyl Species** | | |
| | 774.5 | 40:6 | O-18:0/22:6 |
| | 750.5 | 38:4 | O-18:0/20:4 |
| | 778.5 | 40:4 | O-18:0/22:4 |

Carboxylate anions ([RCOO]-) are detected through the fragmentation of PE in the negative mode. Neutral loss of the fatty acids as carboxylic acids ([M-H-RCOOH]-) in combination with the carboxylate anions allow the characterization of the fatty acids present in the PE molecular species [128, 156] (**Figure 27**).

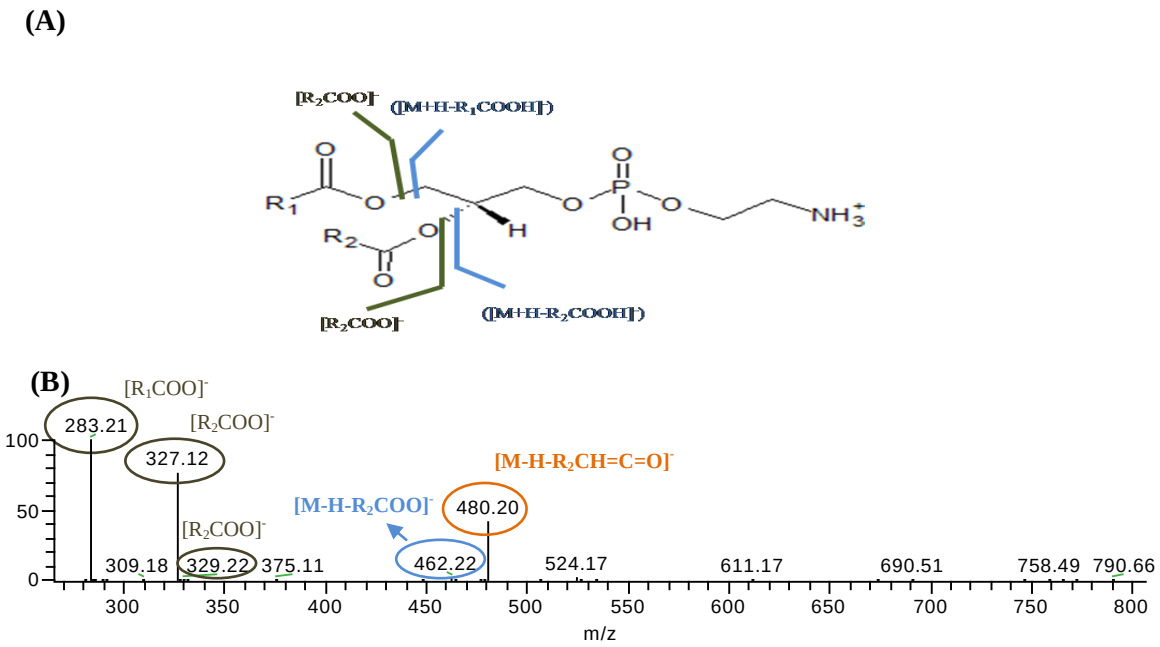


**Figure 27:** Characteristic fragmentation of PE in the negative mode (A); HPLC-ESI-MS/MS spectrum of ion at *m/z* 790 corresponding to PE 18:0/22:6 and PE 18:1/22:6 in the negative mode (B). Ions at *m/z* 283; 327 and 329 correspond to the carboxylate ions ($[RCOO]^-$) of the 18:0, 22:6 and 22:5 fatty acids respectively. Ion at *m/z* 462 corresponds to the loss of the fatty acid 20:0 as a carboxylic acid ($[M-H-RCOOH]^-$), and ion at *m/z* 480 corresponds to the loss of the fatty acid as ketene.

### 5.3.5. Evaluation of Phosphatidylserine Profile in Mitochondria

PS species were also analyzed in the negative mode that allowed the formation of $[M-H]^-$ ions. The MS spectra obtained for PS are shown in Figure 28 and PS species identified are resumed in Table 7. The identification of PS class was confirmed by MS/MS that showed the loss of the head group serine with formation of the product ion $[M-H-87]^-$ and $[M-H-87-RCOOH]^-$, corresponding to the neutral loss of the serine and subsequent loss of the fatty acid. Analyzing HPLC-MS spectra of PS (**Figure 28**) we can identified the ion at *m/z* 790.5, PS (18:0/18:0) as the most abundant specie, followed by the ion at *m/z* 834.5 PS(18:0/22:6) for control and 828.4 PS(18:3/22:6) for cancer-related cachexia situations. This profile is once again according with increased longer fatty acid chains relative content with GC-FID analysis.

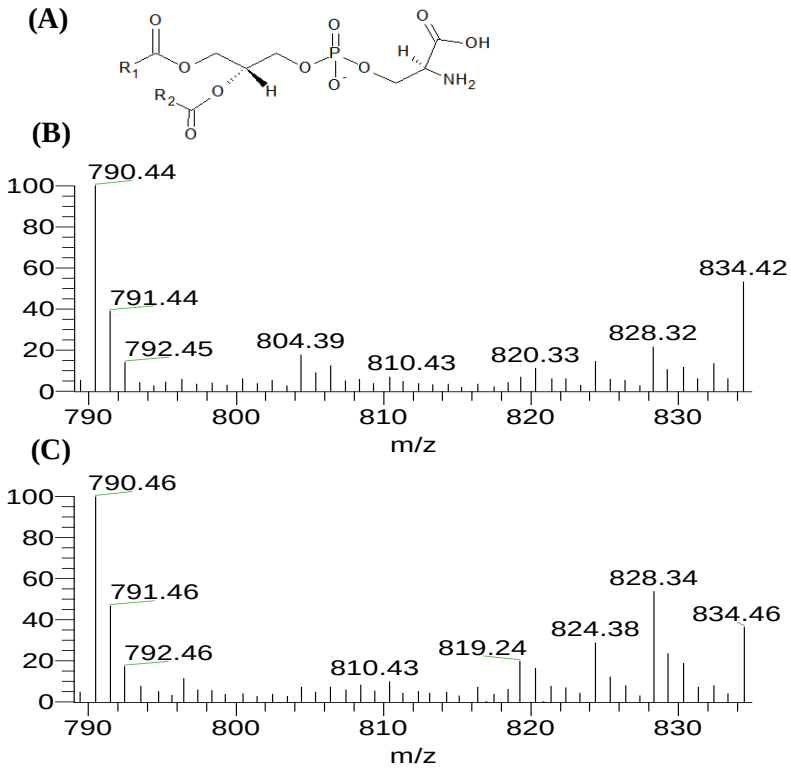


**Figure 28:** General structure of Phosphatidylserine (PS) (A); HPLC-MS spectra of PS class in the negative mode with formation of $[M-H]^-$ ions (B) in control (CONT) and (C) in cachexia situations (BBN). Y-axis: Relative abundance considering the highest abundant ion as 100 %; X-axis: *m/z* for each ion.

**Table 7:** Identification of the $[M-H]^-$ ions observed in the HPLC-ESI-MS spectra of PS. The identification of the fatty acyl composition was done according to the interpretation of the correspondent MS/MS. C:N – number of carbons in the chain : number of double bonds.

| | **$[M-H]^-$ *m/z*** | **Molecular Species (C:N)** | **Fatty Acyl Chains** |
|---|---|---|---|
| **PS** | 790.5 | 36:0 | 18:0/18:0 |
| | 828.4 | 40:9 | 18:3/22:6 |
| | 834.5 | 40:6 | 18:0/22:6 |

### 5.3.6. Evaluation of Phosphatidylinositol Profile in Mitochondria

The molecular species of PI class were analyzed in the negative ion mode, with the formation of $[M-H]^-$ ions. The PI profile spectra are presented in Figure 29 and the identification of the $[M-H]^-$ ions resumed in Table 8. The identification of PI class in MS spectrum was confirmed by MS/MS that showed neutral loss of fatty acyl species combined with loss of inositol (-162 Da).

The analysis of PI spectra allow us to identify four major $[M-H]^-$ ions observed at *m/z* 861.6, 885.6, 887.5 and 909.6 and, corresponding to PI(18:0/18:2), PI(18:0/20:4), PI(18:0/20:3) and PI(18:0/22:6) . Although analysis of phospholipid content showed a slight decrease in the relative content of PI class, no differences were observed in the MS spectra of control and cachexia situations.

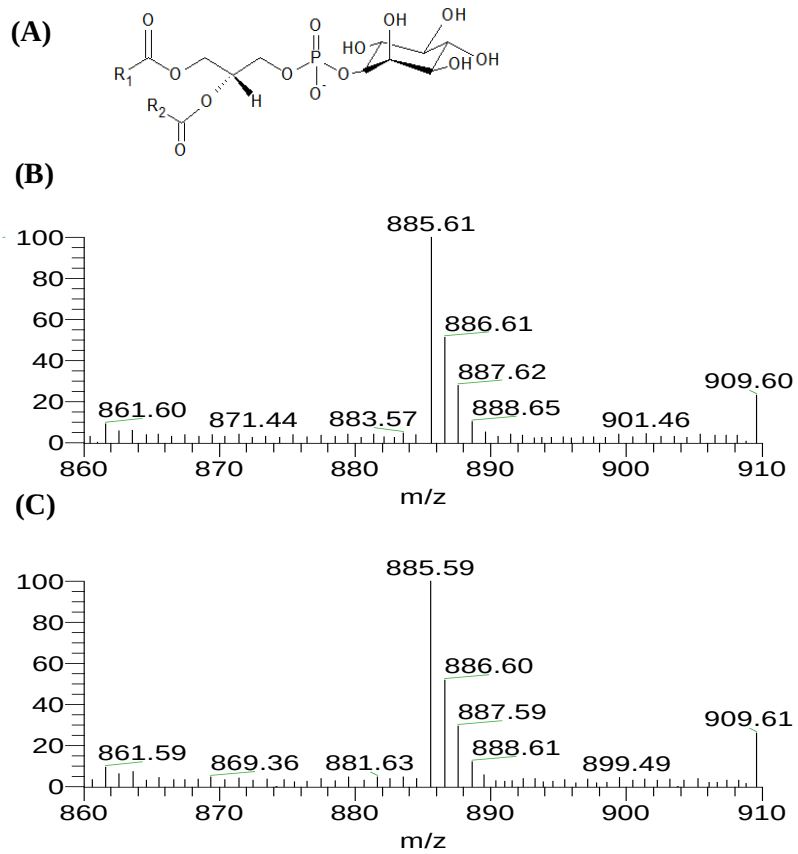


**Figure 29:** General structure of Phosphatidylinositol (PI) (A); HPLC-MS spectra of PI class in the negative mode with formation of $[M-H]^-$ ions (B) in control (CONT) and (C) in cachexia situations (BBN). Y-axis: Relative abundance considering the highest abundant ion as 100%; X-axis: *m/z* for each ion.

**Table 8:** Identification of the $[M-H]^-$ ions observed in the HPLC-ESI-MS spectra of PI. The identification of the fatty acyl composition was done according to the interpretation of the correspondent MS/MS. C:N – number of carbons in the chain : number of double bonds.

| | $[M-H]^-$ *m/z* | Molecular Species (C:N) | Fatty Acyl Chains |
|---|---|---|---|
| **PI** | 861.6 | 36:2 | 18:0/18:2 |
| | 885.6 | 38:4 | 18:0/20:4 |
| | 887.5 | 38:3 | 18:0/20:3 |
| | 909.6 | 40:6 | 18:0/22:6 |

### 5.3.7. Evaluation of Phosphatidylglycerol Profile in Mitochondria

PG molecular species were also analyzed in the negative mode, with the formation of $[M-H]^-$ ions. The MS spectra of PG class are presented in Figure 30 and the identification of the $[M-H]^-$ ions resumed in Table 9. Also in this class (as we can see in Figure 30) the differences between the two spectra are not significant despite the decrease showed by phospholipids relative content quantification.

Analyzing HPLC-MS spectra of PG (**Figure 30**), we can identified the ion at *m/z* 747.6 (16:0/18:1) as the most abundant, followed by the ion at *m/z* 773.6 (18:1/18:1; 18:0/18:2) and 775.6 (18:0/18:0). No differences between control and BBN situations are observed in PG profile.

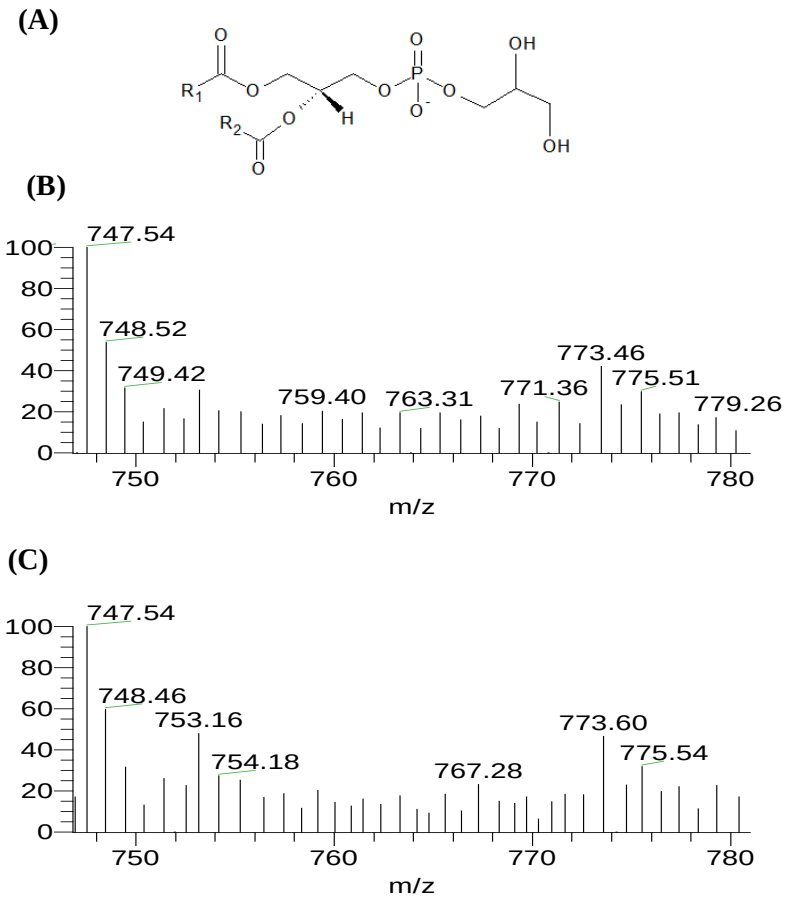


**Figure 30:** General structure of Phosphatidylglycerol (PG) (A); HPLC-MS spectra of PG class in the negative mode with formation of $[M-H]^-$ ions (B) in control (CONT) and (C) in cachexia situations (BBN). Y-axis: Relative abundance considering the highest abundant ion as 100%; *737.6 peak correspondent to the eluent.

**Table 9:** Identification of the [M-H]- ions observed in the HPLC-ESI-MS spectra of PG. The identification of the fatty acyl composition was done according to the interpretation of the correspondent MS/MS. C:N – number of carbons in the chain : number of double bonds.

| | $[M-H]^-$ *m/z* | Molecular Species (C:N) | Fatty Acyl Chains |
|---|---|---|---|
| **PG** | 747.6 | 34:1 | 16:0/18:1 |
| | 773.6 | 36:2 | 18:1/18:1 |
| | | | 18:0/18:2 |
| | 775.6 | 36:1 | 18:0/18:0 |

### 5.3.8. Evaluation of Cardiolipin Profile in Mitochondria

The molecular species of CL class were analyzed in the negative ion mode. This phospholipid has four alkyl groups and ionize with the formation of $[M-H]^-$ or $[M-2H]^{2-}$ ions (mono or double charge species). The CL profile spectra are presented in Figure 31. The analysis was achieved by direct interpretation of MS/MS spectra of each ion identified in the MS spectra, both $[M-H]^-$ and $[M-2H]^{2-}$. By analysis of MS spectra (**Figure 31**), we can identify only one ion $[M-H]^-$ at *m/z* 1447.8 corresponding to CL(18:2/18:2/18:2/18:2). No differences were observed between the MS spectra from the two studied conditions.

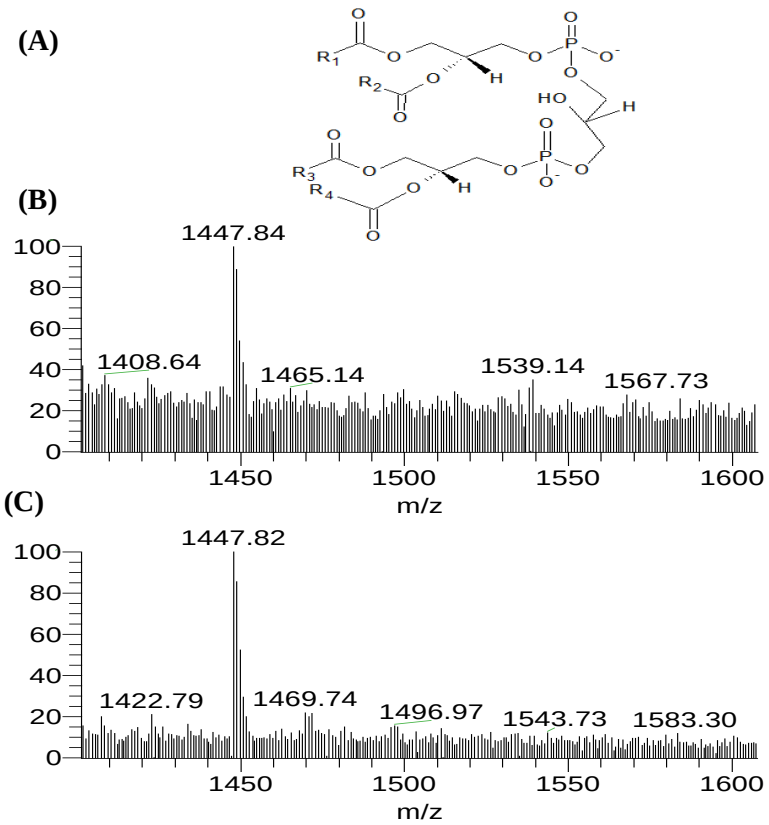


**Figure 31:** General structure of Cardiolipin (CL) (A); HPLC-MS spectra of CL class in the negative mode with formation of $[M-H]^-$ ions (B) in control (CONT) and (C) in cachexia situations (BBN). Y-axis: Relative abundance considering the highest abundant ion as 100%;

The MS/MS spectra of the $[M-H]^-$ ions allows the structural characterization of CL and can be divided in three distinct zones, as described by Hsu and Turk [157]: the phosphatidic acid $[PA-H]^-$, *m/z* 695; the $[(PA-H)+136]^-$, *m/z* 831 and the mono phosphatidic with loss of the fatty acyl chains ($[PA-RCOOH]^-$), *m/z* 415, as it is schematically represented in Figure 32. By MS/MS spectra of the $[M-2H]^{2-}$ ions we can

achieved the structure of the product ions resulting from the fragmentation CL $[M-2H]^{2}$ (**Figure 32C**) with the product ions $[(M-2H)-RCOO^{-}]^{-}$, at *m/z* 1167, formed by the loss of fatty acyl anion and the double charged ion $[M-2H-R=C=O]^{2-}$, at *m/z* 592, formed by the loss of fatty acyl as ketene. Other abundant product ions are the carboxylate anions, $RCOO^{-}$, observed at *m/z* 279, the $[M-H]^{-}$ ions of phosphatidic acid (PA), at *m/z* of 695. The ion at *m/z* 415 is also visible and corresponds to the loss of RCOOH from the phosphatidic acid (PA), with formation of the ion $[PA-RCOOH-H]^{-}$. In this spectrum we can also observe similar fragmentation pathways as previously described by Hsu and Turk [157].

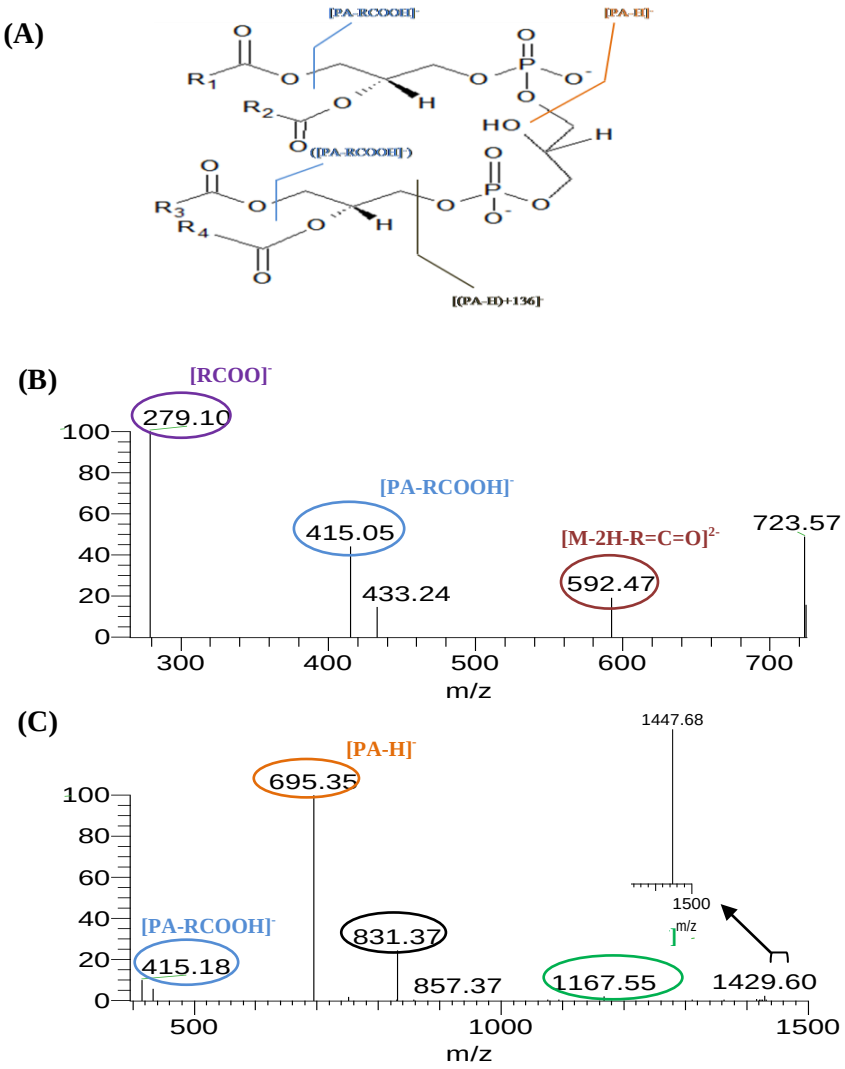


**Figure 32:** Typical CL fragmentation products and CL molecular structure (A); HPLC-ESI-MS/MS spectrum of the $[M-2H]^{2-}$ ion at *m/z* 723 corresponding to CL $(18:2)_4$ in the negative mode (B); HPLC-ESI-MS/MS spectrum of the $[M-H]^{-}$ ion at *m/z* 1447 corresponding to CL $(18:2)_4$ in the negative mode (C).

# CHAPTER IV

# Discussion

# IV. Discussion

Cancer cachexia (CC) is a complex pathophysiological condition related to increased morbidity and mortality in cancer patients [1]. Since the poor quality of life and intolerance to treatment is related to muscle wasting, it is needed a better understand of the molecular mechanisms underlying cancer-induced skeletal muscle wasting [10]. In order to mimic cancer cachexia and its complications, a well characterized animal model of bladder cancer was used. For this purpose, Wistar rats were subjected to N-butyl-N-(4-hydroxybutyl)-nitrosamine (BBN) oral administration for 20 weeks followed by 8 weeks of tap water consumption. The loss of 17% body weight and 12% muscle mass evidenced by animals with notorious bladder nodular hyperplasia confirmed the occurrence of cachexia (**Table 1**). Additionally, mitochondria isolated from *gastrocnemius* muscle seem less functional in cachectic animals considering the decreased activity of OXPHOS complexes II and V (**Table 2**). These results are supported by the decreased expression of ATP synthase β evaluated by western blotting analysis, which synthesis impairment has been related in skeletal muscle wasted conditions [21, 158]. Also the lower levels of cytochrome c observed in mitochondria from animals with urothelial carcinoma might be related to decreased electron transporter function (**Figure 10**). Furthermore, the decreased expression of ETFβ and ETFDH might be associated to mitochondrial respiratory chain impairment considering their function as electron carrier in the respiratory chain [60]. Indeed, ETF transfers electrons to ubiquinone in the mitochondrial respiratory chain [60]. The decreased oxidative activity was paralleled by the accumulation of oxidatively modified proteins in BBN-induced cachexia, specifically carbonylated proteins, which has been associated with impaired cellular function in aged muscle [101, 159]. These data seem to reflect greater susceptibility to oxidative modifications in cancer cachexia, which are consistent with the association between mitochondrial dysfunction and oxidative damage to proteins [66].

Taken together, our data suggest the accumulation of dysfunctional mitochondria in the *gastrocnemius* of cachectic animals. Indeed, mitochondrial dysnfunction has been recently suggested in cancer-related muscle wasting; however the mechanisms involved are not fully elucidated [21]. Moreover, UCP-3 an uncoupling protein was found in increased levels in the skeletal muscle mitochondria of BBN animals (**Figure 11C**). This

protein forms a channel in the inner mitochondrial membrane that allows protons to reenter the mitochondrial matrix without passing through the ATP synthase complex, leading to uncoupling of ATP synthesis rate [72]. An important role in fatty acid transport for further oxidation in situations of increased supply of fatty acids has been attributed to UCP-3 in skeletal muscle, since most part of ATP is generated via fatty acid oxidation [101]. In this way, the overexpression of this protein might be related not only with the diminished OXPHOS activity but also with changes in the phospholipid profile, with the increase of metabolites from the glycosphingolipid pathway and PC, and reduction of metabolites content from the glycerophospholipid pathway, PG, PA and CL (**Figures 16 and 17**). The general phospholipid composition of rat *gastrocnemius* muscle was similar to that reported for this and other skeletal muscles of the same or different species [116]: PC and PE were the prominent species, by far exceeding the rest (**Figure 16**). No significant alterations of PE relative content were verified. Böttinger *et al.* [160] suggested that PE plays an important role for mitochondrial functionality, given the decreased cyt c activity when PE levels were decreased. Phosphatidylserine (PS) similarly to CL has been related to oxidative damage and apoptosis, these alterations are leading by exposure on the outer leaflet of the membrane in a process so-called PS externalization [85]. Finally, regarding phosphotidylinositol (PI), no oxidation products in mitochondria of *gastrocnemius* muscle were found after BBN administration, though this phospholipid contains polyunsaturated potentially oxidizable species [133]. Concomitantly, significant lower levels of PG and CL were observed in BBN-related muscle wasting. Their decrease seem to affect electron transfer efficiency and mitochondrial energy production, taking into account the mitochondrial membrane phospholipids functions. Furthermore, the decreased expression of cytochrome c appears to be correlated with cytochrome c peroxidase activity and oxidataion of cardiolipin [88]. Indeed, lower levels of this protein were detected in mitochondria from *gastrocnemius* of BBN rats (**Figure 10A**), which together with PL profile alterations highlight the implications of the disruption of specific protein-lipid interactions for the appropriate performance of mitochondria. Oxidation of CL by cyt c is associated with the release of cyt c to the cytosol and also associated to loss of CL content. In addition, the loss of CL content has been related with mitochondrial dysfunction, increased membrane permeability and impair respiratory rate also due to its association with complexes I, III, IV and V for their optimal activity [80, 85].

Lipid peroxidation has been hypothesized to be associated to mitochondrial dysfunction [81, 124] and CL comprises a vulnerable target of this oxidative damage due to their high content of unsaturated fatty acids, namely linoleic acid and docosahexaenoic acid [80]. However, no oxidation products of CL were observed. This could be due to loss of oxidized CL because of UCP3 activation. In fact UCP3 is activated by lipid hydroperoxides and is involved in mediating the translocation of LOOH across the mitochondrial membrane and in LOOH-dependent mitochondrial uncoupling [161]. It has been suggested that higher levels of UCP-3 were able to protect mitochondria from ROS and by eliminate or extrude lipid hydroperoxides. UCP3 has been also suggested as responsable by exporting LOOH to outer mitochondrial matrix. This effect may protect mitochondria from lipid damage, but on the other side, may affect membrane properties in consequence of changes in the PL relative content which can affect protein assembly and function [161]. However, mitochondrial proteins were not protect from the oxidative damage once we verified an increase of carbonylated proteins (**Figure 12**). In fact, the accumulation of carbonylated mitochondrial proteins has also been associated with impaired respiratory function [65], playing a crucial role in the pathogenesis of cancer-related cachexia. Since skeletal muscle is multi-nucleated along with the high concentration of endogenous apoptosis inhibitor molecules, apoptosis occur under some conditions such as skeletal muscle atrophy [162]. Additionally, the decreased functionality of mitochondria (**Table 2**) seems related to greater susceptibility to apoptosis as previously suggested [68]. In fact, an increase of the Bax/Bcl-2 ratio was observed in BBN mitochondria. In apoptotic processes, caspases are the main enzymes involved in the initiation and execution of apoptosis and the balance between pro- and anti-apoptotic proteins of Bcl-2 family can control caspases activation. Bax is pro-apoptotic and Bcl-2 anti-apoptotic. An imbalance in this shift results in the release of the pro-apoptotic factor cytochrome c [95], validating the decreased cytochrome c levels observed. The decreased levels of CL (**Figure 15**) also contribute to cyt c release, since the interaction between both is required for cytochrome c attachment and also for an efficient respiratory activity [80, 85, 160]. This release leads to radical species production that could accelerate apoptotic processes [92, 160].

# CHAPTER V

# Conclusions

# V. Conclusions

In order to elucidate the molecular mechanisms underlying cancer-induced muscle wasting in skeletal muscle, 23 *Wistar* rats were randomly divided in two groups: animals with bladder cancer induced by the administration of N-butyl-N-(4-hydroxybutyl)-nitrosamine for 20 weeks (BBN, n=13) or healthy ones (CONT, n=10) and mitochondria were isolated from *gastrocnemius* muscle and biochemically analyzed. Data obtained allowed to conclude that:

i. Urothelial carcinoma induced by BBN administration resulted in a 17% decrease of body weight and 12% of muscle mass as compared to healthy animals. The activity of respiratory chain complexes II and V diminished and was accompanied by decreased expression of metabolic proteins.
ii. The increased susceptibility of mitochondrial proteins to carbonylation seems to justify, at least partially, the mitochondrial dysfunction underlying muscle wasting.
iii. Decreased OXPHOS activity of *gastrocnemius* muscle was parallel to PL profile remodelling characterized by higher PC levels, lower PG, PA and CL content and increased degree of unsaturation of fatty acyl chains.
iv. Skeletal muscle from BBN animals seem more susceptibility to apoptosis, represented by decreased cytochrome c expression levels, increased Bax/Bcl-2 ratio and decreased CL content.
v. The decreased CL content may be responsible for the decrease in cyt c activity and thus affect mitochondria functionality.
vi. Higher levels of UCP-3 seem to protect mitochondrial from lipid mediated oxidative damage since no MS evidences of lipid peroxidation and TBARS levels were observed between groups.

Taken together, urothelial carcinoma induced by BBN administration resulted in muscle wasting due to mitochondrial dysfunction, which was underlied by PL remodeling with higher content of long fatty acyl side chains, accumulation of oxidized mitochondrial proteins that ultimately might lead to muscle apoptosis. Future work focused on therapeutic strategies to counteract cancer-related muscle wasting will be crucial aiming to improve patients' quality of life.

# CHAPTER VI

# References

## VI. References


[1] *World Health Organization*. Available: http://www.who.int/mediacentre/factsheets/fs297/en/

[2] M. J. Tisdale, "Mechanisms of Cancer Cachexia," *Physiological Reviews,* vol. 89, pp. 381-410, Apr 2009.

[3] J. M. Argilés, F. J. López-Soriano, and S. Busquets, "Mechanisms and treatment of cancer cachexia," *Nutrition, Metabolism and Cardiovascular Diseases,* 2012.

[4] J. Argilés, F. López-Soriano, M. Toledo, A. Betancourt, R. Serpe, and S. Busquets, "The cachexia score (CASCO): a new tool for staging cachectic cancer patients," *J Cachexia Sarcopenia Muscle,* vol. 2, pp. 87-93, 2011.

[5] J. M. Argiles, S. Busquets, A. Felipe, and F. J. Lopez-Soriano, "Molecular mechanisms involved in muscle wasting in cancer and ageing: cachexia versus sarcopenia," *International Journal of Biochemistry & Cell Biology,* vol. 37, pp. 1084-1104, May 2005.

[6] S. Dodson, V. E. Baracos, A. Jatoi, W. J. Evans, D. Cella, J. T. Dalton, *et al.*, "Muscle wasting in cancer cachexia: clinical implications, diagnosis, and emerging treatment strategies," *Annu Rev Med,* vol. 62, pp. 265-79, 2011.

[7] C. L. Donohoe, A. M. Ryan, and J. V. Reynolds, "Cancer cachexia: mechanisms and clinical implications," *Gastroenterol Res Pract,* vol. 2011, p. 601434, 2011.

[8] F. A. Guarnier, A. L. Cecchini, A. A. Suzukawa, A. L. G. C. Maragno, A. N. C. Simao, M. D. Gomes, *et al.*, "Time Course of Skeletal Muscle Loss and Oxidative Stress in Rats with Walker 256 Solid Tumor," *Muscle & Nerve,* vol. 42, pp. 950-958, Dec 2010.

[9] R. A. Murphy, M. S. Wilke, M. Perrine, M. Pawlowicz, M. Mourtzakis, J. R. Lieffers, *et al.*, "Loss of adipose tissue and plasma phospholipids: Relationship to survival in advanced cancer patients," *Clinical Nutrition,* vol. 29, pp. 482-487, Aug 2010.

[10] A. Saini, S. Faulkner, N. Al-Shanti, and C. Stewart, "Powerful signals for weak muscles," *Ageing Research Reviews,* vol. 8, pp. 251-267, Oct 2009.

[11] K. Sakuma and A. Yamaguchi, "Sarcopenia and cachexia: the adaptations of negative regulators of skeletal muscle mass," *J Cachexia Sarcopenia Muscle,* vol. 3, pp. 77-94, Jun 2012.

[12] M. J. Tisdale, "Molecular pathways leading to cancer cachexia," *Physiology,* vol. 20, pp. 340-348, Oct 2005.

[13] J. M. Argiles, R. Moore-Carrasco, G. Fuster, S. Busquets, and F. J. Lopez-Soriano, "Cancer cachexia: the molecular mechanisms," *International Journal of Biochemistry & Cell Biology,* vol. 35, pp. 405-409, Apr 2003.

[14] M. J. Tisdale, "Metabolic abnormalities in cachexia and anorexia," *Nutrition,* vol. 16, pp. 1013-1014, Oct 2000.

[15] I. DeBlaauw, N. E. P. Deutz, and M. F. VonMeyenfeldt, "Metabolic changes in cancer cachexia - first of two parts," *Clinical Nutrition,* vol. 16, pp. 169-176, Aug 1997.

[16] P. W. Emery, R. H. Edwards, M. J. Rennie, R. L. Souhami, and D. Halliday, "Protein synthesis in muscle measured in vivo in cachectic patients with cancer," *British medical journal (Clinical research ed.),* vol. 289, pp. 584-586, 1984.

[17] J. M. Argilés, B. Alvarez, and F. J. López-Soriano, "The metabolic basis of cancer cachexia," *Medicinal Research Reviews,* vol. 17, pp. 477-498, 1997.

[18] A. I. Padrão, P. Oliveira, R. Vitorino, B. Colaço, M. J. Pires, M. Márquez, *et al.*, "Bladder cancer-induced skeletal muscle wasting: Disclosing the role of mitochondria plasticity," *The international journal of biochemistry & cell biology,* vol. 45, pp. 1399-1409, 2013.

[19] X. Wang, A. M. Pickrell, T. A. Zimmers, and C. T. Moraes, "Increase in Muscle Mitochondrial Biogenesis Does Not Prevent Muscle Loss but Increased Tumor Size in a Mouse Model of Acute Cancer-Induced Cachexia," *Plos One,* vol. 7, Mar 2012.

[20] C. Julienne, J.-F. Dumas, C. Goupille, M. Pinault, C. Berri, A. Collin, *et al.*, "Cancer cachexia is associated with a decrease in skeletal muscle mitochondrial oxidative capacities without alteration of ATP production efficiency," *J Cachexia Sarcopenia Muscle,* vol. 3, pp. 265-275, 2012/12/01 2012.

[21] C. Constantinou, C. C. Fontes de Oliveira, D. Mintzopoulos, S. Busquets, J. He, M. Kesarwani, *et al.*, "Nuclear magnetic resonance in conjunction with functional genomics suggests mitochondrial dysfunction in a murine model of cancer cachexia," *International journal of molecular medicine,* vol. 27, pp. 15-24, 2011.

[22] M. J. Tisdale, "Cancer cachexia: Metabolic alterations and clinical manifestations," *Nutrition,* vol. 13, pp. 1-7, 1997.

[23] M. J. Lorite, M. G. Thompson, J. L. Drake, G. Carling, and M. J. Tisdale, "Mechanism of muscle protein degradation induced by a cancer cachectic factor," *British journal of cancer,* vol. 78, pp. 850-856, 1998.

[24] W. J. Evans, "Skeletal muscle loss: cachexia, sarcopenia, and inactivity," *The American journal of clinical nutrition,* vol. 91, pp. 1123S-1127S, 2010.

[25] K. C. H. Fearon, "Cancer cachexia: Developing multimodal therapy for a multidimensional problem," *European Journal of Cancer,* vol. 44, pp. 1124-1132, 2008.

[26] M. J. Tisdale, "Pathogenesis of Cancer Cachexia," *THE JOURNAL OF SUPPORTIVE ONCOLOGY,* vol. 1, pp. 159-168, 2003.

[27] J. M. Argilés, R. Moore-Carrasco, G. Fuster, S. l. Busquets, and F. J. López-Soriano, "Cancer cachexia: the molecular mechanisms," *The International Journal of Biochemistry & Cell Biology,* vol. 35, pp. 405-409, 2003.

[28] S. Al-Majid and H. Waters, "The Biological Mechanisms of Cancer-Related Skeletal Muscle Wasting: The Role of Progressive Resistance Exercise," *Biological Research For Nursing,* vol. 10, pp. 7-20, July 1, 2008 2008.

[29] T. Cannon, M. Couch, X. Yin, D. Guttridge, V. Lai, and C. Shores, "Comparison of Animal Models for Head and Neck Cancer Cachexia," *The Laryngoscope,* vol. 117, pp. 2152-2158, 2007.

[30] L. G. Melstrom, K. A. Melstrom, X. Z. Ding, and T. E. Adrian, "Mechanisms of skeletal muscle degradation and its therapy in cancer cachexia," *Histology and Histopathology,* vol. 22, pp. 805-814, Jul 2007.

[31] M. Llovera, C. García-Martínez, N. Agell, F. J. López-Soriano, and J. M. Argilés, "TNF can directly induce the expression of ubiquitin-dependent proteolytic system in rat soleus muscles," *Biochemical and biophysical research communications,* vol. 230, pp. 238-241, 1997.

[32] S. A. Beck and M. J. Tisdale, "Production of lipolytic and proteolytic factors by a murine tumor-producing cachexia in the host," *Cancer Research,* vol. 47, pp. 5919-5923, 1987.

[33] N. MacDonald, A. M. Easson, V. C. Mazurak, G. P. Dunn, and V. E. Baracos, "Understanding and managing cancer cachexia," *Journal of the American College of Surgeons*, vol. 197, pp. 143-161, 2003.

[34] R. Cabal-Manzano, P. Bhargava, A. Torres-Duarte, J. Marshall, and I. W. Wainer, "Proteolysis-inducing factor is expressed in tumours of patients with gastrointestinal cancers and correlates with weight loss," *British journal of cancer*, vol. 84, pp. 1599-1601, 2001.

[35] P. Matthys, H. Heremans, G. Opdenakker, and A. Billiau, "Anti-interferon-γ antibody treatment, growth of Lewis lung tumours in mice and tumour-associated cachexia," *European Journal of Cancer and Clinical Oncology*, vol. 27, pp. 182-187, 1991.

[36] M. J. Smith Kl Fau - Tisdale and M. J. Tisdale, "Increased protein degradation and decreased protein synthesis in skeletal muscle during cancer cachexia," 1993.

[37] S. Temparis, Asensi, M., Taillandier, D., et al., "Increased ATP-Ubiquitin-dependent Proteolysis in Skeletal Muscles of Tumor-bearing Rats," *Cancer Research*, vol. 54, pp. 5568-5573, 1994.

[38] J. A. Norton, R. Shamberger, T. P. Stein, G. W. A. Milne, and M. F. Brennan, "The influence of tumor-bearing on protein metabolism in the rat," *Journal of Surgical Research*, vol. 30, pp. 456-462, 1981.

[39] M. J. Lorite, Smith, H. J., Arnold, J. A:, Morris, A., Thompson, M. G., & Tisdale, M. J., "Activation of ATP-ubiquitin-dependent proteolysis in skeletal muscle in vivo and murine myoblasts in vitro by a proteolysis-inducing factor (PIF)

" *British Journal of Cancer*, vol. 85, pp. 297-302, 2001.

[40] A. Fanzani, V. Conraads, F. Penna, and W. Martinet, "Molecular and cellular mechanisms of skeletal muscle atrophy: an update," *J Cachexia Sarcopenia Muscle*, vol. 3, pp. 163-179, 2012/09/01 2012.

[41] B. B. Lowell, Ruderman, N. B., Goodman, M. N. , "Evidence that lysosomes are not involved in the degradation of myofibriliar proteins in rat skeletal muscle," *Biochemistry Journal*, vol. 234, pp. 237-240, 1986.

[42] S. H. Lecker, A. L. Goldberg, and W. E. Mitch, "Protein Degradation by the Ubiquitin–Proteasome Pathway in Normal and Disease States," *Journal of the American Society of Nephrology*, vol. 17, pp. 1807-1819, July 2006 2006.

[43] P. Costelli, R. D. Tullio, F. M. Baccino, and E. Melloni, "Activation of Ca2+-dependent proteolysis in skeletal muscle and heart in cancer cachexia," ed: Nature Publishing Group, 2001.

[44] J. Khal, A. V. Hine, K. C. Fearon, C. H. Dejong, and M. J. Tisdale, "Increased expression of proteasome subunits in skeletal muscle of cancer patients with weight loss," *The international journal of biochemistry & cell biology*, vol. 37, pp. 2196-2206, 2005.

[45] H. Crossland, D. Constantin-Teodosiu, S. M. Gardiner, D. Constantin, and P. L. Greenhaff, "A potential role for Akt/FOXO signalling in both protein loss and the impairment of muscle carbohydrate oxidation during sepsis in rodent skeletal muscle," *The Journal of physiology*, vol. 586, pp. 5589-5600, November 15, 2008 2008.

[46] T. N. Stitt, D. Drujan, B. A. Clarke, F. Panaro, Y. Timofeyva, W. O. Kline, *et al.*, "The IGF-1/PI3K/Akt Pathway Prevents Expression of Muscle Atrophy-Induced Ubiquitin Ligases by Inhibiting FOXO Transcription Factors," *Molecular Cell*, vol. 14, pp. 395-403, 2004.

[47] A. Amirouche, A.-C. Durieux, S. Banzet, N. Koulmann, R. Bonnefoy, C. Mouret, *et al.*, "Down-Regulation of Akt/Mammalian Target of Rapamycin Signaling Pathway in Response to Myostatin Overexpression in Skeletal Muscle," *Endocrinology*, vol. 150, pp. 286-294, January 1, 2009 2009.

[48] R. A. Frost and C. H. Lang, "Protein kinase B/Akt: a nexus of growth factor and cytokine signaling in determining muscle mass," *Journal of Applied Physiology*, vol. 103, pp. 378-387, July 2007 2007.

[49] T. Schmitt, M. Martignoni, J. Bachmann, K. Fechtner, H. Friess, R. Kinscherf, *et al.*, "Activity of the Akt-dependent anabolic and catabolic pathways in muscle and liver samples in cancer-related cachexia," *Journal of Molecular Medicine*, vol. 85, pp. 647-654, 2007.

[50] S. C. Bodine, T. N. Stitt, M. Gonzalez, W. O. Kline, G. L. Stover, R. Bauerlein, *et al.*, "Akt/mTOR pathway is a crucial regulator of skeletal muscle hypertrophy and can prevent muscle atrophy in vivo," *Nature cell biology*, vol. 3, pp. 1014-1019, 2001.

[51] P. H. Haran, D. A. Rivas, and R. A. Fielding, "Role and potential mechanisms of anabolic resistance in sarcopenia," *J Cachexia Sarcopenia Muscle*, vol. 3, pp. 157-162, 2012.

[52] S. Schiaffino and C. Mammucari, "Regulation of skeletal muscle growth by the IGF1-Akt/PKB pathway: insights from genetic models," *Skeletal Muscle*, vol. 1, p. 4, 2011.

[53] M. Sandri, C. Sandri, A. Gilbert, C. Skurk, E. Calabria, A. Picard, *et al.*, "Foxo transcription factors induce the atrophy-related ubiquitin ligase atrogin-1 and cause skeletal muscle atrophy," *Cell*, vol. 117, pp. 399-412, 2004.

[54] D. J. Glass, "Skeletal muscle hypertrophy and atrophy signaling pathways," *The international journal of biochemistry & cell biology*, vol. 37, pp. 1974-1984, 2005.

[55] A. E. Frazier, C. Kiu, D. Stojanovski, N. J. Hoogenraad, and M. T. Ryan, "Mitochondrial morphology and distribution in mammalian cells," *Biological Chemistry*, vol. 387, pp. 1551-1558, 2006.

[56] B. Su, X. Wang, L. Zheng, G. Perry, M. A. Smith, and X. Zhu, "Abnormal mitochondrial dynamics and neurodegenerative diseases," *Biochimica et Biophysica Acta (BBA) - Molecular Basis of Disease*, vol. 1802, pp. 135-142, 2010.

[57] A. M. Distler, J. Kerner, and C. L. Hoppel, "Proteomics of mitochondrial inner and outer membranes," *Proteomics*, vol. 8, pp. 4066-4082, 2008.

[58] R. Dudkina Nv Fau - Kouril, K. Kouril R Fau - Peters, H.-P. Peters K Fau - Braun, E. J. Braun Hp Fau - Boekema, and E. J. Boekema, "Structure and function of mitochondrial supercomplexes," *Biochim Biophys Acta*, vol. 1797, pp. 664-70, 2010.

[59] M. L. Lenaz G Fau - Genova and M. L. Genova, "Structural and functional organization of the mitochondrial respiratory chain: a dynamic super-assembly," *Int J Biochem Cell Biol.*, vol. 41, pp. 1750-1772, 2009.

[60] W.-C. Liang, A. Ohkuma, Y. K. Hayashi, L. C. López, M. Hirano, I. Nonaka, *et al.*, "ETFDH mutations, CoQ10 levels, and respiratory chain activities in patients with riboflavin-responsive multiple acyl-CoA dehydrogenase deficiency," *Neuromuscular Disorders*, vol. 19, pp. 212-216, 2009.

[61] S. R. Pieczenik and J. Neustadt, "Mitochondrial dysfunction and molecular pathways of disease," *Experimental and molecular pathology*, vol. 83, pp. 84-92, 2007.

[62] G. L. Bellot, D. Liu, and S. Pervaiz, "ROS, autophagy, mitochondria and cancer: Ras, the hidden master?," *Mitochondrion*, 2012.

[63] K. B. Choksi, J. E. Nuss, J. H. DeFord, and J. Papaconstantinou, "Age-related alterations in oxidatively damaged proteins of mouse skeletal muscle mitochondrial electron transport chain complexes," *Free Radical Biology and Medicine,* vol. 45, pp. 826-838, 2008.

[64] A. I. Padrão, R. M. P. Ferreira, R. Vitorino, R. M. P. Alves, M. J. Neuparth, J. A. Duarte, *et al.*, "OXPHOS susceptibility to oxidative modifications: The role of heart mitochondrial subcellular location," *Biochimica et Biophysica Acta (BBA) - Bioenergetics,* vol. 1807, pp. 1106-1113, 2011.

[65] M. K. Shigenaga, T. M. Hagen, and B. N. Ames, "Oxidative damage and mitochondrial decay in aging," *Proceedings of the National Academy of Sciences of the United States of America,* vol. 91, pp. 10771-10778, 1994.

[66] B. D. Doria E., Focarelli A., Marzatico F., "Relationship between Human Aging Muscle and Oxidative System Pathway," *Oxidative Medicine and Cellular Longevity,* vol. 2012, p. 13, 2012.

[67] E. Zinser, C. D. Sperka-Gottlieb, E. V. Fasch, S. D. Kohlwein, F. Paltauf, and G. Daum, "Phospholipid synthesis and lipid composition of subcellular membranes in the unicellular eukaryote Saccharomyces cerevisiae," ed, 1991.

[68] K. A. White Jp Fau - Baltgalvis, M. J. Baltgalvis Ka Fau - Puppa, S. Puppa Mj Fau - Sato, J. W. Sato S Fau - Baynes, J. A. Baynes Jw Fau - Carson, and J. A. Carson, "Muscle oxidative capacity during IL-6-dependent cancer cachexia," 2011.

[69] H. R. Remels Ah Fau - Gosker, P. Gosker Hr Fau - Schrauwen, P. P. H. Schrauwen P Fau - Hommelberg, P. Hommelberg Pp Fau - Sliwinski, M. Sliwinski P Fau - Polkey, J. Polkey M Fau - Galdiz, *et al.*, "TNF-alpha impairs regulation of muscle oxidative phenotype: implications for cachexia?."

[70] T. Y. Aw and D. P. Jones, "Nutrient Supply and Mitochondrial Function," *Annual Review of Nutrition,* vol. 9, pp. 229-251, 1989.

[71] A. Ushmorov, V. Hack, and W. Dröge, "Differential Reconstitution of Mitochondrial Respiratory Chain Activity and Plasma Redox State by Cysteine and Ornithine in a Model of Cancer Cachexia," *Cancer Research,* vol. 59, pp. 3527-3534, July 15, 1999 1999.

[72] J. M. Argilés, S. l. Busquets, and F. J. López-Soriano, "The role of uncoupling proteins in pathophysiological states," *Biochemical and biophysical research communications,* vol. 293, pp. 1145-1152, 2002.

[73] S. Busquets, V. Almendro, E. Barreiro, M. Figueras, J. M. Argilés, and F. J. López-Soriano, "Activation of UCPs gene expression in skeletal muscle can be independent on both circulating fatty acids and food intake: Involvement of ROS in a model of mouse cancer cachexia," *FEBS Letters,* vol. 579, pp. 717-722, 2005.

[74] D. Sanchís, S. l. Busquets, B. Alvarez, D. Ricquier, F. J. López-Soriano, and J. M. Argilés, "Skeletal muscle UCP2 and UCP3 gene expression in a rat cancer cachexia model," *FEBS Letters,* vol. 436, pp. 415-418, 1998.

[75] S. Busquets, C. Garcia-Martínez, M. Olivan, E. Barreiro, F. J. López-Soriano, and J. M. Argilés, "Overexpression of UCP3 in both murine and human myotubes is linked with the activation of proteolytic systems: A role in muscle wasting?," *Biochimica et Biophysica Acta (BBA)-General Subjects,* vol. 1760, pp. 253-258, 2006.

[76] J. S. Moylan and M. B. Reid, "Oxidative stress, chronic disease, and muscle wasting," *Muscle & Nerve,* vol. 35, pp. 411-429, 2007.

[77] J. R. Lancaster jr, S. M. Laster, and L. R. Gooding, "Inhibition of target cell mitochondrial electron transfer by tumor necrosis factor," *FEBS Letters,* vol. 248, pp. 169-174, 1989.

[78] Y. Yamada and H. Harashima, "Mitochondrial drug delivery systems for macromolecule and their therapeutic application to mitochondrial diseases," *Advanced Drug Delivery Reviews,* vol. 60, pp. 1439-1462, 2008.

[79] M. A. Kiebish, X. Han, H. Cheng, A. Lunceford, C. F. Clarke, H. Moon, *et al.*, "Lipidomic analysis and electron transport chain activities in C57BL/6J mouse brain mitochondria," *Journal of Neurochemistry,* vol. 106, pp. 299-312, 2008.

[80] A. J. Chicco and G. C. Sparagna, "Role of cardiolipin alterations in mitochondrial dysfunction and disease," *American Journal of Physiology - Cell Physiology,* vol. 292, pp. C33-C44, January 2007 2007.

[81] E. Niki, "Lipid peroxidation: Physiological levels and dual biological effects," *Free Radical Biology and Medicine,* vol. 47, pp. 469-484, 2009.

[82] V. Ott M Fau - Gogvadze, S. Gogvadze V Fau - Orrenius, B. Orrenius S Fau - Zhivotovsky, and B. Zhivotovsky, "Mitochondria, oxidative stress and cell death," 2007.

[83] H. Bayir, V. A. Tyurin, Y. Y. Tyurina, R. Viner, V. Ritov, A. A. Amoscato, *et al.*, "Selective early cardiolipin peroxidation after traumatic brain injury: an oxidative lipidomics analysis," *Annals of Neurology,* vol. 62, pp. 154-169, 2007.

[84] V. A. Tyurin, Y. Y. Tyurina, P. M. Kochanek, R. Hamilton, S. T. DeKosky, J. S. Greenberger, *et al.*, "Chapter Nineteen Oxidative Lipidomics of Programmed Cell Death," in *Methods in Enzymology*. vol. Volume 442, Z. Z. R. A. L. Roya Khosravi-Far and P. Mauro, Eds., ed: Academic Press, 2008, pp. 375-393.

[85] V. E. Kagan, G. G. Borisenko, Y. Y. Tyurina, V. A. Tyurin, J. Jiang, A. I. Potapovich, *et al.*, "Oxidative lipidomics of apoptosis: redox catalytic interactions of cytochrome c with cardiolipin and phosphatidylserine," *Free Radical Biology and Medicine,* vol. 37, pp. 1963-1985, 2004.

[86] Y. Y. Tyurina, V. A. Tyurin, A. M. Kaynar, V. I. Kapralova, K. Wasserloos, J. Li, *et al.*, "Oxidative lipidomics of hyperoxic acute lung injury: mass spectrometric characterization of cardiolipin and phosphatidylserine peroxidation," *American Journal of Physiology - Lung Cellular and Molecular Physiology,* vol. 299, pp. L73-L85, July 1, 2010 2010.

[87] M. T. Jiang F Fau - Ryan, M. Ryan Mt Fau - Schlame, M. Schlame M Fau - Zhao, Z. Zhao M Fau - Gu, M. Gu Z Fau - Klingenberg, N. Klingenberg M Fau - Pfanner, *et al.*, "Absence of cardiolipin in the crd1 null mutant results in decreased mitochondrial membrane potential and reduced mitochondrial function."

[88] M. Bogdanov, E. Mileykovskaya, and W. Dowhan, "Lipids in the assembly of membrane proteins and organization of protein supercomplexes: implications for lipid-linked disorders," *Sub-cellular biochemistry,* vol. 49, pp. 197-239, 2008.

[89] M. Nabben and J. Hoeks, "Mitochondrial uncoupling protein 3 and its role in cardiac- and skeletal muscle metabolism," *Physiology & behavior,* vol. 94, pp. 259-269, 2008.

[90] T. Nagase I Fau - Yoshida, M. Yoshida T Fau - Saito, and M. Saito, "Up-regulation of uncoupling proteins by beta-adrenergic stimulation in L6 myotubes," *FEBS Lett.,* vol. 494, pp. 175-80, 2001.

[91] C. Wang and R. J. Youle, "The Role of Mitochondria in Apoptosis," *Annual review of genetics,* vol. 43, pp. 95-118, 2009.

[92] J. Cai, J. Yang, and D. Jones, "Mitochondrial control of apoptosis: the role of cytochrome c," *Biochimica et Biophysica Acta (BBA) - Bioenergetics,* vol. 1366, pp. 139-149, 1998.

[93] E. Finucane Dm Fau - Bossy-Wetzel, N. J. Bossy-Wetzel E Fau - Waterhouse, T. G. Waterhouse Nj Fau - Cotter, D. R. Cotter Tg Fau - Green, and D. R. Green,

"Bax-induced caspase activation and apoptosis via cytochrome c release from mitochondria is inhibitable by Bcl-xL."

[94] A. Takahashi, A. Masuda, M. Sun, V. E. Centonze, and B. Herman, "Oxidative stress-induced apoptosis is associated with alterations in mitochondrial caspase activity and Bcl-2-dependent alterations in mitochondrial pH (pHm)," *Brain Research Bulletin,* vol. 62, pp. 497-504, 2004.

[95] J. M. Adams and S. Cory, "The Bcl-2 protein family: Arbiters of cell survival. (Cover story)," *Science,* vol. 281, p. 1322, 1998.

[96] M. F. Beal, "Oxidatively modified proteins in aging and disease," *Free Radical Biology and Medicine,* vol. 32, pp. 797-803, 2002.

[97] I. Dalle-Donne, R. Rossi, D. Giustarini, A. Milzani, and R. Colombo, "Protein carbonyl groups as biomarkers of oxidative stress," *Clinica Chimica Acta,* vol. 329, pp. 23-38, 2003.

[98] M. A. Pellegrino, J. F. Desaphy, L. Brocca, S. Pierno, D. C. Camerino, and R. Bottinelli, "Redox homeostasis, oxidative stress and disuse muscle atrophy," *The Journal of physiology,* vol. 589, pp. 2147-2160, 2011.

[99] C. E. Robinson, A. Keshavarzian, D. S. Pasco, T. O. Frommel, D. H. Winship, and E. W. Holmes, "Determination of Protein Carbonyl Groups by Immunoblotting," *Analytical biochemistry,* vol. 266, pp. 48-57, 1999.

[100] D. L. Meany, H. Xie, L. V. Thompson, E. A. Arriaga, and T. J. Griffin, "Identification of carbonylated proteins from enriched rat skeletal muscle mitochondria using affinity chromatography-stable isotope labeling and tandem mass spectrometry," *Proteomics,* vol. 7, pp. 1150-1163, 2007.

[101] J. Feng, H. Xie, D. L. Meany, L. V. Thompson, E. A. Arriaga, and T. J. Griffin, "Quantitative proteomic profiling of muscle type-dependent and age-dependent protein carbonylation in rat skeletal muscle mitochondria," *The journals of gerontology. Series A, Biological sciences and medical sciences,* vol. 63, pp. 1137-1152, 2008.

[102] G. M. Enns, "The contribution of mitochondria to common disorders," *Molecular Genetics and Metabolism,* vol. 80, pp. 11-26, 2003.

[103] G. A. Cortopassi and A. Wong, "Mitochondria in organismal aging and degeneration," *Biochimica et Biophysica Acta (BBA) - Bioenergetics,* vol. 1410, pp. 183-193, 1999.

[104] J. WANAGAT, Z. CAO, P. PATHARE, and J. M. AIKEN, "Mitochondrial DNA deletion mutations colocalize with segmental electron transport system abnormalities, muscle fiber atrophy, fiber splitting, and oxidative damage in sarcopenia," *The FASEB Journal,* vol. 15, pp. 322-332, February 1, 2001 2001.

[105] L. K. Kwong and R. S. Sohal, "Age-Related Changes in Activities of Mitochondrial Electron Transport Complexes in Various Tissues of the Mouse," *Archives of Biochemistry and Biophysics,* vol. 373, pp. 16-22, 2000.

[106] V. G. Desai, R. Weindruch, R. W. Hart, and R. J. Feuers, "Influences of Age and Dietary Restriction on Gastrocnemius Electron Transport System Activities in Mice," *Archives of Biochemistry and Biophysics,* vol. 333, pp. 145-151, 1996.

[107] S. M. Tanhauser and P. J. Laipis, "Multiple deletions are detectable in mitochondrial DNA of aging mice," *The Journal of biological chemistry,* vol. 270, pp. 24769-24775, 1995.

[108] S. Sugiyama, Takasawa, M., Hayakawa, M., and Ozawa, T., "Changes in skeletal muscle, heart and liver mitochondrial electron transport activities in rats and dogs of various ages," *Biochem. Mol. Biol. Int.* , vol. 30, pp. 937–944, 1993.

[109] C. M. Lee, M. E. Lopez, R. Weindruch, and J. M. Aiken, "Association of age-related mitochondrial abnormalities with skeletal muscle fiber atrophy," *Free Radical Biology and Medicine,* vol. 25, pp. 964-972, 1998.

[110] C. M. Lee, S. S. Chung, J. M. Kaczkowski, R. Weindruch, and J. M. Aiken, "Multiple Mitochondrial DNA Deletions Associated With Age in Skeletal Muscle of Rhesus Monkeys," *Journal of Gerontology,* vol. 48, pp. B201-B205, November 1, 1993 1993.

[111] C. Meissner, P. Bruse, and M. Oehmichen, "Tissue-specific deletion patterns of the mitochondrial genome with advancing age," *Experimental Gerontology,* vol. 41, pp. 518-524, 2006.

[112] P. Schrauwen, V. Schrauwen-Hinderling, J. Hoeks, and M. K. C. Hesselink, "Mitochondrial dysfunction and lipotoxicity," *Biochimica et Biophysica Acta (BBA) - Molecular and Cell Biology of Lipids,* vol. 1801, pp. 266-271, 2010.

[113] G. O. Fruhwirth, A. Loidl, and A. Hermetter, "Oxidized phospholipids: From molecular properties to disease," *Biochimica et Biophysica Acta (BBA) - Molecular Basis of Disease,* vol. 1772, pp. 718-736, 2007.

[114] K. Kolanjiappan, C. R. Ramachandran, and S. Manoharan, "Biochemical changes in tumor tissues of oral cancer patients," *Clinical Biochemistry,* vol. 36, pp. 61-65, 2003.

[115] H. B. Clay, S. Sillivan, and C. Konradi, "Mitochondrial dysfunction and pathology in bipolar disorder and schizophrenia," *International Journal of Developmental Neuroscience,* vol. 29, pp. 311-324, 2011.

[116] G. Daum and J. E. Vance, "Import of lipids into mitochondria," *Progress in Lipid Research,* vol. 36, pp. 103-130, 1997.

[117] S. Pope, J. M. Land, and S. J. R. Heales, "Oxidative stress and mitochondrial dysfunction in neurodegeneration; cardiolipin a critical target?," *Biochimica et Biophysica Acta (BBA) - Bioenergetics,* vol. 1777, pp. 794-799, 2008.

[118] M. Schlame and M. Ren, "The role of cardiolipin in the structural organization of mitochondrial membranes," *Biochimica et Biophysica Acta (BBA) - Biomembranes,* vol. 1788, pp. 2080-2083, 2009.

[119] L. J. Sparvero, A. A. Amoscato, P. M. Kochanek, B. R. Pitt, V. E. Kagan, and H. Bayır, "Mass-spectrometry based oxidative lipidomics and lipid imaging: applications in traumatic brain injury," *Journal of Neurochemistry,* vol. 115, pp. 1322-1336, 2010.

[120] D. L. Nelson, Lehninger, A. L., Cox, M. M., *Lehninger principles of biochemistry*. New York: W.H. Freeman, 2008.

[121] M. Schlame, S. Brody, and K. Y. Hostetler, "Mitochondrial cardiolipin in diverse eukaryotes. Comparison of biosynthetic reactions and molecular acyl species," *European journal of biochemistry / FEBS,* vol. 212, pp. 727-735, 1993.

[122] M. Schlame and D. Haldar, "Cardiolipin is synthesized on the matrix side of the inner membrane in rat liver mitochondria," *The Journal of biological chemistry,* vol. 268, pp. 74-79, 1993.

[123] R. Pamplona, M. Portero-Otín, J. R. Requena, S. R. Thorpe, A. Herrero, and G. Barja, "A low degree of fatty acid unsaturation leads to lower lipid peroxidation and lipoxidation-derived protein modification in heart mitochondria of the longevous pigeon than in the short-lived rat," *Mechanisms of Ageing and Development,* vol. 106, pp. 283-296, 1999.

[124] G. Paradies, G. Petrosillo, M. Pistolese, N. Di Venosa, D. Serena, and F. M. Ruggiero, "Lipid peroxidation and alterations to oxidative metabolism in

mitochondria isolated from rat heart subjected to ischemia and reperfusion," *Free Radical Biology and Medicine,* vol. 27, pp. 42-50, 1999.

[125] A. Reis, P. Domingues, A. J. V. Ferrer-Correia, and M. R. M. Domingues, "Fragmentation study of short-chain products derived from oxidation of diacylphosphatidylcholines by electrospray tandem mass spectrometry: identification of novel short-chain products," *Rapid Communications in Mass Spectrometry,* vol. 18, pp. 2849-2858, 2004.

[126] A. Reis, P. Domingues, A. J. V. Ferrer-Correia, and M. R. M. Domingues, "Tandem mass spectrometry of intact oxidation products of diacylphosphatidylcholines: evidence for the occurrence of the oxidation of the phosphocholine head and differentiation of isomers," *Journal of Mass Spectrometry,* vol. 39, pp. 1513-1522, 2004.

[127] A. Reis, M. R. M. Domingues, F. M. L. Amado, A. J. V. Ferrer-Correia, and P. Domingues, "Separation of peroxidation products of diacyl-phosphatidylcholines by reversed-phase liquid chromatography–mass spectrometry," *Biomedical Chromatography,* vol. 19, pp. 129-137, 2005.

[128] M. R. M. Domingues, A. Reis, and P. Domingues, "Mass spectrometry analysis of oxidized phospholipids," *Chemistry and Physics of Lipids,* vol. 156, pp. 1-12, 2008.

[129] E. Niki, Y. Yoshida, Y. Saito, and N. Noguchi, "Lipid peroxidation: Mechanisms, inhibition, and biological effects," *Biochemical and biophysical research communications,* vol. 338, pp. 668-676, 2005.

[130] V. A. Tyurin, Y. Y. Tyurina, W. Feng, A. Mnuskin, J. Jiang, M. Tang, *et al.*, "Mass-spectrometric characterization of phospholipids and their primary peroxidation products in rat cortical neurons during staurosporine-induced apoptosis," *J Neurochem,* vol. 107, pp. 1614-33, Dec 2008.

[131] F.-F. Hsu and J. Turk, "Electrospray ionization with low-energy collisionally activated dissociation tandem mass spectrometry of glycerophospholipids: Mechanisms of fragmentation and structural characterization," *Journal of Chromatography B,* vol. 877, pp. 2673-2695, 9/15/ 2009.

[132] O. I. Shadyro, I. L. Yurkova, M. A. Kisel, O. Brede, and J. Arnhold, "Radiation-induced fragmentation of cardiolipin in a model membrane," *International Journal Of Radiation Biology,* vol. 80, pp. 239-245, 2004.

[133] Y. Y. Tyurina, V. A. Tyurin, V. I. Kapralova, K. Wasserloos, M. Mosher, M. W. Epperly, *et al.*, "Oxidative lipidomics of γ-radiation-induced lung injury: mass spectrometric characterization of cardiolipin and phosphatidylserine peroxidation," *Radiation research,* vol. 175, pp. 610-621, 2011.

[134] V. A. Tyurin, Y. Y. Tyurina, M.-Y. Jung, M. A. Tungekar, K. J. Wasserloos, H. Bayır, *et al.*, "Mass-spectrometric analysis of hydroperoxy- and hydroxy-derivatives of cardiolipin and phosphatidylserine in cells and tissues induced by pro-apoptotic and pro-inflammatory stimuli," *Journal of Chromatography B,* vol. 877, pp. 2863-2872, 2009.

[135] N. Gebert, M. T. Ryan, N. Pfanner, N. Wiedemann, and D. Stojanovski, "Mitochondrial protein import machineries and lipids: A functional connection," *Biochimica et Biophysica Acta (BBA) - Biomembranes,* vol. 1808, pp. 1002-1011, 2011.

[136] B. G. Gugiu, C. A. Mesaros, M. Sun, X. Gu, J. W. Crabb, and R. G. Salomon, "Identification of Oxidatively Truncated Ethanolamine Phospholipids in Retina and Their Generation from Polyunsaturated Phosphatidylethanolamines," *Chemical Research in Toxicology,* vol. 19, pp. 262-271, 2006/02/01 2006.

[137] L. V. Basova, I. V. Kurnikov, L. Wang, V. B. Ritov, N. A. Belikova, I. I. Vlasova, *et al.*, "Cardiolipin Switch in Mitochondria: Shutting off the Reduction of Cytochrome c and Turning on the Peroxidase Activity†," *Biochemistry,* vol. 46, pp. 3423-3434, 2007/03/01 2007.

[138] H. Oudart, C. Calgari, M. Andriamampandry, Y. L. Maho, and A. Malan, "Stimulation of brown adipose tissue activity in tumor-bearing rats," *Canadian Journal of Physiology and Pharmacology,* vol. 73, pp. 1625-1631, 1995/11/01 1995.

[139] J.-F. Dumas, C. Goupille, C. M. Julienne, M. Pinault, S. Chevalier, P. Bougnoux, *et al.*, "Efficiency of oxidative phosphorylation in liver mitochondria is decreased in a rat model of peritoneal carcinosis," *Journal of Hepatology,* vol. 54, pp. 320-327, 2011.

[140] E. Maciel, P. Domingues, D. Marques, C. Simões, A. Reis, M. M. Oliveira, *et al.*, "Cardiolipin and oxidative stress: Identification of new short chain oxidation products of cardiolipin in in vitro analysis and in nephrotoxic drug-induced disturbances in rat kidney tissue," *International Journal of Mass Spectrometry,* vol. 301, pp. 62-73, 3/30/ 2011.

[141] K. S. M. Tonkonogi, "Rate of oxidative phosphorylation in isolated mitochondria from human skeletal muscle: effect of training status," *Acta Physiol Scand,* vol. 161, pp. 345-353, 1997.

[142] O. H. Lowry, N. J. Rosebrough, A. L. Farr, and R. J. Randall, "PROTEIN MEASUREMENT WITH THE FOLIN PHENOL REAGENT," *Journal of Biological Chemistry,* vol. 193, pp. 265-275, November 1, 1951 1951.

[143] M. A. Birch-Machin, H. L. Briggs, A. A. Saborido, L. A. Bindoff, and D. M. Turnbull, "An evaluation of the measurement of the activities of complexes I-IV in the respiratory chain of human skeletal muscle mitochondria," *Biochemical medicine and metabolic biology,* vol. 51, pp. 35-42, 1994.

[144] N. Simon, C. Morin, S. Urien, J.-P. Tillement, and B. Bruguerolle, "Tacrolimus and sirolimus decrease oxidative phosphorylation of isolated rat kidney mitochondria," *British Journal of Pharmacology,* vol. 138, pp. 369-376, 2003.

[145] U. K. Laemmli, "Cleavage of structural proteins during the assembly of the head of bacteriophage T4," *Nature,* vol. 227, pp. 680-685, 1970.

[146] J. R. Bertholf Rl Fau - Nicholson, M. R. Nicholson Jr Fau - Wills, J. Wills Mr Fau - Savory, and J. Savory, "Measurement of lipid peroxidation products in rabbit brain and organs (response to aluminum exposure)," *Ann Clin Lab Sci.* , vol. 17, pp. 418-23, 1987.

[147] D. W. Bligh EG, "A rapid method of total lipid extraction and purification," *Canadian Journal Of Biochemistry And Physiology,* vol. 37(8), pp. 911–7, 1959.

[148] E. a. D. L. Bartlett, "Spectrophotometric determination of phosphate esters in the presence and absence of orthophosphate," *Analytical biochemistry,* vol. 36(1), pp. 159-167, 1970.

[149] S. Aued-Pimentel, J. H. G. Lago, M. H. Chaves, and E. E. Kumagai, "Evaluation of a methylation procedure to determine cyclopropenoids fatty acids from Sterculia striata St. Hil. Et Nauds seed oil," *Journal of Chromatography A,* vol. 1054, pp. 235-239, 2004.

[150] P. T. Ivanova, S. B. Milne, M. O. Byrne, Y. Xiang, and H. A. Brown, "Glycerophospholipid Identification and Quantitation by Electrospray Ionization Mass Spectrometry," in *Methods in Enzymology*. vol. Volume 432, H. A. Brown, Ed., ed: Academic Press, 2007, pp. 21-57.

[151] D. C. Wallace, "A mitochondrial paradigm of metabolic and degenerative diseases, aging, and cancer: a dawn for evolutionary medicine," *Annual review of genetics,* vol. 39, pp. 359-407, 2005.

[152] J. Gao, V. G. Tarcea, A. Karnovsky, B. R. Mirel, T. E. Weymouth, C. W. Beecher, *et al.*, "Metscape: a Cytoscape plug-in for visualizing and interpreting metabolomic data in the context of human metabolic networks," *Bioinformatics (Oxford, England),* vol. 26, pp. 971-973, 2010.

[153] A. M. Hicks, C. J. DeLong, M. J. Thomas, M. Samuel, and Z. Cui, "Unique molecular signatures of glycerophospholipid species in different rat tissues analyzed by tandem mass spectrometry," *Biochimica et Biophysica Acta (BBA) - Molecular and Cell Biology of Lipids,* vol. 1761, pp. 1022-1029, 2006.

[154] E. E. Kooijman and K. N. J. Burger, "Biophysics and function of phosphatidic acid: A molecular perspective," *Biochimica et Biophysica Acta (BBA) - Molecular and Cell Biology of Lipids,* vol. 1791, pp. 881-888, 2009.

[155] W. Stillwell, L. Jenski, F. Thomas Crump, and W. Ehringer, "Effect of docosahexaenoic acid on mouse mitochondrial membrane properties," *Lipids,* vol. 32, pp. 497-506, 1997/05/01 1997.

[156] M. Pulfer and R. C. Murphy, "Electrospray mass spectrometry of phospholipids," *Mass Spectrometry Reviews,* vol. 22, pp. 332-364, 2003.

[157] J. Hsu Ff Fau - Turk, E. R. Turk J Fau - Rhoades, D. G. Rhoades Er Fau - Russell, Y. Russell Dg Fau - Shi, E. A. Shi Y Fau - Groisman, and E. A. Groisman, "Structural characterization of cardiolipin by tandem quadrupole and multiple-stage quadrupole ion-trap mass spectrometry with electrospray ionization."

[158] S. Fontes-Oliveira Cc Fau - Busquets, M. Busquets S Fau - Toledo, F. Toledo M Fau - Penna, M. Penna F Fau - Paz Aylwin, S. Paz Aylwin M Fau - Sirisi, A. P. Sirisi S Fau - Silva, *et al.*, "Mitochondrial and sarcoplasmic reticulum abnormalities in cancer cachexia: altered energetic efficiency?."

[159] J. E. Nuss, J. K. Amaning, C. E. Bailey, J. H. DeFord, V. L. Dimayuga, J. P. Rabek, *et al.*, "Oxidative modification and aggregation of creatine kinase from aged mouse skeletal muscle," *Aging,* vol. 1, pp. 557-572, 2009.

[160] L. Böttinger, S. E. Horvath, T. Kleinschroth, C. Hunte, G. Daum, N. Pfanner, *et al.*, "Phosphatidylethanolamine and cardiolipin differentially affect the stability of mitochondrial respiratory chain supercomplexes," *Journal of molecular biology,* vol. 423, pp. 677-686, 2012.

[161] A. Lombardi, R. A. Busiello, L. Napolitano, F. Cioffi, M. Moreno, P. de Lange, *et al.*, "UCP3 translocates lipid hydroperoxide and mediates lipid hydroperoxide-dependent mitochondrial uncoupling," *J Biol Chem,* vol. 285, pp. 16599-605, May 28 2010.

[162] E. E. Dupont-Versteegden, "Apoptosis in skeletal muscle and its relevance to atrophy."